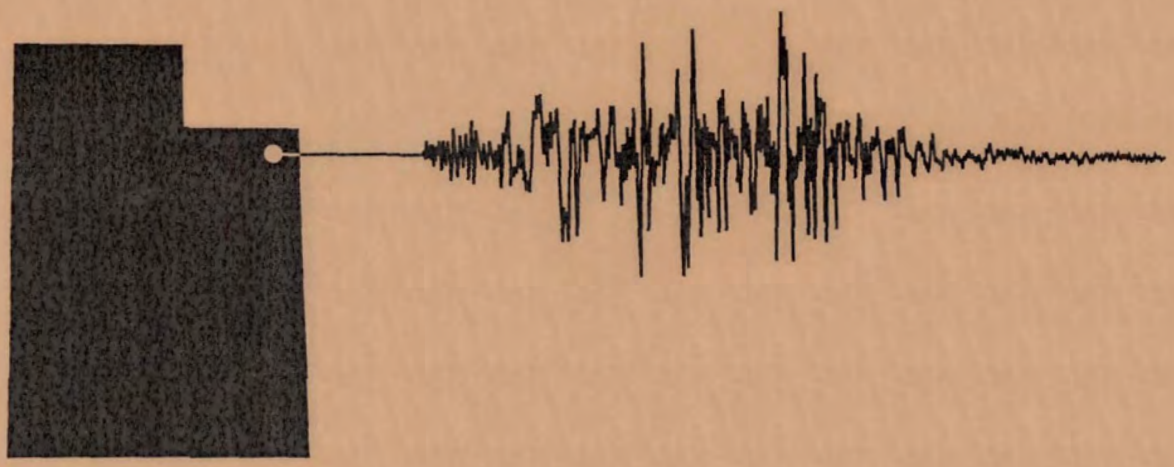

Seismotectonic Study

for
Flaming Gorge Dam,
Colorado River Storage Project, Utah

U.S. DEPARTMENT OF INTERIOR
BUREAU OF RECLAMATION
TECHNICAL SERVICE CENTER
GEOPHYSICS, PALEOHYDROLOGY, AND SEISMOTECTONICS GROUP
DENVER, COLORADO

SEISMOTECTONIC REPORT FOR FLAMING GORGE DAM, COLORADO RIVER STORAGE PROJECT, NORTHEASTERN UTAH

by
Lucille A. Piety
and
Ute R. Vetter

SEISMOTECTONIC REPORT 98-2

Geophysics, Paleohydrolgy, and Seismotectonics Group
Technical Service Center
Bureau of Reclamation
Denver, Colorado

July 1999

SEISMOTECTONIC REPORT FOR FLAMING GORGE DAM, COLORADO RIVER STORAGE PROJECT, NORTHEASTERN UTAH

Seismotectonic Report 98-2

Prepared by:

L. A. Piety — 7/29/99

Lucille A. Piety — Date

U. Vetter — 7/30/99

Ute R. Vetter — Date

Peer review by:

Larry W. Anderson — 7/30/99

Larry W. Anderson — Date

JmP A — 8/2/99.

Jon P. Ake — Date

Summary

This report presents the conclusions of the seismotectonic study for Flaming Gorge Dam, Colorado River Storage Project, in northeastern Utah. These conclusions are based on a review of literature about the geology, seismicity, and tectonics of the region, an examination of 1:40,000-scale, black-and-white aerial photographs for several faults identified in the literature as exhibiting evidence for Quaternary rupture, a field reconnaissance of scarps and lineaments identified by their expression on the aerial photographs as possibly having a tectonic origin, a compilation of regional seismicity using historical records, and a calculation of ground motions on the basis of historical seismicity. No additional studies are recommended at this time.

Flaming Gorge Dam is located on the Green River on the north flank of the eastern Uinta Mountains, an east-trending range of the middle Rocky Mountains. The area surrounding the dam has experienced a complex late Cenozoic (since about 65 Ma) tectonic history, and faults are associated with both the north and south flanks of the mountains. Although most of the tectonic activity ceased by about 10 Ma, evidence for Quaternary ($\leq$1.6 Ma) surface displacement has been reported for a few of these faults. However, none of these faults had been studied in enough detail to adequately evaluate the age and extent of any possible Quaternary ruptures. Scarps and lineaments that may have a tectonic origin and could indicate Quaternary surface rupture are preserved along or near four faults within about 50 km of Flaming Gorge Dam. These scarps are dissected and have a rounded form. They are usually short (<10 km). The average Quaternary displacement rates for all of these faults is low (<0.01 mm/yr). Surfaces that are at least a few tens of thousands of years old cross the projected traces of all of the faults. These faults have not experienced recurrent, large surface ruptures during the latest Quaternary (since about 15 ka to 20 ka) and possibly not for a much greater time. The probability of surface displacement on any of these faults is considered low. None are considered to be potential seismic sources for Flaming Gorge Dam.

Seismicity in the region surrounding Flaming Gorge Dam has been moderate. Earthquakes are mostly of magnitude 4.0 and smaller, but eight events greater than magnitude 4.5 have been reported. The largest of these was a magnitude (M_W) 5.5 event that occurred on October 11, 1960, near Montrose, Colorado.

Because none of the faults in the region are considered to be potential seismic sources, the greatest hazard for Flaming Gorge Dam is from random earthquakes, unrelated to any mapped faults in the region. Earthquake recurrence parameters were calculated on the basis of the historical seismic catalog, which includes events through the end of 1995. A probabilistic seismic hazard analysis (PSHA) was performed for the random seismicity, incorporating uncertainties in seismicity rates. The attenuation relations of Sadigh and others (1997) and of Spudich and others (1996) were used with equal weights.

Results of the PSHA are hazard curves (peak horizontal acceleration (PHA) ground motions vs. annual probability of exceedance) at 5% damping. For an annual probability of exceedance of 2×10^{-5} (50,000-year return period), the resulting median PHA value is 0.4 g, and for an annual probability of exceedance of 1×10^{-4} (10,000-year return period) it is 0.25 g. Empirical time histories were selected to represent the hazard for return periods of 50,000 and 10,000 years. The recommended time histories to represent the 50,000-year return period are records from the Mammoth Lake earthquake on May 27, 1980, 14:51 UTC, M_W 6.0 (M_L 6.2) recorded at the Long Valley Dam, upper left abutment station. For the 10,000-year return period, records from the Whittier Narrows earthquake on October 1, 1987, 14:42 UTC, M_W 6.0 (M_L 5.9) recorded at the Castlegate Street station in Compton, are recommended.

SEISMOTECTONIC REPORT FOR FLAMING GORGE DAM, COLORADO RIVER STORAGE PROJECT, NORTHEASTERN UTAH

Seismotectonic Report 98-2

Page

Summary iii
1. Introduction 1
    1.1. Acknowledgments 3
2. Late Cenozoic Geologic and Tectonic Setting 4
3. Evaluation of Possible Quaternary Faults Along or Adjacent to the North Flank of the Uinta Mountains 9
    3.1. Scarps Along the North Flank of Phil Pico Mountain 9
        3.1.1. Alluvial geomorphic surfaces 13
        3.1.2. Scarps 15
        3.1.3. Quaternary activity on the Phil Pico Mountains scarps 21
        3.1.4. Tectonic significance of the Phil Pico Mountain scarps 21
    3.2. Sparks Fault 25
    3.3. Uinta Fault 28
    3.4. Faults Between Bear Mountain and Browns Park 28
        3.4.1. Dutch John fault 28
        3.4.2. Mountain Home fault 29
        3.4.3. Beaver Creek fault 31
4. Evaluation of Possible Quaternary Faults Along or Adjacent to the South Flank of the Uinta Mountains 33
    4.1. Diamond Gulch Fault 33
        4.1.1. Surficial expression of the Diamond Gulch fault 33
        4.1.2. Quaternary activity on the Diamond Gulch fault 37
    4.2. Pot Creek Fault 38
        4.2.1. Surficial expression of the Pot Creek fault 40
        4.2.2. Quaternary activity on the Pot Creek fault 41
    4.3. South Flank or Marsh Peak Fault 42
        4.3.1. Surficial expression of the eastern South Flank fault 42
        4.3.2. Quaternary activity on the eastern South Flank fault 44
5. Seismicity 45
    5.1. Earthquake Recurrence 47
6. Evaluation of Faults As Potential Seismic Sources 54
7. Probabilistic Seismic Hazard Analysis 58
    7.1. Methodology 58
    7.2. Results 60
        7.2.1. Peak Horizontal Acceleration (PHA) Hazard Curves 60
        7.2.2. Spectrum Intensities 61
        7.2.3. Uniform Hazard Spectra 62
8. Acceleration Time Histories 64
9. References 75

Figures

Figure Page
1. Location map showing Flaming Gorge Dam, physiographic features, and selected faults 2
2. Faults on the north flank of the eastern Uinta Mountains between Bear Mountain and Browns Park 6
3. Aerial photograph showing the surficial expression of the scarps along the north flank of Phil Pico Mountain 10
4. Map of scarps and lineaments along the north flank of Phil Pico Mountain 11
5. Topographic profile across the south graben on the north flank of Phil Pico Mountain 17
6. Comparison of scarp height and scarp-slope angle at Phil Pico Mountain with regression lines derived for these parameters for fault scarps in western Utah 20
7. Aerial photographs showing the possible surficial expression of the Sparks fault along the south flanks of Diamond Peak and Middle Mountain 26
8. Aerial photographs showing the surficial expression of the Mountain Home fault 30
9. Aerial photographs showing the surficial expression of the Diamond Gulch fault 34
10. Aerial photographs showing the best surficial expression of the Pot Creek fault 39
11. Map of the eastern South Flank or Marsh Peak fault between the Whiterocks River and Ashley Creek 43
12. Location of Flaming Gorge Dam in relation to tectonic provinces 45
13. Seismicity of magnitude 2 and greater in study area 46
14. Number of earthquakes in three different magnitude ranges over time 49
15a. Time versus latitude plot of independent events of magnitude ≥3 within Flaming Gorge study area 50
15b. Time versus longitude plot of independent events of magnitude ≥3 within Flaming Gorge study area 50
16. Earthquakes used in recurrence calculation, Flaming Gorge study area 51
17. Incremental recurrence curve for the Flaming Gorge Dam study area 52
18. Cumulative recurrence curve for the Flaming Gorge Dam study area 52
19. Depth histogram of earthquakes in the area of Ridgway seismic network 59
20. Schematic probability density functions of focal depths for the magnitude ranges used in the probabilistic analysis 59
21. Median PHA hazard curves for Flaming Gorge Dam, calculated with the attenuation curves of Sadigh and others (1997) and Spudich and others (1996) 60
22. PHA hazard curves for Flaming Gorge Dam 61
23. PHA hazard surface with contours indicating 5,000-, 10,000-, 20,000-, 35,000-, and 50,000-year return periods 62
24. 5% damped acceleration response spectra for 10,000- and 50,000-year return periods, Flaming Gorge Dam 63
25. Median UHS for return periods of 50,000 and 10,00 years, Flaming Gorge Dam 63

Figures (Cont.)

Figure Page

26. Comparison between median 50,000-year UHS (target) and two horizontal components (LVD000 and LVD090) of records from the May 27, 1980, 14:51 UTC Mammoth Lakes earthquake, M_W 6.0, recorded at the Long Valley Dam station 65
27. Comparison between median 50,000-year UHS (target) and the average of the two empirical horizontal spectra shown in Figure 26 66
28a. 000-component of the Long Valley Dam record of the Mammoth Lakes earthquake of May 27, 1980, 14:51 UTC, M_W 6.0 67
28b. 090-component of the same record as in Figure 28a 67
28c. Vertical component of the same record as in Figure 28a 68
29. Comparison between median 10,000-year UHS (target) and the two horizontal components (CCAS000 and CCAS270) of records from the October 1, 1987, 14:42 UTC Whittier Narrows earthquake, M_W 6.0, recorded at the Compton-Castlegate Street station 69
30. Comparison between median 10,000-year UHS (target) and the average of the two empirical horizontal spectra shown in Figure 29 70
31a. 000-component of the Compton-Castlegate Street record of the Whittier Narrows earthquake of October 1, 1987, 14:42 UTC, M_W 6.0 71
31b. 270-component of the same record as in Figure 31a 71
31c. Vertical component of the same record as in Figure 31a 72
32. Comparison of UHS for 50,000 years to average spectrum of suggested horizontal records of the Mammoth Lakes earthquake of May 27, 1980 73
33. Comparison of UHS for 10,000 years to average spectrum of suggested horizontal records of the Whittier Narrows earthquake of October 1, 1987 74

Tables

Table Page
1. Characteristics of surfaces along the north flank of Phil Pico Mountain....14
2. Characteristics of the two scarps bounding the south graben along the north flank of Phil Pico Mountain....18
3. Relationship between alluvial surfaces and possible fault-related features along the north flank of Phil Pico Mountain....19
4. Properties of fault scarps at Phil Pico Mountain, Towanta Flat, and Elizabeth Ridge....24
5. Characteristics of scarps along the Diamond Gulch and Pot Creek faults....36
6. Completeness periods and event counts used in recurrence calculation....48
7. Recurrence parameters....51
8. Observed and predicted return periods, with upper and lower bounds at 95% confidence for Flaming Gorge Dam....53
9. Characteristics of the faults examined for evidence of Quaternary activity in the area surrounding Flaming Gorge Dam....55
10. PHA and spectrum intensities....61
11. Suggested ground motion characteristics....72

Abbreviations and symbols used in report

Abbreviation	Meaning
ASI	Acceleration Spectrum Intensity
CCAS	Compton, Castlegate Street
cm	centimeters
comp	component
ft	foot, feet
g	acceleration of gravity
hor	horizontal
in	inches
ka	kilo-annum (10^3 yr); years before present
km	kilometers
kyr	thousands of years; interval of time
LVD	Long Valley Dam
Ma	Mega-annum (10^6 yr); years before present
m	meters
mm	millimeters
mi	miles
PHA	peak horizontal acceleration
PSHA	probabilistic seismic hazard analysis
sec	seconds
UHS	Uniform Hazard Spectrum (Spectral)
UTC	Universal Time (Greenwich Mean Time or World Time)
VSI	Velocity Spectrum Intensity
yr	years
~	about
o	degrees
>	greater than
≥	greater than or equal to
<	less than
≤	less than or equal to
%	percent
±	plus or minus

1. Introduction

Flaming Gorge Dam is located in Red Canyon on the Green River in the northeastern corner of Utah (Figure 1). It is on the north flank of the eastern Uinta Mountains, an east-trending range of the middle Rocky Mountains. The Uinta Mountains lie between the Colorado Plateau to the south and the Wyoming Basin to the north. The Basin and Range Province is to the west of the Uinta Mountains in central Utah.

In the Safety of Existing Dams (SEED) report, Peterson (1989, his Table 1) identified four faults with reported Quaternary rupture as potential seismic sources for Flaming Gorge Dam: the Diamond Gulch fault, which is 26 km (16 mi) south of Flaming Gorge Dam; the Pot Creek fault, which is 26 km (16 mi) southeast of the dam; the Marsh Peak fault (or the eastern South Flank fault), which is 35 km (21 mi) southwest of the dam; and the Sparks fault, which is 35 km (21 mi) east of the dam (Figure 1). He assigned preliminary maximum credible earthquakes between 6-1/2 (M_L) and 7 (M_S) to these faults primarily on the basis of their potential rupture length. However, evidence for Quaternary rupture on these faults is from regional, reconnaissance-level studies and has not been verified by detailed fault assessments. Peterson (1989) recommended a more detailed study or studies of these and other nearby faults (e.g., the Dutch John and Uinta faults).

The purpose of the present study was to examine the potential seismic sources identified by Peterson (1989) for evidence of Quaternary surface rupture and to determine, if possible, the ages and number of Quaternary ruptures. Additional faults for which evidence for Quaternary surface rupture has been reported in published literature also were included in our assessment.

The area surrounding the dam has experienced a complex late Cenozoic (since about 65 Ma) tectonic history (discussed in Chapter 2), and faults along and near both the north and south flanks of the eastern Uinta Mountains have markedly displaced, deformed, and tilted an erosion surface (the Gilbert Peak erosion surface) that was nearly flat about 25 Ma. Although most of the tectonic activity ceased by about 10 Ma, several faults along or adjacent to the flanks of the eastern Uinta Mountains have deformed a widespread sandstone (Browns Park Formation) that dates from this time. Limited Quaternary surface displacement has been reported for a few faults (e.g., one north of Phil Pico Mountain and the Sparks fault along the north flank of the Uinta Mountains, and the Diamond Gulch and Pot Creek faults along the south flank of the mountains). However, the evidence for these displacements is poorly documented and has not been examined in any detail. Consequently, several faults reported to deform either possible Quaternary ($\leq$1.6 Ma) features or the youngest beds of the Browns Park Formation (~10 Ma) were considered during this study. We focused on those faults that have reported evidence for Quaternary surface rupture, those that are closest to Flaming Gorge Dam, or those that are related to faults that extend close to the dam.

On the basis of examination of aerial photographs and limited field inspection that were conducted as part of this study, we conclude that, although a few faults in the region within about 50 km of the dam have features suggestive of Quaternary surface rupture, none has evidence for recurrent, large, latest Quaternary (since about 15 ka to 20 ka) ruptures (Chapters 3 and 4). Thus, none of the faults are considered to be potential seismic sources for Flaming Gorge Dam (Chapter 6).

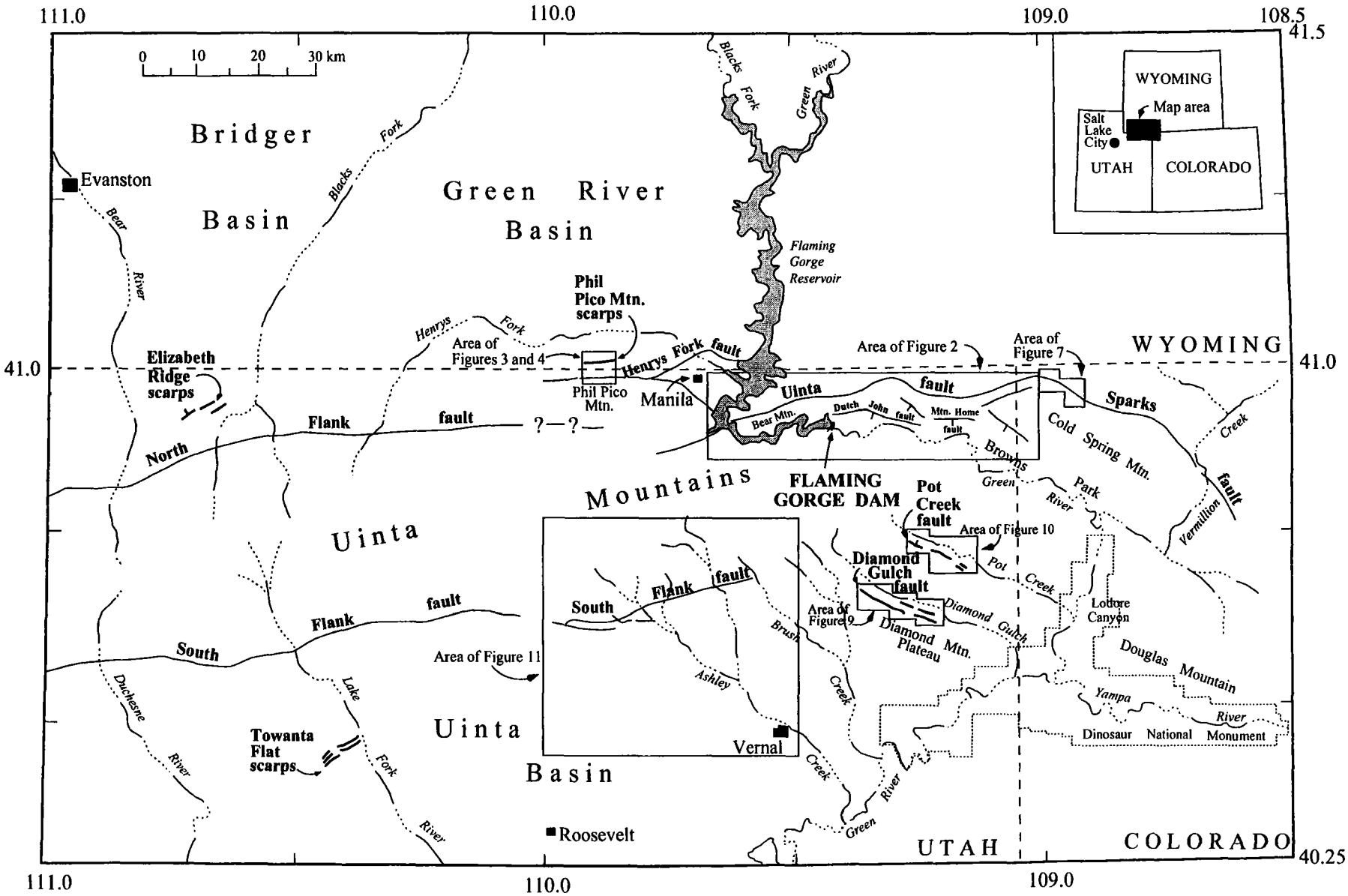

Figure 1. Location map showing Flaming Gorge Dam, physiographic features, and selected faults. Modified from Hansen (1986, his Figures 2 and 25).

Seismicity was also examined as part of our study. In the region around Flaming Gorge Dam, including northeast Utah, southwest Wyoming, and northwest Colorado, earthquakes have been recorded since about 1870. However, seismograph coverage has been limited and heterogeneous over time. Since about 1960 seismograph stations have been concentrated along the western boundary, and since 1985 also along the southern boundary of the area. Consequently, the detection threshold has been markedly variable within the region. Recorded earthquakes are primarily of magnitude 4.0 and smaller, but eight events $\geq$4.5 have been reported. The largest of these was a magnitude (M_W) 5.5 event that occurred on October 11, 1960, near Montrose, Colorado (Chapter 5). The correlation between seismicity and tectonic provinces is very weak. Therefore, the seismicity of the whole study area was treated as one homogeneous areal seismic source. Because none of the faults in the region are considered to be potential seismic sources, the greatest hazard for Flaming Gorge Dam is generated by the random seismicity in the region (Chapters 7 and 8).

1.1. Acknowledgments

We thank Lynn and Ralph Siddoway of the Siddoway Sheep Company of Vernal, Utah, for allowing access to their land in the Diamond Gulch area and Larry Anderson of the Geophysics, Paleohydrology, and Seismotectonics Group for input into the geologic field studies.

2. Late Cenozoic Geologic and Tectonic Setting

The late Cenozoic geologic and tectonic history of the eastern Uinta Mountains is complex and has been controlled, at least in part, by older tectonic features. The geologic history of the region is discussed in detail in Hansen (1965, 1969, 1984, 1986). It is summarized from these sources in the following paragraphs.

The Uinta Mountains are a 260-km-long (156-mi-long), east-trending range that is a compound anticline whose axis extends from the Wasatch Range in central Utah on the west to western Colorado on the east (Tweto, 1976, 1979; Hansen, 1984, p. 5). The eastern end of the anticline merges with smaller folds of the White River Plateau (Tweto, 1976, 1979; Hansen, 1984, p. 5). The main anticline is composed of two elongate domes separated along a north-south line located approximately between Vernal and Manila, Utah (Figure 1; Hansen, 1984, p. 6). The geologic and tectonic history of the two domes is similar during the initial stages of Laramide uplift, although the east dome rose higher and is more deeply dissected than the west dome. During the late Oligocene, the processes operating on the two domes began to differ. The east dome began to tilt and subside (Hansen, 1986, p. 6). Thus, the eastern portion of the Uinta Mountains presently is 1,200 to 1,500 m (3,960 to 4,950 ft) lower than the western part of the range (Hansen, 1984, p. 6). Flaming Gorge Dam and most of the geologic structures examined (except for the Phil Pico Mountain scarps and the eastern South Flank fault) are within or adjacent to the eastern Uinta Mountains.

The Uinta Mountains are bounded on the north by four curving but roughly east-striking faults that overlap (Figure 1). These faults from west to east are the North Flank fault, between Salt Lake City and west of Manila, Utah; the Henrys Fork fault, near Manila; the Uinta fault, between Manila and the Utah-Colorado border; and the Sparks fault, between the Utah-Colorado border and southeast of Vermillion Creek. The Henrys Fork fault, which is shorter than the other faults, may be structurally related to either the North Flank fault or the Uinta fault, or both (Anderman, 1955, p. 131; Hansen, 1986, p. 39). The south flank of the western Uinta Mountains is bounded by the South Flank fault. The south flank of the eastern Uinta Mountains is complicated by southeast-trending folds, which causes the eastern part of the range to be wider and its flank to be less defined than the south flank of the western Uinta Mountains.

Beginning during the late Cretaceous (~65 Ma), uplift of the eastern Uinta Mountains began by north-south-directed compressional forces as part of the Laramide orogeny, which continued into the early to middle Oligocene (~30 Ma; Hansen, 1986, his Figure 26, p. 42). The faults bounding the north and south flanks were thrust or reverse faults at that time (Hansen, 1984, p. 9).

This period of uplift was followed by a long period of tectonic quiescence during which a broad erosion surface (pediment), which sloped gently away from the high peaks, was cut on older rocks on the flanks of the eastern Uinta Mountains (Hansen, 1986, p. 39, his Table 2). This surface has been named the Gilbert Peak erosion surface. The chiefly gravelly alluvium that was deposited on it beginning about 30 Ma, primarily as large alluvial fans, is called the Bishop Conglomerate (Hansen, 1984, p. 6, his Table 2; Hansen, 1986, p. 39-41, his Table 2). The widespread nature of both the Gilbert Peak erosion surface and overlying Bishop Conglomerate, the nearly level original topography of the plain-like erosion surface, and the nearly horizontal original inclination

of the conglomerate deposited on the surface make these units excellent markers with which to evaluate the extent and magnitude of later episodes of tectonic deformation.

Remnants of the Gilbert Peak erosion surface and overlying Bishop Conglomerate form many of the high plateaus or mesas that surround the Uinta Mountains (e.g., Diamond Mountain Plateau; Hansen, 1986, his Figure 5, p. 7). Many of these remnants are between 300 and 600 m (990 to 1,980 ft) above presently active drainages (Hansen, 1986, p. 35). Gravel-free remnants of the surface near Flaming Gorge Dam include Dutch John Bench, Bear Mountain, and Goslin Mountain (Figure 2; Hansen, 1986, p. 12). Other examples in the eastern Uinta Mountains are Mountain Home (in part), Bender Mountain (in part), O-Wi-Yu-Kuts Mountain, and Cold Spring Mountain (Figure 2; Hansen, 1986, p. 35).

The Bishop Conglomerate is composed of a loosely cemented, bouldery, cobbly conglomerate and coarse, poorly sorted, pebbly, friable sandstone. The clasts are subangular to subrounded, although some are well rounded. The most abundant clast lithology is red quartzite or sandstone eroded from the Precambrian Uinta Mountain Group; however, in some places gray Paleozoic limestone dominates clast composition (Hansen, 1986, p. 21). The cementation of the Bishop Conglomerate is variable. Where the calcareous cement is strong, the conglomerate forms cliffs. Where the Bishop Conglomerate is present, it has probably helped to preserve the underlying Gilbert Peak erosion surface (Hansen, 1986, p. 8).

The wide aerial extent and uniform character of the Gilbert Peak erosion surface suggest that a long period existed in the eastern Uinta Mountains during the late Oligocene when climate and tectonics were stable (Hansen, 1986, p. 11). However, this was followed by renewed deformation during the Miocene (~25 Ma), which caused a reversal in the sense of displacement on the faults bounding the mountains (Hansen, 1986, p. 41). North-south-directed extension resulted in normal displacement on the former thrust or reverse faults along the flanks. Additional faults just south of the Uinta fault between Bear Mountain and Browns Park formed in response to extension during this second major period of deformation (Figure 2; Hansen, 1986, his Figure 27). These faults have various orientations, short lengths, and normal displacement. Both Laramide compression and the later extension were greater and more complex along the north flank of the eastern Uinta Mountains than they were along the south flank (Hansen, 1986, p. 41).

Regional warping and extensional fault displacements during the Miocene lowered the crest of the eastern Uinta Mountains and warped the Gilbert Peak erosion surface and the overlying Bishop Conglomerate (Hansen, 1984, p. 6; Hansen, 1986, p. 41). Subsidence along the Uinta fault and other faults just south of it along the north flank of the eastern Uinta Mountains tilted the Gilbert Peak erosion surface southward; whereas subsidence on faults bounding the south flank of the eastern Uinta Mountains tilted the Gilbert Peak erosion surface and related Bishop Conglomerate northward (Hansen, 1986, p. 45). Maximum down-to-the-south subsidence of the Gilbert Peak erosion surface occurred on the north flank along the south side of Goslin Mountain between Bear Mountain and Browns Park at Little Hole (Figure 2; Hansen, 1986, p. 44-45). Between Bear Mountain, or possibly Phil Pico Mountain, on the west and Cold Spring Mountain on the east, the Gilbert Peak erosion surface was tilted southward a maximum of about 120 m/km (673 ft/mi; about 7°) at Goslin Mountain (Hansen, 1986, p. 41). The surface also was tilted westward along this zone by differential displacements on the Uinta and the Dutch John faults (Hansen, 1965, p. 163; 1986, p. 44).

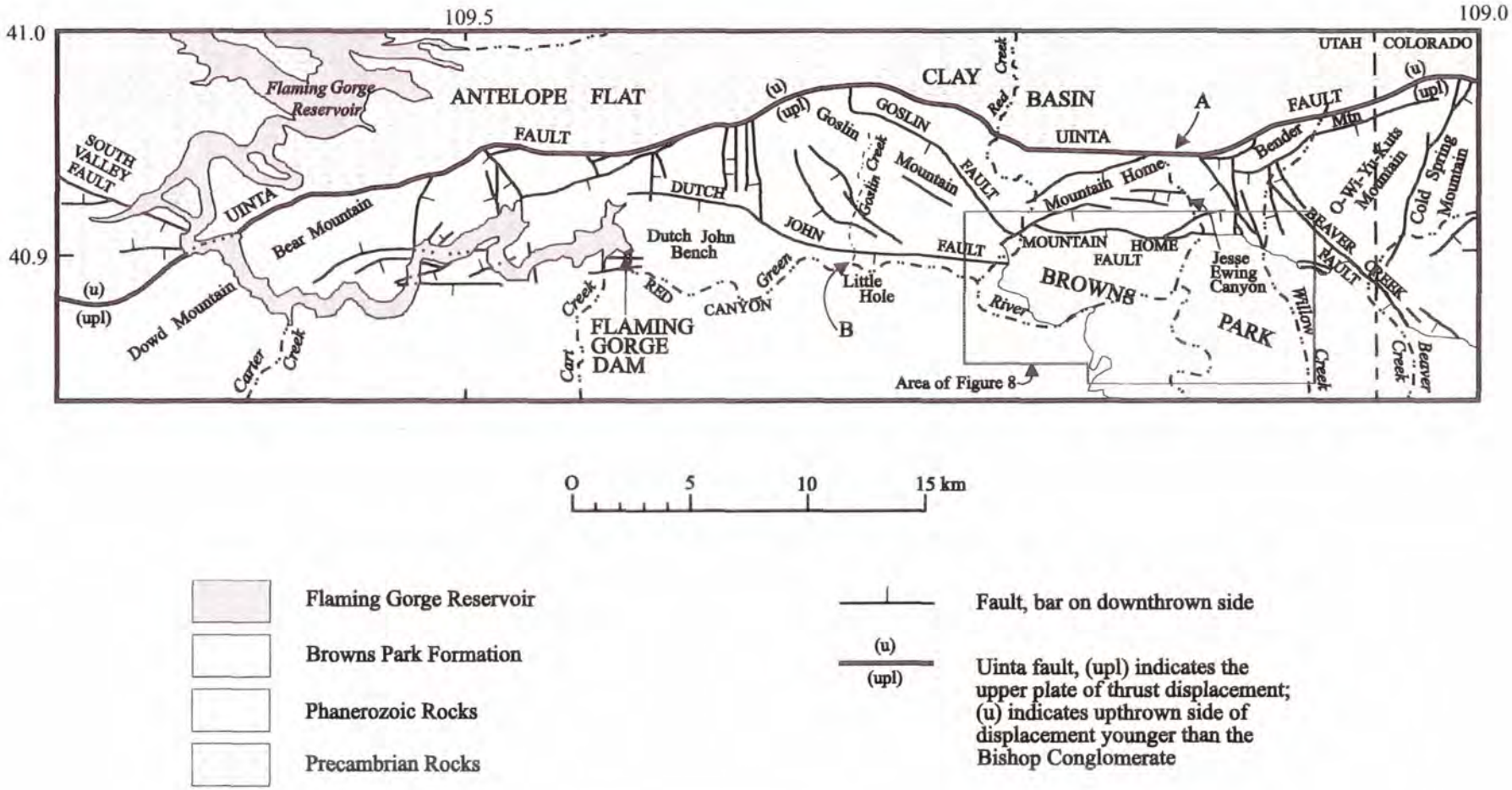

Figure 2. Faults along the north flank of the eastern Uinta Mountains between Bear Mountain and Browns Park. Modified from Hansen (1969, his Figure 27, p. 43). Location is shown on Figure 1.

Minimum northward tilt of about 28 m/km (156 ft/mi; 1.6^{o}) along the south flank occurs near Stuntz Ridge (about 5 km (3 mi) south of Dinosaur National Monument at the boundary between Colorado and Utah; Hansen, 1986, p. 45). In addition to their northward tilt, the Gilbert Peak erosion surface and Bishop Conglomerate also tilt eastward along the south flank (Hansen, 1986, p. 47). The elevation difference between the Uinta River on the west (3,050 m; 10,065 ft) and Diamond Gulch on the east (2,125 m; 7,013 ft) is about 900 m (2,970 ft) (Hansen, 1986, p. 47). The Gilbert Peak erosion surface is also displaced along the north-northeast-striking Island Park fault and the northwest-striking Diamond Gulch fault, both of which are just west of the Green River southwest of Lodore Canyon (Figure 1; Hansen, 1986, p. 48).

Collapse and rotation that tilted the Gilbert Peak erosion surface in the eastern Uinta Mountains also rearranged the established drainage patterns in the region (Hansen, 1986, p. 16, 30-31, 41, 44). This included transforming many north-flowing drainages on the north flank into south-flowing drainages (Hansen, 1986, p. 30-31). Many south-flowing drainages on the south flank were changed into north-flowing drainages, some of which now drain into Browns Park (Hansen, 1986, p. 45). The continued uplift resulted in erosion and dissection of the Gilbert Peak erosion surface as the present canyons of the Green and Yampa Rivers were cut (Hansen, 1986, p. 8).

After most of the deformation ceased during the Miocene, another widespread sedimentary unit was deposited in and adjacent to the eastern Uinta Mountains. The Browns Park Formation, like the Bishop Conglomerate, has been used to assess tectonic relationships in the region because of its relatively uniform characteristics and widespread nature. The Browns Park Formation is light-colored to nearly white, loosely cemented, calcareous sandstone and light-gray to white, vitric and ashy to earthy, friable to firm, rhyolitic tuff (Hansen, 1986, p. 28). Much of the sandstone, where it is intensely cross stratified, is eolian (Hansen, 1986, p. 28). Some of the sandstone, especially near its western extent, may be fluvial (Hansen, 1986, p. 28). The formation was deposited between about 25 Ma and 10 Ma (Hansen, 1986, p. 31). Unlike the Bishop Conglomerate, which was deposited on a widespread erosion surface, the Browns Park Formation fills valleys, buries hills, and locally covers broad areas (Hansen, 1986, p. 37). It is best preserved in Browns Park, a valley northeast of the eastern Uinta Mountains (Figure 2).

Most of the deformation in the area appears to have preceded the deposition of the Browns Park Formation (Hansen, 1986, p. 41), and thus, must be older than about 10 Ma, and perhaps older than about 25 Ma. However, faults along the northeast side of Browns Park displace and are overlapped by the formation (Hansen, 1986, p. 50-51). These relationships suggest that extensional displacements continued as the Browns Park Formation was being deposited and were part of a continuum of alternating periods of displacement and quiescence that began during Miocene and continued into the Pliocene (~5 Ma-1.6 Ma). Deformation of the Browns Park Formation above the Uinta-Sparks fault north of Cold Spring Mountain shows renewed or continued displacement related to collapse of the crest of the eastern Uinta Mountains (Hansen, 1986, p. 51). Similarly, south-side-down displacements on several faults in the zone between Bear Mountain and Browns Park (e.g., the Mountain Home and Beaver Creek faults, Figure 2) have sharply tilted the Browns Park Formation (Hansen, 1986, p. 51). Deformation of the Browns Park Formation along the south flank has been suggested at the southeast end of the range southeast of Douglas Mountain (Figure 1).

Quaternary displacements have been reported for a few faults in the region, but the evidence is sketchy and not well documented. This is in large part because Quaternary deposits in the area are discontinuous and difficult to date and correlate. Hansen (1969, p. 122-123) interpreted episodic Quaternary uplift for the region from evidence for variable incision rates along large drainages, such as the Green River in Lodore Canyon. He concluded that "... gentle but considerable Quaternary uplift" has occurred intermittently and on a regional scale (Hansen and Bonilla, 1954, p. 27). Evidence for latest Quaternary (since about 15 ka to 20 ka) surface ruptures has not been reported for any faults in or adjacent to the eastern Uinta Mountains.

3. Evaluation of Possible Quaternary Faults Along or Adjacent to the North Flank of the Uinta Mountains

Several faults along or adjacent to the north flank of the Uinta Mountains have been reported to exhibit evidence for deformation of Quaternary (≤1.6 Ma) surfaces or Browns Park Formation 25 Ma to 10 Ma). Fault scarps reported along the north flank of Phil Pico Mountain, which is about 40 km (24 mi) northwest of Flaming Gorge Dam, and evidence for possible Quaternary rupture along the Sparks fault, about 35 km (21 mi) east of the dam, were examined (Figure 1).

Displacement of the Browns Park Formation and surficial expression also have been noted for some of the faults that are south of the Uinta fault between Bear Mountain and Browns Park (Figure 2). The closest of these is the Mountain Home fault, which is about 15 km (9 mi) east of the dam. The Dutch John fault, which is about 2 km (1.2 mi) north of Flaming Gorge Dam, is also part of this zone of faults. Although neither displacement of the Browns Park Formation nor surficial expression has been reported for the Dutch John fault, it does displace the Gilbert Peak erosion surface. Because of its association with a zone of faults for which displacement of the Browns Park Formation or Quaternary surfaces has been reported and because of its proximity to the dam, the Dutch John fault also was examined briefly.

3.1. Scarps Along the North Flank of Phil Pico Mountain

Two east- or northeast-trending graben are present along the north flank of Phil Pico Mountain near the Utah-Wyoming border. The graben are each about 1 km (0.6 mi) long and about 150 m (495 ft) wide. They are on a surface that may be older than about 130 ka to 150 ka and younger than about 500 ka. Lineaments on an adjacent surface that may be about 130 ka to 150 ka align with the graben. An inflection on a surface that is likely older than 250 ka to 500 ka is present about 3 km (1.8 mi) east of the graben and could have a tectonic origin. The entire length over which these features extend is about 4 km (2.5 mi).

Hansen (1969, p. 123) cited Max Crittenden, Jr. as noting fault scarps on an alluvial fan on the north flank of Phil Pico Mountain (Figure 1). Phil Pico Mountain is composed of conglomerate of the Green River Formation (Anderman, 1955, p. 131). Clasts in the conglomerate were derived from the Uinta Mountains immediately to the south of Phil Pico Mountain (Anderman, 1955, p. 132). Hansen (1969, p. 123) indicated that although the age of these scarps is uncertain he speculated that they were probably no younger than the Bull Lake Glaciation (about 130 ka to 150 ka). West (1988, p. 61) briefly examined these scarps and judged them to have a tectonic origin. On the basis of the truncation of the scarps by a younger alluvial fan and the eroded nature of the scarps, West (1988, p. 61) concluded that the scarps are older than late Pleistocene or Holocene. The scarps on the north flank of Phil Pico Mountain were not identified in the SEED report (Peterson, 1989) and, consequently, were not assigned an MCE in the preliminary assessment of seismic hazards for Flaming Gorge Dam.

Scarps along the north flank of Phil Pico Mountain are best expressed by an east-trending, 1-km-long (0.6-mi-long), 150-m-wide (495-ft-wide) graben that displaces an alluvial surface graded to the Henrys Fork (Figures 3 and 4). A second graben about 120 m (396 ft) to the north also displaces this same surface. The north graben has a length and width similar to those of the

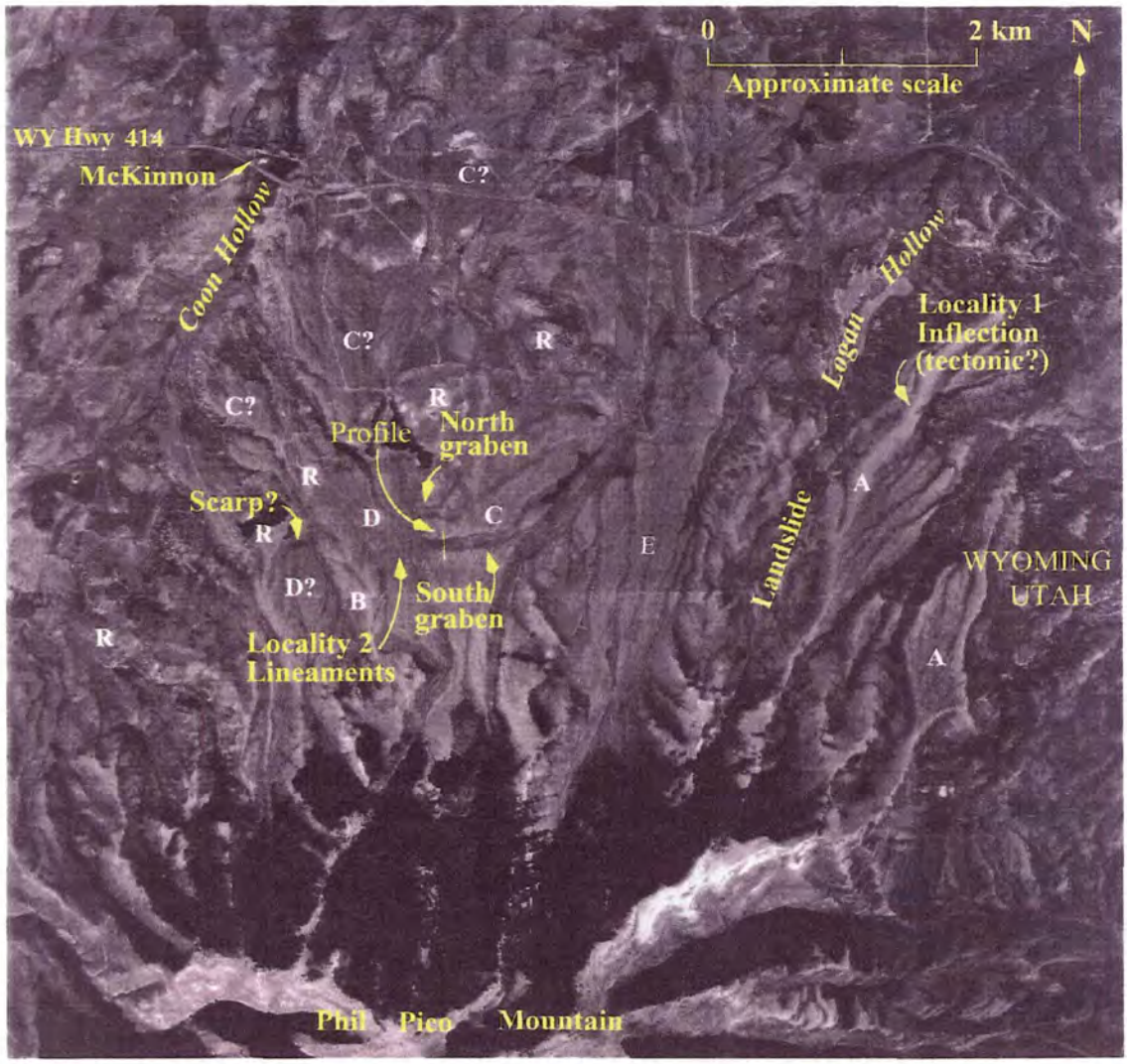

Figure 3. Aerial photograph showing the surficial expression of the scarps along the north flank of Phil Pico Mountain. Photograph is no. 7912-120 from the NAPP project, taken 8/30/94. The original scale is 1:40,000. The localities are discussed in the text. White letters indicate surfaces of different ages as shown on Figure 4 and Table 1 and as discussed in the text. Topographic profile is shown in Figure 5. The location of this figure is shown on Figure 1.

Figure 4. Map of scarps and lineaments along the north flank of Phil Pico Mountain (Figure 1). Geology was mapped on 1:40,000-scale, black-and-white aerial photograph (NAPP, #7912-120, taken 8/30/94; Figure 3). Ages for the units are based on tentative correlation to dated units at Towanta Flat (Martin and others, 1985; Nelson and Weisser, 1985). Towanta Flat is about 75 km (45 mi) southwest of Phil Pico Mountain (Figure 1).

EXPLANATION

- Active wash (≤10 ka)
- Surface F (11 ka to 14 ka)
- Surface E (13 ka-14 ka to 30 ka-40 ka)
- Surface D (130 ka to 150 ka)
- Surface C (>130 ka to 150 ka and ≤500 ka)
- Surface B (250 ka-500 ka to early Quaternary)
- Surface A (250 ka-500 ka to early Quaternary)
- Surface, undifferiated
- Landslide
- Bedrock, primarily Wasatch Formation (Anderman, 1955)
- Probable tectonic scarp; bar on lower side
- Probable tectonic lineament on Quaternary surface
- Inflection in Surface A; possibly tectonic
- Lineament in rock; possibly tectonic
- Scarp on landslide deposit
- Drainage
- Ridge
- Pond
- Scarp profile (Figure 5)

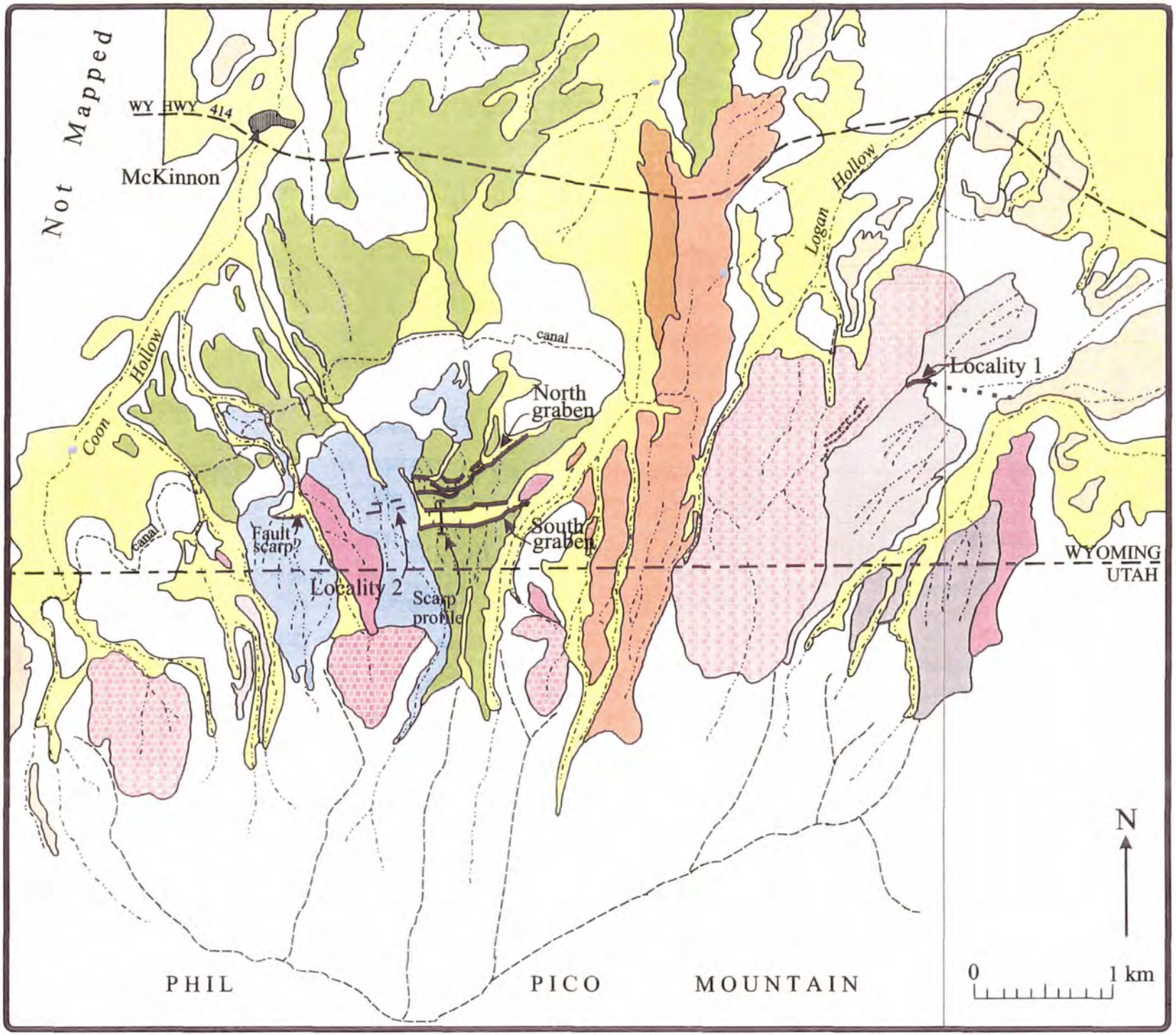
Not Mapped
WY HWY 414
McKinnon
Coon Hollow
canal
canal
Logan Hollow
Locality 1
North graben
South graben
Fault scarp?
Locality 2
Scarp profile
WYOMING
UTAH
41.0
N
0
1 km
PHIL
PICO
MOUNTAIN
109.9

south graben. The east half of the north graben trends northeast and has been enhanced by erosion along a small drainage. Lineaments that roughly align with the north scarp of the south graben extend about 300 m (990 ft) across a younger alluvial surface (Locality 2, Figures 3 and 4). No displacement could be discerned across the lineaments, but bar-and-swale topography could mask up to about 1 m (3 ft) of surface displacement. The scarps that bound the south graben cannot be traced across an active wash and landslide complex to the east. However, an inflection in a markedly older surface (Surface A) about 3 km (1.8 mi) east of the graben aligns with the projection of the graben-bounding scarps and could have a tectonic origin (Locality 1, Figures 3 and 4). The length of the surficial expression, then, could be as much as 4.2 km (2.5 mi). East of Surface A, drainages trend eastward and align with the trend of the graben, so that surficial expression is difficult to trace east of Surface A (Figure 4). A 0.6-km-long (0.4-mi-long) lineament in rock east of the inflection in Surface A (Figure 4) could have a tectonic origin. No evidence for lateral surface displacement was observed.

The alluvial surfaces, scarps, and lineaments along the north flank of Phil Pico Mountains were examined on aerial photographs (NAPP 5863-53 and 54, 5863-75 and 76, 5867-15 and 16, 7912-46 and 47, 7912-119 and 120, 7920-40 and 41; black and white; taken 8/30/94; scale 1:40,000) and briefly on the ground to assess the characteristics and history of Quaternary surface rupture. Ages of the alluvial surfaces were roughly estimated using surface characteristics (Bull, 1991) that are visible on the aerial photographs, primarily, or on the ground. A rough estimate of possible soil properties was also made. These characteristics were then used to tentatively correlate the surfaces on the north flank of Phil Pico Mountain with surfaces described by Martin and others (1985) on the south flank of the Uinta Mountains at Towanta Flat, about 75 km (45 mi) southwest of Phil Pico Mountain (Figure 1). This area is the closest to Phil Pico Mountain where alluvial surfaces have been described and dated in a geologic, tectonic, and topographic setting similar to that along north Phil Pico Mountain. An estimate for the age of most-recent surface rupture along Phil Pico Mountain is bracketed by the ages estimated for the displaced surfaces and for the oldest adjacent undisplaced surface.

In addition, a topographic profile was measured across the south graben, including both the north- and south-bounding scarps. The profile was used to estimate scarp heights, vertical surface displacements, maximum scarp-slope angles, surface slopes above and below each scarp, and net tectonic displacement. These parameters were determined as indicated by Bucknam and Anderson (1979, their Figure 3) or by Machette (1982, his Figure 4). The estimates from the topographic profile were supplemented with scarp heights and maximum scarp-slope angles that were measured in the field at three additional localities. The combined data were used to estimate the ages of the scarps.

3.1.1. Alluvial geomorphic surfaces

Displaced and undisplaced alluvial surfaces that are graded northward toward the Henrys Fork are used to determined the Quaternary surface-rupture history on the scarps along the north flank of Phil Pico Mountain. Alluvial units of at least five, and perhaps six, different ages are preserved along the north flank. The units are defined on the basis of differences in degree of preservation, surface topography, degree of dissection, development of pavement, and possible soil development (Figures 3 and 4, Table 1; Bull, 1991). Although soils were not examined in any detail, the presence or absence of carbonate-coated clasts on the surfaces was noted. The

Table 1. Characteristics of surfaces along the north flank of Phil Pico Mountain

Surface	Appearance on aerial photographs	Preservation	Surface topography	Dissection	Pavement	Possible development of soil carbonate[1]	Possible correlation to Towanta Flat stratigraphy[2]	Estimated age range (correlative glaciation)[2]
A	Mostly light gray; dark along drainages	Thin ridges that extend to the range front; bedrock visible beneath the gravel cap	Ridge-and-ravine	Dissected by large drainages and by small drainages that head on the surface	Contains clasts with thick carbonate rinds; clasts primarily limestone and sandstone	Stage III or better	RAG1, RAG2, or RAG3	Early Quaternary to 250 ka - 500 ka (pre-Bull Lake)
B	Mostly light gray; dark along drainages	A few isolated remnants	Incipient ridge-and-ravine	Dissected by large drainages and by small drainages that head on the surface	--	--		
C	Mottled light and dark gray	Incised into the range front; no bedrock is visible beneath the gravel	Smooth	Dissected by large drainages and by small drainages that head on the surface	Moderately packed; contains clasts with thick carbonate rinds that are laminar near the clasts, but also includes clasts that lack rinds	Stage III or better	RAG4	≤500 ka and >130 ka to 150 ka (pre-Bull Lake)
D	Mottled light and dark gray	Incised into the range front; no bedrock is visible beneath the gravel	Bar and swale with 0.5 m of relief	Dissected by channels about 1 m deep that head on the surface	Moderately to poorly packed; primarily limestone clasts; sand visible	No evidence of strong carbonate	RAG5-6	130 ka to 150 ka (Bull Lake)
E	Medium gray	Incised into the range front; no bedrock is visible beneath the gravel	Bar and swale	--	--	No evidence of strong carbonate	RAG 7-8	30 ka - 40 ka to 13 ka - 14 ka (Pinedale)
F	Medium gray	No bedrock is visible beneath the gravel	Bar and swale	--	--	--	RAG9	11 ka - 14 ka (late Pinedale)

[1]For a description of carbonate terminology, see Birkeland (1984).

[2]Stratigraphic designations and estimated ages are from Martin and others (1985). Possible carbonate development at Phil Pico Mountain was compared to that described by Martin and others (1985) on outwash terraces.

presence of such clasts on the slopes of a surface suggests that relatively strong carbonate is in the soil associated with the surface. It is possible that the preservation of the scarps is related to the strength of carbonate development (likely stage III or more on the surface with the graben; Surface C). Vegetation is low sagebrush and grasses.

The alluvial surfaces on the north flank of Phil Pico Mountain are tentatively correlated with alluvial surfaces at Towanta Flat that were studied by Martin and others (1985). Some of the surfaces at Towanta Flat were dated using paleomagnetic and amino-acid analyses (Martin and others, 1985). On the basis of its preservation in isolated remnants or as narrow ridges well above presently active drainages, development of ridge-and-ravine surface topography, dissection by both large and small drainages that have exposed pre-Quaternary units beneath the alluvium, and surface clasts that are thickly coated with carbonate, we tentatively correlate Surface A, and probably Surface B, with units RAG1, RAG2, or RAG3 of Martin and others (1985) (Table 1). The ages of these units range between early Quaternary for RAG1 and about 250 ka to 500 ka for RAG3.

On the basis of more continuous preservation, a slightly smoother surface topography, and a moderately packed pavement, we conclude that Surface C is younger than Surfaces A and B (Table 1). However, preservation of Surface C about 3 m (10 ft) above presently active drainages, the degree of dissection, and carbonate-coated clasts in the pavement suggest that Surface C is still quite old (Table 1). On the basis of these properties, we tentatively correlate Surface C with RAG4 at Towanta Flat. RAG4 is the youngest unit that has a strongly developed carbonate horizon in the associated soil. The age of RAG4 ranges between 130 ka to 150 ka and 500 ka (Martin and others, 1985). This is correlative to pre-Bull Lake glacial deposits in the region (Martin and others, 1985).

Similarly, the preservation of bar-and-swale topography, the dissection primarily by small drainages that head on the surface, a moderately to poorly packed pavement that lacks carbonate-coated clasts suggest that Surface D at Phil Pico Mountain is markedly younger than Surface C, but still is Pleistocene (Table 1). We tentatively correlate Surface D with RAG5-6 at Towanta Flat. The age of RAG5-6 ranges between 130 ka to 150 ka and correlates with Bull Lake glacial deposits in the region (Martin and others, 1985).

On the basis of smooth topography, no evidence for carbonate development, and incision into Surface D, we tentatively correlate Surface E with RAG7-8 at Towanta Flat (Table 1). The age of RAG7-8 ranges between 30 ka to 40 ka and 13 ka to 14 ka and correlates with Pinedale glacial deposits. Surface F, which is preserved at only one locality in the mapped area at Phil Pico Mountain, is tentatively correlated with RAG 9 at Towanta Flat. The age of RAG9 at Towanta Flat is 11 ka to 14 ka (correlative to late Pinedale glacial deposits).

Deposits in the graben (mapped as active wash, Figure 4) at Phil Pico Mountain and along active washes are young as indicated by their loose, sandy character and poorly packed pavement. The deposits are probably late Holocene.

3.1.2. Scarps

A topographic profile was measured across both the scarps that bound the south graben in order to roughly estimate the ages of the scarps and the number of surface ruptures, if possible. The profile was measured using a measuring rod adjusted to lengths of 1, 2, or 3 m (3, 6, and 10 ft) and

a Brunton compass. Slope measurements are probably accurate to $\pm 0.5^{o}$. The profile was extended well beyond the scarps to both the north and south to estimate the slope of the pre-displacement surface (Figure 5). The scarps have been modified by the erosion of gullies and general scarp degradation. The floor of the graben is filled with colluvium and alluvial-fan deposits shed from the scarps and transported laterally within the graben. The location for the profile was selected to try to minimize the effects of erosion and deposition along and adjacent to the scarps.

Scarp heights and vertical surface displacements were estimated by the differences in elevation between projections of the steepest scarp slope and the average surface slopes above and below the scarp as shown in Bucknam and Anderson (1979) (Figure 5). Maximum scarp-slope angles were measured both on the plotted topographic profile and in the field along the profile using a Brunton compass at the point where the scarps appear to be the steepest (Table 2). The measurements from the two methods are in general agreement (Table 2). Scarp heights and maximum scarp slope angles also were measured with a Brunton compass at two additional localities on the south scarp and at one additional locality on the north scarp (Table 2).

The total height for the south scarp of the south graben (10 m; 33 ft) may indicate that the scarp is compound and represents multiple surface ruptures. Terraces inset adjacent to gullies eroded into the 10-m-high (33-ft-high) south scarp could signal up to three surface-rupturing events. No evidence for multiple events was noted along the 5-m-high (17-ft-high) north scarp (Figure 5).

The total net vertical tectonic displacement across the south graben was estimated graphically from the topographic scarp profile (Figure 5) assuming that the original slope of the alluvial surface was the same as that of the present surface above the south scarp (about 6°). This slope was projected northward down the alluvial surface. The net vertical tectonic displacement across the south graben could be as much as about 1.5 m (5 ft). The south (mountainward) side is up relative to the north side. This amount would be a maximum because any decrease in the original slope of the alluvial surface in a downfan direction would decrease this value. Depending upon the original slope, the net vertical tectonic displacement across the south graben could be zero.

The graben are preserved on Surface C, and perhaps on Surface D. A possible tectonic scarp is preserved about 0.8 km (0.5 mi) west of the graben on Surface C. However, an erosional origin for this scarp seems to be more likely. The graben do not extend onto Surface E (Figures 3 and 4, Table 3). These relationships and the estimated ages of the surfaces suggest that the latest surface rupture on the graben-bounding scarps is older than at least 13 ka to 14 ka, and is probably older than 30 ka to 40 ka (before the Pinedale Glaciation). It may be older than 130 ka to 150 ka. These ages are based on a tentative correlation of the alluvial surfaces at Phil Pico Mountain with those at Towanta Flat.

Surface displacement of Surface D (130 ka to 150 ka) is not conspicuous. Discontinuous lineaments that roughly align with the north scarp of the south graben are visible on the aerial photographs (Figures 3 and 4). They appear as alignments of darker vegetation on the photographs, but could not be detected on the ground. In addition, the relief across the bar-and-swale topography on the surface of Surface D could mask scarps up to about 1 m (3 ft). Consequently, displacement of about 1 m on Surface D cannot be precluded across the lineaments, although evidence for such displacement was not observed. Because displacement of Surface D is limited to no more than about 1 m (3 ft), any additional displacement across the graben appears to have occurred before Surface D formed. Alternatively, it may be that Surface D

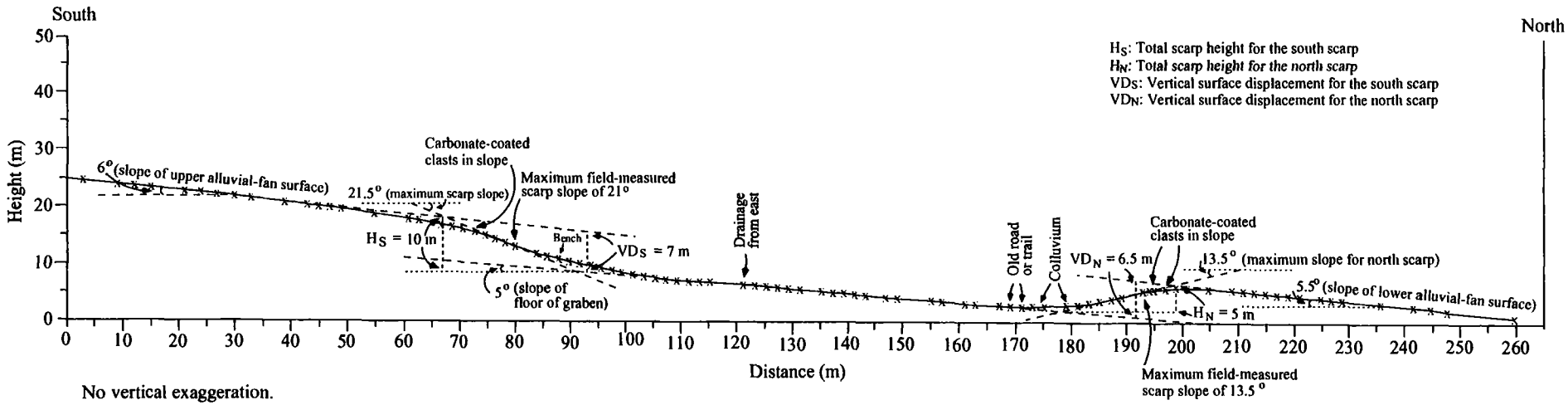

Figure 5. Topographic profile across the south graben on the north flank of Phil Pico Mountain. Location of profile is shown on Figures 3 and 4.

Table 2. Characteristics of the two scarps bounding the south graben along the north flank of Phil Pico Mountain[1]

Scarp	Total scarp height (m)	Vertical surface displacement (m)	Surface-slope angle (°)		Maximum scarp-slope angle (°)	
			Above scarp	Below scarp	Measured on the profile	Measured in the field
South (north-facing)	10	7	6 (to north)	5 (to north; graben floor)	21.5 (to north)	21 (to north)
	9.6	--	--	--	--	22
	8	--	--	--	--	15
North (south-facing)	5	6.5	5.5 (to north)	5 (to north; graben floor)	13.5 (to south)	13.5 (to south)
	4.5	--	--	--	--	11

[1]Properties were estimated graphically from the plotted topographic profile (Figure 5) as defined by Bucknam and Anderson (1979, their Figure 3) or Machette (1982, his Figure 4) or were measured directly in the field.

Table 3. Relationship between alluvial surfaces and possible fault-related features along the north flank of Phil Pico Mountain

Alluvial surface	Estimated age range	Possible fault-related feature
A	Early Quaternary to 250 ka - 500 ka	Inflection
B		?
C	≤500 ka and >130 ka - 150 ka	Scarps (graben)
D	130 ka to 150 ka	Lineaments (visible on 1:40,000-scale, black-and-white aerial photographs but could not be identified on the ground)
E	30 ka - 40 ka to 13 ka - 14 ka	None
F	11 ka to 14 ka	None
Active wash	≤10 ka	None

is not displaced. Faults buried by Surface D may be a source for water that allows the growth of thicker vegetation. Thus, the lineaments may not represent actual surface rupture since deposition of Surface D. If Surface D is not displaced, then the youngest rupture on the scarps bounding the graben occurred before 130 ka to150 ka.

An attempt was made to use the relationship between scarp height and maximum scarp-slope angle to estimate the ages of the two scarps bounding the south graben along the north flank of Phil Pico Mountain. This comparison was based on the quantitative relationship between scarp heights and maximum scarp-slope angles developed by Bucknam and Anderson (1979). Bucknam and Anderson (1979, their Figure 5) established this relationship using a series of regression lines that vary systematically with scarps of different ages in western Utah (Figure 6). Scarp heights and maximum scarp-slope angles at Phil Pico Mountain are similar to those for scarps at Panguitch, Utah (Figure 6), where the scarps formed about 100 ka. However, the large, possibly multiple-event scarps and the small number of data points at Phil Pico Mountain, along with the differences in lithology and climate between the two areas, do not allow a rigorous comparison of scarp characteristics. An age of about 100 ka for the scarps bounding the south graben at Phil Pico Mountain is in general agreement with the age estimated using alluvial-fan stratigraphy.

A comparison of the scarp heights and maximum scarp-slope angles along the south graben at Phil Pico Mountain with those for fault scarps at Towanta Flat suggests general similarities in scarp characteristics. Scarps with heights of 11 m (36 ft) at Towanta Flat have maximum scarp-

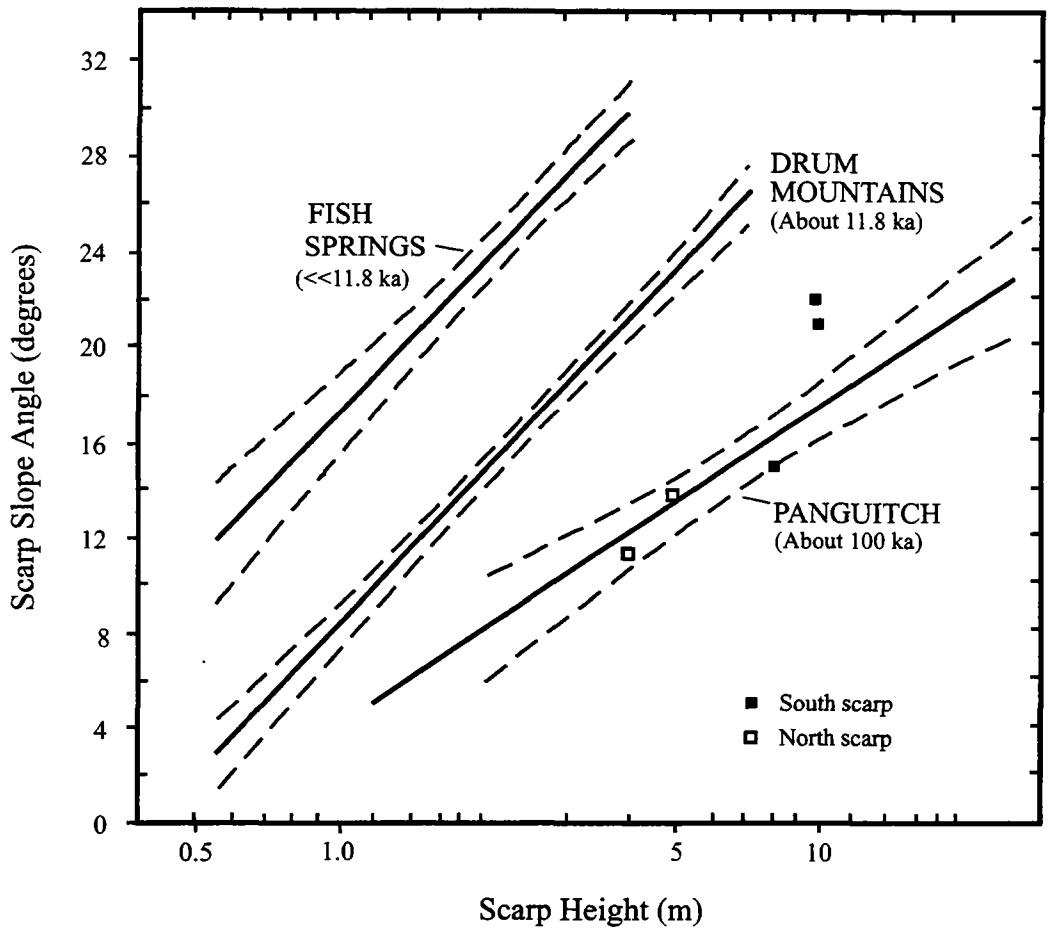

Figure 6. Comparison of scarp height and scarp-slope angle at Phil Pico Mountain with regression lines derived for these parameters for fault scarps in western Utah (Bucknam and Anderson, 1979). Dashed lines are 95 percent confidence intervals. Data are in Table 2.

1985, their Figure 4.5, p. 59). The 10-m-high (33-ft-high) scarp bounding the south graben at Phil Pico Mountain has a maximum scarp-slope angle of 21.5°, and the 5-m-high scarp has a maximum angle of 13.5° (Table 2). The scarps at Towanta Flat are on surfaces with ages between 130 ka-150 ka and 250 ka-500 ka.

3.1.3. Quaternary activity on the Phil Pico Mountain scarps

Our observations of the scarps and alluvial surfaces on the north flank of Phil Pico Mountain suggest that surface rupture probably occurred about 100 ka to 150 ka or earlier. The last surface rupture can be no younger than about 13 ka to 14 ka, the minimum age estimated for Surface E, which contains no evidence for surface displacement. This surface may be as old as 30 ka to 40 ka, so that surface rupture may pre-date this time. Weakly expressed lineaments on Surface D, which has an estimated age of 130 ka to 150 ka, and bar-and-swale topography that could mask as much as 1 m of displacement suggest that surface displacement cannot be entirely ruled out during the last about 130 ka to 150 ka, although direct evidence for such displacement was not observed. The dissection of the scarps that bound the graben on Surface C, which has an estimated age between 130 ka to 150 ka and 500 ka, the presence of small alluvial fans at the base of the scarps, and the degraded character of the bounding scarps support an age of at least 130 ka to150 ka for the last surface rupture. Most of the displacement across the graben (maximum of 1.5 m (5 ft)) likely occurred before this last event.

Using a maximum of 1 m (3 ft) of surface displacement since 130 ka to 150 ka, the maximum displacement rate since that time is 0.007 to 0.008 mm/yr. Using a maximum of 1.5 m (5 ft) of net vertical displacement across the south graben on a surface estimated to be older than 130 ka to 150 ka and younger than 500 ka, the maximum average displacement rate since 500 ka is 0.003 mm/yr. The lack of displacement on a surface that has an estimated age of at least 13 ka to 14 ka and probably 30 ka to 40 ka suggests that the displacement rate has been 0 mm/yr during the last tens of thousands of years. Because a surface that has an estimated age of 130 ka to 150 ka has only equivocal evidence for surface displacement, it is possible that the displacement rate has been negligible since that time. On the basis of these observations, the return period for surface displacements could be 100 kyr or longer.

3.1.4. Tectonic significance of the Phil Pico Mountain scarps

The limited extent of the scarps along the north flank of Phil Pico Mountain, the small amount ($\leq$1.5 m; $\leq$5 ft) of net vertical surface displacement across the graben, and the presence of rock outcrops in the area suggest that a nontectonic origin for the scarps should be considered. Although fluvial erosion or landslide movement can explain some features, neither seems to account for the total expression of the surficial features along the north flank. Although the graben themselves may be explained by a nontectonic origin, the lineaments to the west of the graben and the inflection in the older surface to the east that align with the graben are more difficult to account for without a tectonic origin.

The scarps that bound the graben have been modified by fluvial processes. The eastern portion of the north graben, in particular, has been enhanced by erosion along a northeast-flowing drainage. However, the orientation of the scarps approximately perpendicular to the main drainages from

Phil Pico Mountain suggests that the scarps are not entirely erosional features. In addition, the lineaments on a surface that is younger than the one with the graben cannot be easily explained by fluvial erosion.

Landslide movement could be responsible for the scarps and graben. Several landslides, including a relatively large one east of the graben, are present along the north flank of Phil Pico Mountain (Figure 4). The bedrock in this area is primarily Wasatch Formation, which has interfingering beds of conglomerate, sandstone, siltstone, and clay (Hansen, 1965, p. 111). The variability in the lithology of the formation results in marked differences in the properties of the rock (Hansen, 1965, p. 113-114). Some parts (chiefly the conglomerate and sandstone) are resistant to erosion and other parts (chiefly those that are silty and clayey) can be unstable, especially when wet (Hansen, 1965, p. 114). Conglomerate and sandstone constitute the greater part of the formation. The presence of landslides along the north flank of Phil Pico Mountain indicates that at least some of the underlying Wasatch Formation is unstable. The mapped landslides generally occur adjacent to drainages where erosion has removed gravel and underlying Wasatch Formation leaving an exposed, relatively steep slope. The surface containing the graben has been incised but not to the point of exposing the underlying Wasatch Formation, which is nearly horizontal here, in a steep slope.

Although a nontectonic origin is possible, a tectonic origin cannot be ruled out and seems to be the best explanation for all of the surficial features. The relationship between the scarps on the north flank of Phil Pico Mountain and a mapped tectonic structure is not known. However, the limited extent of and small net tectonic displacement across the scarps on Quaternary surfaces and the preservation of older rocks (primarily Tertiary Wasatch Formation) north of the scarps suggest that a related fault with normal displacement has not experienced recurrent, late Quaternary surface ruptures.

The closest mapped fault is the curving, east-to-northeast-striking Henrys Fork fault that has been shown by Ritzma (1971) and Hansen (1986, his Figure 25, p. 38) along the north flank of Phil Pico Mountain (Figure 1). The Henrys Fork fault may be related structurally to either the North Flank fault or the Uinta fault, or both. Thus, the Henrys Fork fault could be one of the faults that bound the north flank of the eastern Uinta Mountains.

Hansen (1954, p. 18) concluded that the Henrys Fork fault has less displacement than the Uinta fault but is similar to it structurally. Both are high-angle reverse faults, and a component of strike-slip displacement seems likely (Hansen, 1954, p. 18; Anderman, 1955, p. 132). The two faults overlap near Manila (Figure 1; Anderman, 1955, p. 132). Stratigraphic displacement on the Henrys Fork fault is at least 3,500 m (12,000 ft) at Phil Pico Mountain, where displacement on the Uinta fault has decreased to near 0 m (Anderman, 1955, p. 132). Major displacement on the Henrys Fork fault occurred during the middle Eocene, somewhat later than most of the displacement on the Uinta fault (Anderman, 1955, p. 131-132). Later reversed movement similar to that recorded along the Uinta fault and related to collapse of the eastern Uinta Mountains has not been recognized on the Henrys Fork fault, although such displacement probably affected the area near Phil Pico Mountain (Anderman, 1955, p. 133).

Other scarps that are thought to represent Quaternary fault rupture along bounding faults of the Uinta Mountains are preserved at two other localities adjacent to the western Uinta Mountains

west of Phil Pico Mountain: at Towanta Flat on the south flank of the mountains (Martin and others, 1985; Nelson and Weisser, 1985) and at Elizabeth Ridge on the north flank (Figure 1; West, 1988). Some properties of the scarps in these three localities are similar (Table 4). In general, the scarps at all three localities are short, bound graben, include evidence for multiple surface ruptures, have tens of meters of displacement across individual scarps but little net tectonic displacement across the graben, and have been modified by erosion and deposition. Subsidence or displacement rates on all of the scarps are low (<0.1 mm/yr).

The relationship between the Quaternary fault scarps at Towanta Flat and Elizabeth Ridge and regional geologic structures also is unclear. The scarps at Towanta Flat parallel the Uinta Basin fault and the related South Flank fault, both of which are covered by undisplaced Oligocene through Holocene units along most of their lengths (Nelson and Weisser, 1985, p. 147). Aftershocks to a magnitude 4.5 (M_L) earthquake that occurred on September 30, 1977, near the Towanta Flat scarps suggest east-west horizontal extension in this area along the south flank of the Uinta Mountains (Carver and others, 1983, p. 439). The east-west extension does not agree with displacement on east-northeast-striking normal faults (Martin and others, 1985, p. 62). A similar problem exists for the Elizabeth Ridge scarps, which roughly parallel the east-northeast-striking North Flank fault (West, 1988, p. 58). However, there is no evidence to suggest a relationship between displacement on the North Flank fault and formation of the scarps along Elizabeth Ridge (West, 1988, p. 106). West (1988, p. 107) speculated that the scarps might instead be related to displacement on the northeast-striking Darby thrust at the eastern edge of a north-trending belt of thrust faults.

Faults associated with the scarps at Towanta Flat and Elizabeth Ridge were not considered by Martin and others (1985, p. 71) or Sullivan and Ostenaa (1988, p. 1, 5) to be potential seismic sources. In fact, Martin and others (1985, p. 71) concluded that faults associated with the scarps at Towanta Flat may have a nonseismogenic origin. Similarly, faults associated with the scarps along the north flank of Phil Pico Mountain are not considered to be a seismic source for Flaming Gorge Dam. The eroded character of the scarps and the undisplaced alluvial-fan deposits of at least two and perhaps three different ages suggest that if the scarps are indeed the result of fault displacement, then surface rupture has not occurred in a long time: since at least 13 ka to 14 ka, probably not since 30 ka to 40 ka, and perhaps not since 130 ka to 150 ka. The short length of the surficial expression (about 4 km; 2 mi) and the small amount of net vertical displacement ($\leq$1.5 m; $\leq$5 ft) across the best-expressed graben imply that the fault associated with these scarps has not experienced recurrent, late Quaternary surface rupture.

Table 4. Properties of fault scarps at Phil Pico Mountain, Towanta Flat, and Elizabeth Ridge

Property	Phil Pico Mountain	Towanta Flat[1]	Elizabeth Ridge[2]
Location (see Figure 1)	On the north flank of Phil Pico Mountain about 4 km north of the mountain front, Wyoming, just north of the Utah border	On south side of Uinta Mountains about 6 km south of range front; south of the surface trace of Uinta Basin fault that bounds the south flank of the western Uinta Mountains, Utah	About 6.5 km north of mapped trace of the North Flank fault on the crest and the west flank of Elizabeth Ridge, western Uinta Mountains, Utah
Individual scarp lengths (km)	1	2 to 2.5	1 to 1.5
Total mapped length (km)	4.2	5	4
Number of scarps	4	9	3
Number of graben; width (m)	2; 150	1; 170 to 610	0?
Trend	East to northeast	N. 50-55° E. for primary set; N. 70° E. for secondary set	N. 70° E.
Direction	Down to the north and down to the south	Down to the northwest and down to the southeast	East one is down to the south; other two are down to the north
Scarp height (m)	10 for the south scarp of the south graben; 5 for the north scarp of the south graben	1 to 15 on surface 250 ka to 500 ka; 1 to 8 on surface >130 ka	2.3 to 2.5
Maximum scarp angle (°)	21.5 for 10-m scarp; 13.5 for 5-m scarp	26.5 to 40 for 15-m scarp; 19 for 11-m scarp; 14.5 for 5-m scarp	5 to 5.5
Surface slope angle (°)	5 to 6	--	1 to 2
Vertical surface displacement (m)	6.5 to 7	>8	1.5 to 2.5
Total net vertical tectonic displacement (m)	≤1.5 across south graben	0	--
Displacement per event (m)	--	2 to 3	1.5 to 2.5
Number of surface ruptures	≤1 since 130 ka to 150 ka; 1 to 3? since 500 ka	≥3 ruptures since 250 ka to 500 ka	1
Age of youngest displaced unit	130 ka to 150 ka for lineaments where ≤1 m displacement cannot be ruled out; ≤500 ka and >130 ka to 150 ka for the graben	250 ka to 500 ka	East scarp displaces Bishop Conglomerate (about 25 Ma to 30 Ma) on the Gilbert Peak erosion surface (Oligocene)
Age of unfaulted units	30 ka - 40 ka to 13 ka - 14 ka; perhaps 130 ka to 150 ka	60 ka to 150 ka	--
Average late Quaternary subsidence or displacement rate (mm/yr)	0.007 to 0.008 (maximum since 130 ka-150 ka); 0.003 (maximum since 500 ka)	0.02 to 0.06 (minimum) ≤0.09 (maximum)	--
Average recurrence	≥100 kyr?	50 kyr to 100 kyr (may be a maximum)	--
Total vertical stratigraphic offset (m)	--	--	2.1 to 2.5

[1]From Martin and others (1985) and Nelson and Weisser (1985)
[2]From West (1988)
Dashes indicate that data were not given in the references or are not known.

3.2. Sparks Fault

The Sparks fault is a generally northwest-striking, southwest-dipping, 20-to-30-km-long (12-to-18-mi-long) fault that forms the northeastern boundary of the Uinta Mountains in northwestern Colorado (Figure 1). It has been discussed by Weber (1971, p. 170), Kirkham and Rogers (1981, p. 158), and Colman (1985, his fault #37, the Sparks Ranch fault and related faults). Weber (1971, p. 170) reported that the Sparks fault is primarily a high-angle reverse fault. However, Kirkham and Rogers (1981, their Plate 1) and Colman (1985) show the fault as having several strands that all have normal fault displacement. It is likely that the Sparks fault, like the Uinta fault that bounds the Uinta Mountains to the west, has experienced both types of displacement at different times (Chapter 2). Izett (1975, p. 190, his Sparks Ranch fault), Kirkham and Rogers (1981, p. 80), and Hansen (1986) all considered the Sparks fault to be an eastern extension of the Uinta fault.

Ritzma (1971, p. 148) noted a maximum displacement of about 5,500 m (18,000 ft) on the Sparks fault. Colman (1985, his Table 1, *citing* Izett, 1975) reported 200 m (660 ft) of displacement on the Sparks fault and a related fault at Talamantes Creek since about 10 Ma (since deposition of the Browns Park Formation).

Hansen (1984, p. 11) concluded that post-Bishop Conglomerate displacement had occurred on the Sparks fault because Middle Mountain and Diamond Peak (Figure 7), which are capped with the conglomerate, are now higher than correlative surfaces that are closer to the Uinta Mountains and should be higher. Izett (1975, p. 190, *citing* H.W. Roehler, written communication, 1973) and Kirkham and Rogers (1981, their Plate 1, p. 80, 158) reported that the Browns Park Formation is faulted against Cretaceous and Tertiary rocks. Although the major displacement along the Sparks fault probably occurred during the Eocene (Ritzma, 1971, p. 149), unconformities within the Browns Park Formation suggest that displacement continued at least into the Miocene (Izett, 1975, p. 190, *citing* a field sketch by H.W. Roehler; Kirkham and Rogers, 1981, p. 80). Colman (1985) shows the youngest documented displacement as Neogene (about 2 Ma to 24 Ma), but he did not preclude younger ruptures that have not been documented because of a lack of deposits of appropriate ages or because of severe erosion.

Kirkham and Rogers (1981, p. 80) noted that Quaternary displacement has not been documented on the Sparks fault or any of the faults related to it. Furthermore, they (their Plate 1, p. 158) indicated that Quaternary deposits are the oldest units not displaced by the Sparks fault. However, they (p. 80) also noted that many of the faults in the zone that includes the Sparks fault and related faults have "distinctive linear scarps" associated with them. Weber (1971, his Figure 4) delineated four Quaternary terraces along and adjacent to Talamantes Creek in the vicinity of the Sparks fault. Although ages for the terraces are not specified, he noted that none of them shows evidence for displacement (Weber, 1971, p. 169). On the basis of changes in the course of the Vermillion Creek drainage, Hansen (1984, p. 25, 1986, his Table 2, p. 40) interpreted the youngest displacement on the Sparks fault as down-to-the-northeast movement that occurred during the Quaternary. This is opposite to the sense of displacement that is shown by Kirkham and Rogers (1981, their Plate 1) and by Colman (1985). Consequently, the age of the youngest rupture on the Sparks fault is unclear and poorly documented.

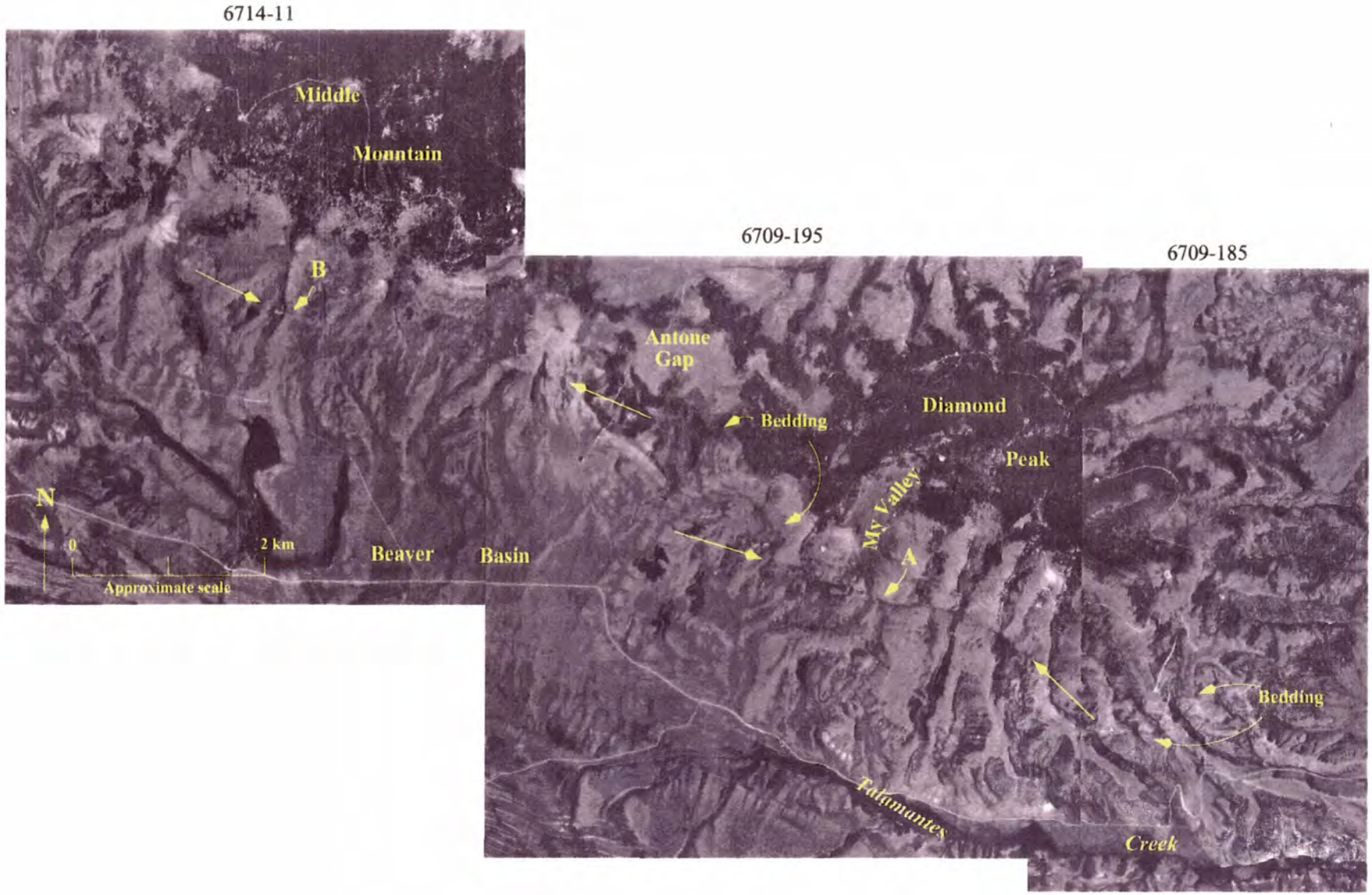

Figure 7. Aerial photographs showing the possible surficial expression of the Sparks fault along the south flanks of Diamond Peak and Middle Mountain. Long arrows point to the zones of lineaments along the range fronts. Areas identified with capital letters are discussed in the text. Photographs are from the NAPP project, were taken in July or August 1993, and have an original scale of 1:40,000. Photograph numbers are shown at the top of each photograph. The location of this figure is shown on Figure 1.

Using 200 m (660 ft) of displacement since about 10 Ma, Colman (1985, his Table 1) estimated a long-term average slip rate of 0.02 mm/yr for the Sparks fault and related faults at Talamantes Creek.

Surficial expression of the Sparks fault was examined on aerial photographs (NAPP, scale 1:40,000, #6709-184, 6709-185, 6709-186, 6709-194 and 6709-195 taken 7/1/93; #6714-11 and 6714-12, taken 8/1/93) and on the ground at one locality in Beaver Basin.

On the southwest side of Diamond Peak, lineaments are visible on alluvial surfaces that extend southward from the mountain (Figure 7). The length of the zone of lineaments is about 2.5 km (1.5 mi; Figure 7). Similarly, northwest-trending lineaments are visible on the southwest flank of Middle Mountain (Figure 7). These lineaments are collectively about 3.5 km (2 mi) long. Between the two peaks in the area of Antone Gap, a 2.5-km-long (1.5-mi-long) gap in the possible tectonic lineaments exists. A few lineaments that appear to be related to bedding are all that exist in the Antone Gap area. If the two sets of lineaments are related, then the total length of surficial expression is about 8.5 km (5 mi), which includes the 2.5-km-long (1.5-mi-long) gap in surficial expression.

Just east of My Valley, which is a drainage on the southwest flank of Diamond Peak, an alluvial fan has a slope break that coincides with a lineament on the aerial photographs (Locality A, Figure 7). A change in vegetation from tall sagebrush above (north) of the scarp to grasses below (south) of the scarp occurs at this locality. Because the slope break is approximately perpendicular to the drainages on the slope of Diamond Peak, it is likely that the slope break has a tectonic origin. About 2 m (7 ft) of displacement could have occurred across the scarp since the alluvial fan stabilized. The alluvial fan has a steep slope; its surface is smooth. The age of the alluvial fan is unknown. Quartzite clasts are pitted, indicating that the alluvial-fan deposit has some antiquity. However, these clasts could have been eroded from the Bishop Conglomerate, which caps Diamond Peak (Weber, 1971, his Figure 4), so that their weathered appearance may not reflect the age of the alluvial-fan deposit.

At an unnamed drainage on the flank of Middle Mountain (Locality B, Figure 7), an alluvial surface crosses the zone of lineaments and has no surficial expression that would suggest fault displacement. The age of the surface is unknown. The surface has been dissected by adjacent drainages, and so it is likely Pleistocene.

The presence of the lineaments and a possible scarp along the southwest flanks of Diamond Peak and Middle Mountain suggest Quaternary tectonic displacement. The close proximity of these features to the mapped trace of the Sparks fault implies a connection, although the relationship between the scarps and the fault has not been established. The eroded character, short length, and discontinuity of the scarps and lineaments suggest that any associated fault rupture is older than latest Pleistocene (15 ka to 20 ka) and could be much older. Older Quaternary displacement is difficult to evaluate because surfaces or deposits of older Quaternary age are not preserved along most of the fault. On the basis of the characteristics of the lineaments and scarps, we conclude that the late Quaternary displacement rate has been very low, and thus, the fault should not be considered a seismic source for Flaming Gorge Dam.

3.3. Uinta Fault

The Uinta fault is an east-northeast-striking structure that is at least 160 km (100 mi) long (Hansen, 1965, p. 156). It borders the eastern Uinta Mountains or adjacent plateaus between southwest of Manila, Utah, on the west and northwest Colorado on the east. Dips range between about 45° and vertical; the mean is 60° to 70° (Hansen and Bonilla, 1954, p. 15). Maximum stratigraphic throw across the fault is probably greater than about 9,000 m (30,000 ft), which occurs east of Clay Basin (Figure 2; Hansen and Bonilla, 1954, p. 15).

No evidence for Quaternary rupture has been reported on the Uinta fault. However, the length and continuity of the fault as mapped in rock, its relationship as a bounding fault of the Uinta Mountains along with the Henrys Fork fault and the Sparks fault, both of which may have had Quaternary displacement, and the proximity of the fault to Flaming Gorge Dam suggested to us that the Uinta fault should be evaluated, if possible, as part of our study. Most of the Uinta fault has been mapped primarily in the Precambrian Uinta Group, which often forms steep slopes that are not readily covered by Quaternary sediment even where drainages cross the fault.

We attempted to examine the Uinta fault in one area where it was reported to be exposed so that the location of the fault is known (Locality A, Figure 2). This was north of Jesse Ewing Canyon, where erosion has exposed the fault along the south side of Clay Basin (photographs NAPP, scale 1:40,000, 5858-145 and 585-146, taken 6/24/93). A fault near the location where the Uinta fault has been mapped does deform Browns Park Formation, which dips steeply near the fault trace.

The slope along the north side of the range front in Clay Basin west of the road through the canyon has an irregular surface, although no well-defined, individual scarps were observed. The general hummocky character of this surface suggests solifluction features rather than surface fault rupture. Near the mouth of the canyon on the east side of the road, the Uinta fault probably is south (mountainward) of a hogback composed of rocks younger than the Precambrian Uinta Quartzite. Surficial expression of the fault is not readily apparent. The hogback may be the result of differential erosion of previously faulted rocks that have variable resistance to weathering and erosion. No evidence for Quaternary displacement on the Uinta fault was observed at this locality.

3.4. Faults Between Bear Mountain and Browns Park

Three faults south of the Uinta fault and between Bear Mountain on the west and Browns Park on the east were examined as part of our study: the Dutch John fault, the Mountain Home fault, and the Beaver Creek fault (Figure 2).

3.4.1. Dutch John fault

The Dutch John fault is a west-northwest-striking, down-to-the-south normal fault that bounds the south side of Goslin Mountain separating it from Dutch John Bench on the west and Little Hole on the east (Figure 2; Hansen,1986, his Figures 27 and 28, p. 43-44). The Gilbert Peak erosion surface is displaced 300 m (990 ft) down to the south along the Dutch John fault (Figure 2; Hansen, 1984, his Figure 14, p. 18; 1986, his Figure 28, p. 44-45).

The Gilbert Peak erosion surface is the youngest, easily identifiable, and most extensive stratigraphic marker to cross the fault (Hansen, 1984, his Figure 14, p. 18). Hansen (1986, p. 12)

noted that Dutch John Bench is a remnant of the Gilbert Peak erosion surface that lacks a cap of Bishop Conglomerate. The surface here probably developed as a pediment mountainward of gravel deposition (Hansen, 1986, p. 12). This surface is an excellent marker with which to evaluate displacement on the Dutch John fault.

The Dutch John fault was examined on aerial photographs (NAPP, scale 1:40,000, 5858-252 and 5858-253, taken 6/24/93, 5861-136, 5861-137, 5861-156, and 5861-157, taken 8/1/93) and briefly on the ground where it is easily accessible. The fault is expressed on the aerial photographs as a lineament on the north edge of Dutch John Bench at the base of the slope of Goslin Mountain. A small alluvial fan extending from a drainage at the west end of the fault, just west of the well-defined lineament, shows no evidence for surface rupture. There is also no surficial expression of the fault east of Dutch John Bench along a road and power line where trees have been cleared.

A southward-sloping alluvial surface at the mouth of Goslin Creek, near the center of the fault as mapped by Hansen (1986), has a smooth surface and shows no evidence for fault rupture or tilting to the north into the Dutch John fault (Locality B, Figure 2). The surface is graded to an elevation about 80 m (260 ft) above the present level of the Green River at Little Hole. At least four well-developed terraces related to the Green River are preserved at Little Hole below the level of the high alluvial surface from Goslin Creek. The terrace deposits are composed of a quartzite-rich cobbly and bouldery gravel and are cut on a light-colored silty sand that may be Browns Park Formation. The highest of these terraces is about 60 m (200 ft) above the Green River; the high surface at Goslin Creek is graded well above this level. A moderate-to-well-developed soil on the second terrace above the Green River suggests that this terrace may be correlative with the Bull Lake Glaciation in the Uinta Mountains and could be 130 ka to 150 ka. Because two terraces are preserved above the level of this terrace along the Green River and the high alluvial surface at the mouth of Goslin Creek is even higher than the highest of these, the alluvial surface at Goslin Creek could be quite old, perhaps several hundred thousand years. This suggests that any displacement on the Dutch John fault is quite old, perhaps even pre-Quaternary.

3.4.2. Mountain Home fault

The Mountain Home fault is an east-striking, down-to-the-south normal fault that bounds the northeastern edge of Browns Park between east of Red Creek on the west and Jesse Ewing Canyon on the east (Figures 2 and 8; Hansen, 1957; Izett, 1975, p. 190; Hansen, 1986, his Figure 27, p. 43). It is about 9 km (5.5 mi) long as mapped by Hansen (1986). Browns Park Formation is displaced against older rocks along most of the fault (Hansen, 1965, his Plate 1). Several hundred meters of displacement has been reported on the fault since the Browns Park Formation was deposited (Izett, 1975, p. 190, *citing* Hansen, 1973, written communication).

Although Browns Park Formation is definitely displaced along the Mountain Home fault, no evidence for Quaternary displacement has been reported (Kirkham and Rogers, 1981, p. 78). Hansen (1957, 1965, his Plate 1) shows the fault as concealed by Pleistocene gravels (his units Qb2 and Qb3) and by Holocene alluvium along both Red Creek and an unnamed tributary west of Jesse Ewing Canyon.

The Mountain Home fault was examined on aerial photographs (photographs NAPP, scale 1:40,000, 5858- 144 and 5858-145, taken 6/24/93, 5861-162 and 5861-163, taken 8/1/93) and briefly on the ground. The fault is expressed as a linear slope break at the base of the range

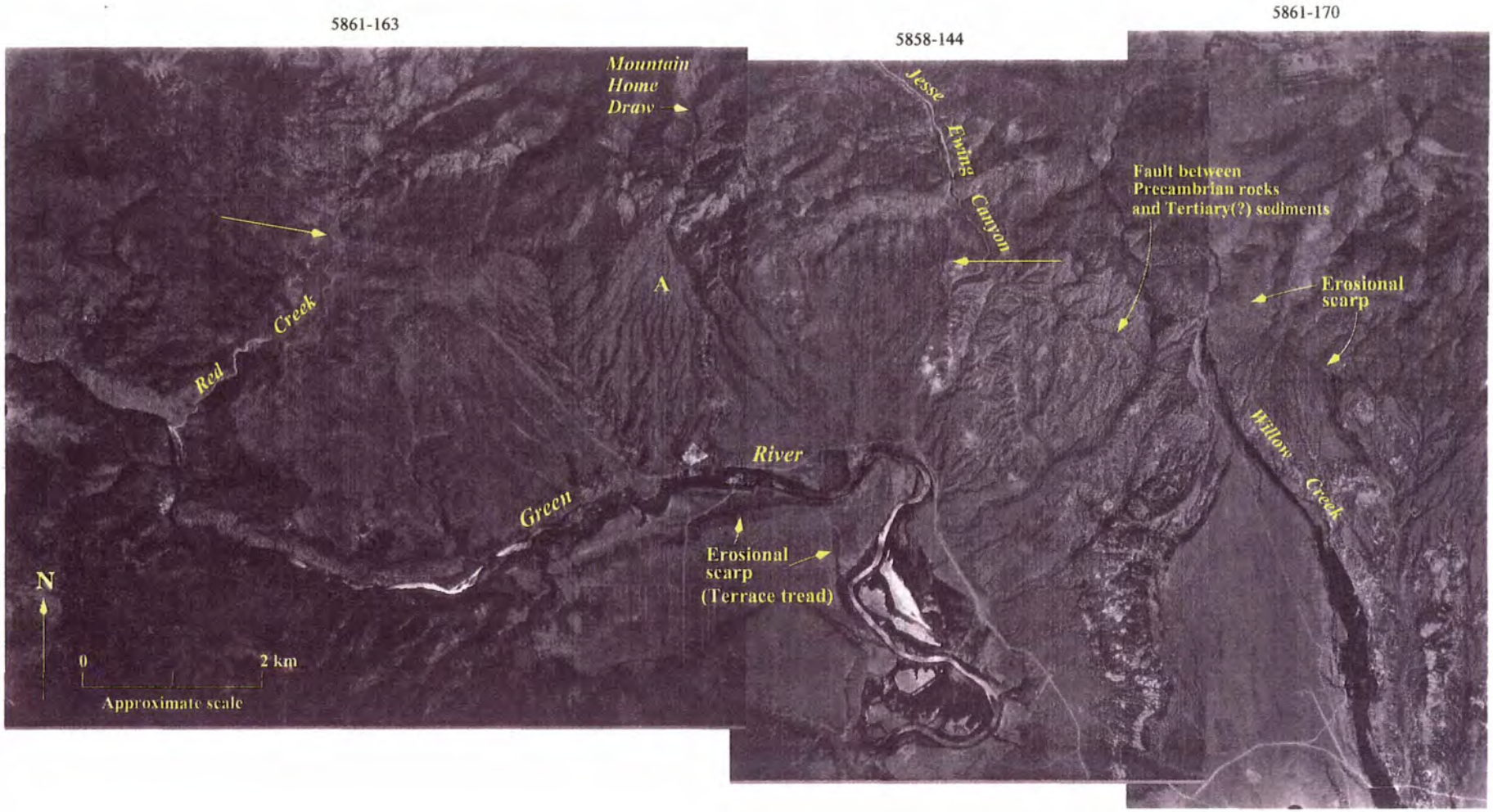

Figure 8. Aerial photographs showing the surficial expression of the Mountain Home fault. Photographs are from the NAPP project, were taken 8/1/93, and have an original scale of 1:40,000. Photograph numbers are shown at the top of each photograph. Long arrows indicate the linear front along the Mountain Home fault. Letter A shows the location of an unfaulted alluvial fan as explained in the text. The location of this figure is shown on Figure 2.

between east of Red Creek and Jesse Ewing Canyon. The length of the linear slope break is about 8 km (5 mi). A large, deeply incised alluvial fan at Mountain Home Draw, about 3.5 km (2 mi) east of Red Creek, crosses the range front and exhibits no evidence of a scarp or lineament (Locality A, Figure 8). This alluvial fan is graded to a fluvial terrace that is about 60 m (200 ft) above the present level of the Green River. Although the age of this alluvial fan is not known, its dissected character and height above present channel of the Green River suggest that it is older than latest Pleistocene (15 ka to 20 ka), and that it is probably much older than this (perhaps 100 ka or more). Other surfaces between Red Creek and Jesse Ewing Canyon are probably younger than the one just discussed. They also lack any evidence for Quaternary surface rupture.

The Mountain Home fault is not mapped east of Jesse Ewing Canyon by Hansen (1986). Alluvial surfaces east of Jesse Ewing Canyon do not show any evidence for surface rupture. At Willow Creek, a large alluvial fan crosses the range front and shows no evidence for fault displacement. The surface is smooth, has visible drainages, and has been incised 30 m (100 ft) by Willow Creek. These characteristics suggest that the alluvial fan is at least latest Pleistocene (15 ka to 20 ka).

On the basis of our observations, we conclude that the Browns Park Formation (10 Ma to 25 Ma) appears to be the youngest unit displaced by the Mountain Home fault. The few older Quaternary deposits that are preserved along the fault do not show any evidence for surface fault rupture. Thus, displacement on the Mountain Home fault is likely quite old and may be pre-Quaternary.

3.4.3. Beaver Creek fault

The Beaver Creek fault is a N. 45° W.-striking, southwest-dipping, down-to-the-southwest normal fault that in part bounds the north margin of Browns Park in the vicinity of Beaver Creek (Figure 2; Hansen, 1965, his Plate 1; 1986, his Figure 27, p. 43; Kirkham and Rogers, 1981, p. 158; Colman, 1985). The northwest portion of the fault crosses the Precambrian Uinta Group; the southeast portion, southeast of Beaver Creek, is preserved along the range front. In this section, Browns Park Formation is preserved on the southwest (downthrown) side of the fault. The length of the fault is about 8 km (5 mi) as mapped by Hansen (1986). Izett (1975, p. 190, *citing* Hansen, 1965, p. 160) noted 457 m (1,508 ft) of vertical displacement and 1,067 m (3,521 ft) of stratigraphic throw on the Beaver Creek fault. Colman (1985, his Table 1) reported that this amount of vertical displacement had occurred since 10 Ma, or since deposition of the Browns Park Formation (Hansen, 1965, his Plate 1; Izett, 1975, p. 190).

Kirkham and Rogers (1981, p. 158) noted that the Browns Park Formation is the youngest unit displaced by the Beaver Creek fault. Colman (1985) portrayed the youngest documented displacement as Neogene (about 2 Ma to 24 Ma), but he did not preclude younger ruptures that have not been documented because of a lack of deposits of appropriate ages or because of severe erosion. Using 460 m (1,518 ft) of displacement in 10 Ma (the Browns Park Formation), Colman (1985, his Table 1) estimated a long-term average slip rate of 0.046 mm/yr (0.002 in/yr) for the Beaver Creek fault. Hansen (1965, his plate 1) shows the fault as concealed by Pleistocene gravel deposits (his Qb2 and Qb4 units). Unit Qb2 may be pre-Wisconsin (>150 ka?; Hansen, 1965, p. 131).

The Beaver Creek fault was examined on aerial photographs (photographs NAPP, scale 1:40,000, 5861-170 and 5861-171, taken 8/1/93, 5858-148, 5858-245, and 5858-246, taken 6/24/93) and briefly on the ground. The southeastern 4 km (2.5 mi) of the fault near Beaver Creek is expressed

on the aerial photographs as a lineament near the base of the front of Cold Spring Mountain. The fault crosses the mouth of Beaver Creek at the range front. A large alluvial fan is present at the mouth of the creek and crosses the trace of the Beaver Creek fault. The alluvial fan shows no evidence of a fault scarp. The age of this surface is unknown. The surface of this alluvial fan is smooth, has small, parallel drainages, and is incised by Beaver Creek up to about 9 m (30 ft). On the basis of its geomorphic expression and height above the present Beaver Creek, we estimate the surface to be no younger than latest Pleistocene (older than 15 ka to 20 ka), and it could be much older.

4. Evaluation of Possible Quaternary Faults Along or Adjacent to the South Flank of the Uinta Mountains

Several faults that are present along or adjacent to the south flank of the Uinta Mountains have reported evidence for Quaternary or post-Browns Park Formation deformation. The ones examined as part of this study are the northwest-striking Diamond Gulch and Pot Creek faults, for which displacement of Quaternary landforms had been reported, and the eastern South Flank fault (or Marsh Peak fault), which has surficial expression and for which Quaternary displacement had been postulated but not demonstrated.

4.1. Diamond Gulch Fault

The Diamond Gulch fault is located on the Diamond Mountain Plateau just south of and approximately parallel to Diamond Gulch, a tributary to the Green River (Figure 1). The surficial expression of the fault trends west-northwest (Hansen, 1986, p. 46). Displacement is portrayed primarily as down to the northeast (Hansen, 1986, his Figure 30; Hecker, 1993). Graben-bounding faults have both down-to-the-northeast and down-to-the-southwest displacement (Hansen and others, 1981, 1983). Hansen and others (1983) show the southeast end of the Diamond Gulch fault terminating at a large landslide. The fault is not shown in pre-Tertiary rocks southeast of this landslide by either Hansen (1977) or Hansen and others (1983).

Hansen (1986, p. 46-47) used structural contours drawn on the Gilbert Peak erosion surface to show that the Bishop Conglomerate has been displaced by the Diamond Gulch fault, as well as by the northeast-striking Island Park fault directly to the east. The contours suggest a maximum displacement of about 60 m (200 ft) for the Gilbert Peak erosion surface at the southeast end of the Diamond Gulch fault. Hansen and others (1981) reported that the Bishop Conglomerate along the rim of Diamond Mountain is at least 100 m (330 ft) thick, although as much as 90 m (300 ft) of the conglomerate has been eroded in this area.

Hansen (1984, p. 18, 25) reported that the Diamond Gulch fault has displaced both the Bishop Conglomerate and Quaternary landforms during the Quaternary. He did not elaborate about the type, amount, or timing of these displacements or what evidence led to this conclusion. Hansen and others (1981) stated that "the displaced topography on the Bishop [Conglomerate across the Diamond Gulch fault] is clearly of Quaternary age, and [that] some of the faulting, therefore, must also be Quaternary." On the basis of the very subdued topographic expression of the fault, they inferred that the most-recent displacement likely occurred during the early Pleistocene. Hecker (1993) assigned a possible Quaternary age to displacement on the Diamond Gulch fault on the basis of landform characteristics. She reported that the fault cuts pediment and colluvial slopes.

The surficial expression of the Diamond Gulch fault was examined on black-and-white, 1:40,000-scale aerial photographs (#5854-138, 198, 199, and 200 that were taken 6/20/93; #5858-261and 262 taken 6/24/93; #5861-144, 148, and 149 that were taken 8/1/93) and briefly on the ground.

4.1.1. Surficial expression of the Diamond Gulch fault

The surficial expression of the southeastern portion of the Diamond Gulch fault is better defined than that of the northwestern portion (Figure 9). Scarps and lineaments that might be related to the fault extend for about 19.5 km (12 mi).

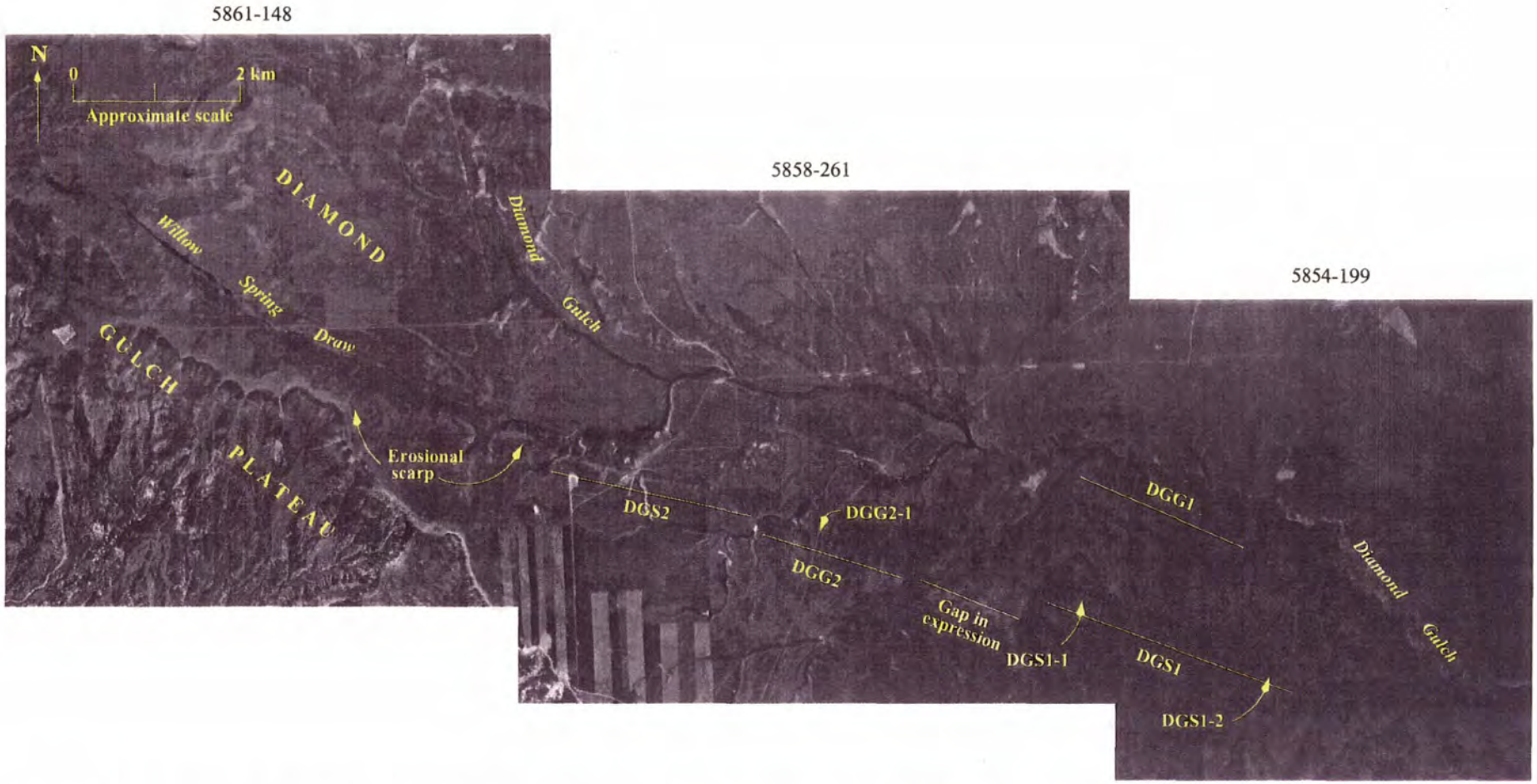

Figure 9. Aerial photographs showing the surficial expression of the Diamond Gulch fault. The photographs are from the NAPP project, were taken in June or August 1993, and have an original scale of 1:40,000. Photograph numbers are shown at the top of each photograph. Labels indicate localities discussed in the text and shown in Table 5. The location of this figure is shown on Figure 1.

The southeastern end of the fault is expressed as a 3.5-km-long (2-mi-long), down-to-the-northeast scarp that is about 1.5 km (0.9 mi) south of Diamond Gulch (Figure 9). This scarp is designated DGS1 on Figure 9. The scarp, which has a rounded form, is on a relatively flat surface that has been deeply dissected (up to about 43 m (142 ft)) by drainages flowing along or across the scarp. Alluvial fans, some fairly large, have accumulated at the base of the scarp. At Locality DGS1-1 a scarp-slope angle of 20° was measured with a Brunton compass at a place that was picked by visual inspection to be the maximum slope (Table 5). The southeast end of scarp DGS1 does not extend across higher surfaces. These higher surfaces have a light color on the aerial photographs and are preserved primarily as ridges separated by incised drainages (Figure 9). These characteristics and the height of these surfaces suggest that they are older than the one with scarp DGS1 and should be displaced if the fault continues to the southeast.

About 1 km north of scarp DGS1, a graben, designated DGG1, is preserved on a surface that could be correlative to the one crossed by scarp DGS1 (Figure 9). The amount of dissection and expression on the aerial photographs are similar. The north fault in graben DGG1 is about 2 km (1.2 mi) long; the south fault is about 1.5 km (0.9 mi) long. The graben is about 0.2 km (0.1 mi) wide and trends northwest, parallel to Diamond Gulch to the north and scarp DGS1 to the south (Figure 9).

Scarp DGS1 does not appear to extend to the northwest to cross a relatively large, unnamed, incised drainage (shown as "Gap in expression" on Figure 9). The drainage appears to have eroded through the scarp resulting in a 1-km-long (0.6-mi-long) break in surficial expression. At least one terrace appears to be inset along the drainage.

To the northwest of this drainage, surficial expression continues as a 2-km-long (1.2-mi-long), 0.1-km-wide (315-ft-wide), northwest-trending graben that is about 2 km (1.2 mi) south of Diamond Gulch (Figure 9). This graben is designated DGG2. The alluvial fan that is displaced by this graben is generally smooth but is dissected by small drainages, especially adjacent to the graben. The dissection of this surface appears to be less than that of the surface with DGS1. At a power line (Locality DGG2-1) that traverses the surface, the scarps bounding the graben are very subdued. A drainage bends sharply around the northwest end of the graben.

About 0.2 km (0.1 mi) northwest of graben DGG2, a northwest-trending, down-to-the-northeast scarp is preserved. This scarp, designated DGS2, extends for about 4.5 km (2.7 mi). The surface with the scarp is less dissected than the one where the graben DGG2 is located. A portion of scarp DGS2, especially the northwest end, appears to be, at least in part, erosional.

About 2.5 km (1.5 mi) from the northwest end of scarp DGS2, Diamond Gulch swings northward. Willow Spring Draw, flows into Diamond Gulch from the northwest (Figure 9). This draw, in which a series of small dams has been built, has a linear, northwest trend, except for the lower 0.5 km (0.3 mi) where the draw turns northward before entering Diamond Gulch. The draw is linear for at least 9 km (5.5 mi) and extends at least 6.5 km (4 mi) northwest of scarp DGS2. The location of Willow Spring Draw could be controlled by the Diamond Gulch fault, but there is no evidence to suggest surface rupture. The drainage is incised into the surface of the Diamond Mountain Plateau. This surface south of Willow Spring Draw is higher than the surface north of the draw. The drainage remains linear to the point where it heads on the plateau.

Table 5. Characteristics of the scarps along the Diamond Gulch and Pot Creek faults

Fault	Locality (Figures 9, 10)	Scarp height (m)	Maximum scarp-slope angle (°)	Length of individual scarps (km)	Total length of scarps (km)	Notes
Diamond Gulch	DGS1-1	25 to 30 (estimated)	20	1.5 to 4.5	13	Scarps are eroded into rounded slopes and incised; alluvial fans head at the scarps
Pot Creek	PCS1-1	8	8	0.4 to 1.3	9.4	Near the southeast end of surficial expression
	PCS2-1	20 to 24	10			At maximum expression of the scarps

4.1.2. Quaternary activity on the Diamond Gulch fault

The scarps associated with the Diamond Gulch fault are shown by Hansen and others (1981, 1983) as displacing the Bishop Conglomerate. This implies that the Gilbert Peak erosion surface, which underlies the conglomerate, is also displaced. Hansen and others (1981) suggested displacement of Quaternary landforms, but they did not describe the properties of this displacement (e.g., type, length, amount, age).

Near the southeast end of scarp DGS1, at locality DGS1-2 (Figure 9), a minimum age for the youngest displacement was estimated. At a drainage that has incised through the scarp, at least one alluvial surface crosses the projection of any fault related to the scarp. This surface is about 4 m (13 ft) above the presently active drainage. A soil has developed in sandy sediment (eolian?) that caps the fluvial gravel associated with the surface. This soil has weak blocky structure and possibly very thin clay films around pebbles. However, the maximum color of this soil is not markedly different from that of unweathered sediment, and no pedogenic carbonate was noted within about 25 cm (10 in) of the ground surface. On the basis of the degree of soil development and the amount of incision, we speculate that this surface is at least early Holocene (8 ka to 10 ka) or latest Pleistocene (10 ka to 15 ka). The lack of surficial expression of the Diamond Gulch fault suggests that surface rupture is no younger than this. It could be much older. The rounded character of the scarp and the marked dissection that has occurred since the scarp formed suggest that most of the displacement and probably also the last event are much older than latest Pleistocene.

It is possible that the scarps reflect displacements of the Bishop Conglomerate and the Gilbert Peak erosion surface that occurred several million years ago and that have been preserved either at the surface or as exhumed features (buried for some time and then exposed by erosion). Preservation of the relatively high scarps may be due to the cementation in the Bishop Conglomerate. The surfaces now appear to be alluvial because of erosion and redeposition of clasts from the Bishop Conglomerate. On the basis of our limited field examination, we could not distinguish between Bishop Conglomerate and younger deposits derived from the Bishop Conglomerate. The absence of a source to provide sediment for large alluvial fans suggests that the large, extensive surfaces are Bishop Conglomerate and have been preserved for quite some time as suggested by Hansen (1984, 1986). Alluvial deposits that are probably Quaternary age are the alluvial fans at the base of the scarps.

Erosion appears to be at least in part responsible for the surficial expression of the Diamond Gulch fault because the best expression of the fault is at its southeastern end where the landscape is more dissected. On at least this part of the fault, erosion may have enhanced the expression of the scarp. Dissection becomes increasingly greater to the southeast, closer to the Green River. As estimated from 1:24,000-scale topographic maps with 20-foot (6-m) and 40-foot ((12-m) contour intervals, incision in the area of scarp DGS2 is about 20 m (70 ft). Adjacent to scarp DGS1, incision is up to about 135 m (440 ft). Just downstream of these scarps, incision increases to about 180 m (580 ft). And at Jones Hole, where Diamond Gulch joins the Green River, Diamond Gulch is incised up to about 720 m (2,360 ft). Incision along the Green River likely occurred since the formation of the Gilbert Peak erosion surface (Hansen, 1986). The Gilbert Peak surface is presently about 610 m (2,000 ft) above the river in Lodore Canyon, so that the Green River has incised this amount since the time when the erosion surface formed.

The progressively better expression of the scarps along the Diamond Gulch fault toward the Green River, where incision has been the greatest along Diamond Gulch, suggests that the expression of the scarps along the Diamond Gulch fault are, at least in part, erosional. The degraded and dissected character of the scarps and the alluvial fans deposited along the base of the scarps indicate that any tectonic displacement has not occurred in quite some time, probably not since at least 100 ka. Displacement could be much older.

4.2. Pot Creek Fault

The Pot Creek fault is located on the Diamond Mountain Plateau just south of and approximately parallel to Pot Creek and about 10 km (6 mi) northeast of the Diamond Gulch fault (Figure 1). The fault strikes west-northwest (Hansen, 1986, p. 47). The southeast end, just west of the Green River, is shown by Hansen and others (1983) as down to the southwest. The length of the Pot Creek fault is about 30 km (18 mi) from near Warren Draw on the northwest to the Green River on the southeast. Hansen and Rowley (1991) suggested that the total length of the inferred fault is about 55 km (33 mi). Throw on the Pot Creek fault was estimated by Hansen and others (1982) to be about 60 to 120 m (200 to 400 ft) in Lodore Canyon along the Green River.

Surficial expression of the fault as scarps is limited to the northwest 9.4 km (5.5 mi) between about Warren Draw and Crouse Reservoir (Figure 10). The scarps are shown by Hansen and others (1981) primarily as northeast side down, except for one west of Crouse Reservoir (scarp labeled PCS4, Figure 10). This scarp is portrayed as southwest side down (Hansen and others, 1981). Hansen (1984, p. 25) and Hecker (1993, p. 97) reported that 5 to 6 m (17 to 20 ft) of displacement may be represented by the scarps along the Pot Creek fault. Although lacking scarps, two additional portions of the Pot Creek drainage are linear. One is a 5-km-long (3-mi-long) section about 2 km (1 mi) east of the southeast end of the scarps. The other is a 4-km-long (2.5-mi-long) section just west of the Green River, where the fault displaces the Precambrian Uinta Group that is exposed along Pot Creek (Hansen and others, 1982, 1983).

Hansen and others (1981, 1982) and Hansen (1986, p. 46) suggested that the Gilbert Peak erosion surface and the overlying Bishop Conglomerate have been displaced by the Pot Creek fault. Hansen and others (1981) and Hansen (1986, p. 46-47) reported that the Pot Creek fault is a zone of very old faults that have experienced Quaternary rupture near Crouse Reservoir (Figure 10). Hansen and others (1981) thought that displaced topography developed on the Bishop Conglomerate "is clearly of Quaternary age," and they went on to conclude that fault displacement must then be Quaternary. However, the eroded character of the scarps led them to speculate that the youngest displacement occurred during the early Pleistocene (Hansen and others, 1981). The youngest deposits reported to overlie the fault are talus, colluvium, and debris fans that are Holocene or Pleistocene (Hansen and others, 1982). Hansen (1984, p. 25) and Hecker (1993, p. 97) indicated that the scarps along Pot Creek are more eroded and more subtle than those associated with the Diamond Gulch fault.

If the scarps along the Diamond Gulch and Pot Creek faults are older features that are being exposed by erosion, then the poorer definition of the scarps along the Pot Creek fault compared to those associated with the Diamond Gulch fault may be the result of less incision by Pot Creek. Both creeks are cutting downward into the Bishop Conglomerate and older rocks. Pot Creek, however, is incising into exhumed ridges of the Precambrian Uinta Mountain Group (shown as R on Figure 10). Consequently, Pot Creek flows in relatively wide valleys on the Bishop Conglomerate and in narrow gorges through the Uinta Mountain Group (Hansen and

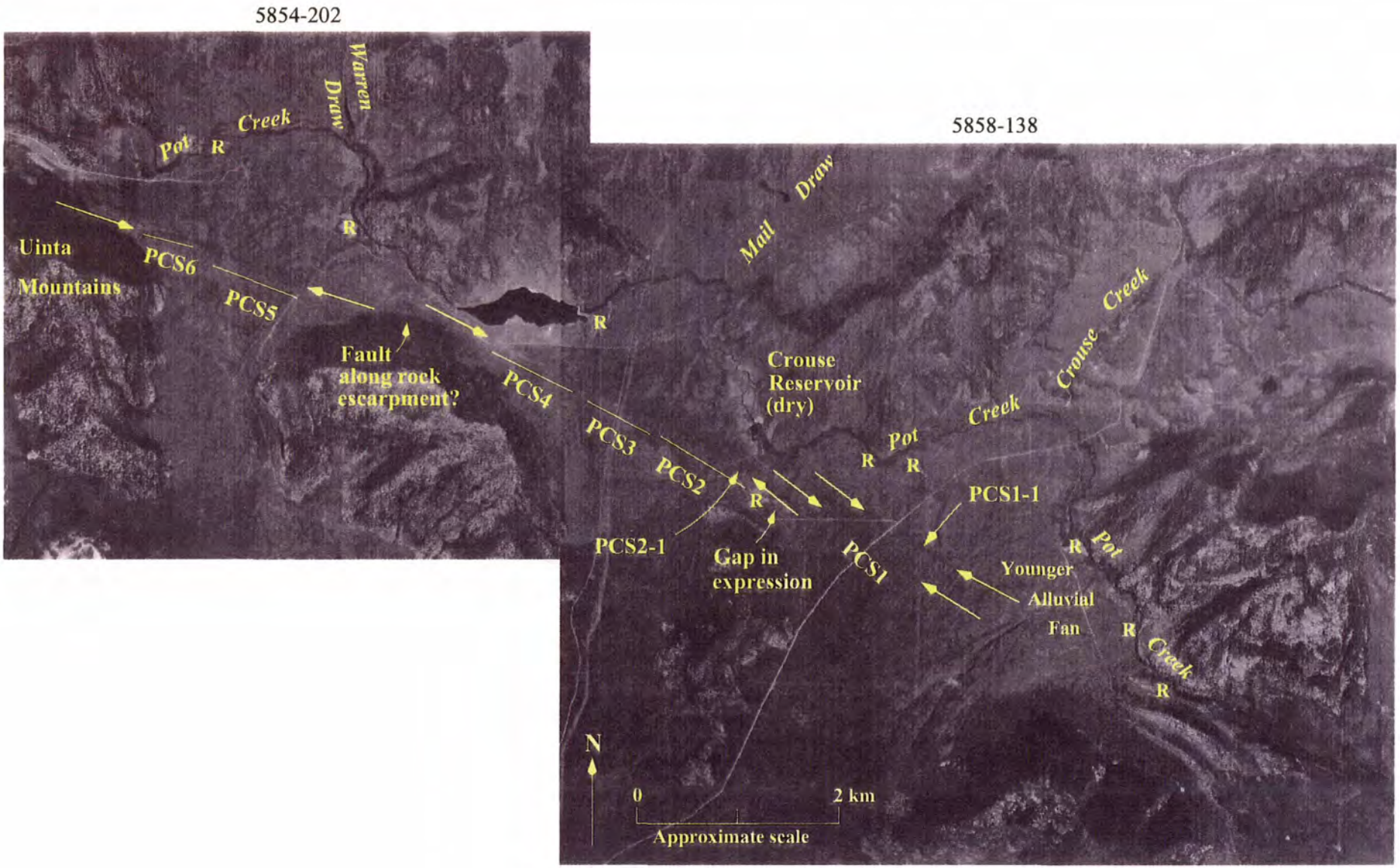

Figure 10. Aerial photographs showing the best surficial expression of the Pot Creek fault. Long, unlabeled arrows indicate scarps or lineaments that may have a tectonic origin, at least in part. Labels indicate localities discussed in the text. Photographs are from the NAPP project, were taken 6/24/93, and have an original scale of 1:40,000. Photograph numbers are shown at the top of each photograph. Outcrops of Precambrian Uinta Mountain Group that are either along the trend of the scarps associated with the Pot Creek fault or crossed by Pot Creek are shown by "R". The location of this figure is shown on Figure 1.

others, 1981). The hardness of the Uinta Mountain Group sandstone slows the downcutting of Pot Creek and, thus, the exhumation of the older scarps.

The surficial expression of the Pot Creek fault was examined on black-and-white, 1:40,000-scale aerial photographs (NAPP, #5854-202 and 5854-203, taken 6/20/93; #5858-137, 5858-138, 5858-257, and 5858-258, taken 6/24/93) and briefly on the ground.

4.2.1. Surficial expression of the Pot Creek fault

Scarps and lineaments that are related to the Pot Creek fault are limited to a section about 9.4 km (5.5 mi) long between about Warren Draw and Crouse Reservoir. These features trend northwest along the south side of Pot Creek (Figure 10).

The southeastern end of surficial expression consists of two zones of scarps both of which trend northwest and are lower to the northeast (scarps designated PCS1 on Figure 10). The two zones overlap by about 0.8 km (0.5 mi). The north scarp is about 1 km (0.6 mi) long, is about 8 m (26 ft) high, and has an estimated maximum scarp-slope angle of 8° (Locality PCS1-1, Figure 10). The south zone is about 0.3 km (0.2 mi) south of the north scarp, has a total length of about 1.3 km (0.8 mi), and consists of three short scarps. Of these three scarps, the southeast and central scarps are each about 0.4 km (0.2 mi) long and have a 0.1-km-long (317-ft-long) break between them. The northwest scarp is about 0.4 km (0.2 mi) long and has a more northern trend than the other two scarps. All the scarps are very rounded and subdued. They are preserved on an extensive alluvial surface that is flat and dissected by relatively large drainages. The scarps cannot be traced to the southeast across an alluvial surface that could be younger than the one on which the scarps are preserved. This younger surface has bars and channels; it is graded to a level about 3 m (10 ft) above Pot Creek.

Northwest of the PCS1 scarps, there is a 0.2-km-long (0.1-mi-long) gap in expression at a tributary to Pot Creek. Northwest of this gap, a 0.5-km-long (0.3-mi-long) linear contact between Precambrian Uinta Mountain Group (R on Figure 10) on the southwest side and unconsolidated deposits on the northeast side aligns with the PSC1 scarps to the southeast and the PCS2 scarps to the northwest. The dip of rocks of the Uinta Mountain Group is 10° south-southwest (Hansen and others, 1981).

Northwest of the linear bedrock contact is a 1.2-km-long (0.7-mi-long), northwest-trending, down-to-the-northeast scarp that is the best surficial expression along the Pot Creek fault (scarp PCS2 on Figure 10). At locality PCS2-1 near the southeast end of this scarp, the estimated scarp height is 22 ± 2 m (73 ± 7 ft) with an estimated maximum scarp-slope angle of 10° (Table 5). This scarp is on an alluvial surface that is flat but dissected. The surface could be the same age as the one with scarps shown as PCS1.

Aligned with and adjacent to the northwest end of the PCS2 scarp, is a poorly defined, northwest-trending scarp that is about 0.6 km (0.4 mi) long (scarp PCS3, Figure 10). The surface on which this scarp is preserved is higher, and presumably older, than the one with scarps to the southeast, yet the expression of the fault is more subtle. A younger alluvial fan eroded from the northeast face of the scarp may in part account for the poorer expression of the fault.

Located immediately northwest of scarp PCS3, the section labeled PCS4 on Figure 10 is a 1-km-long (0.6-mi-long), down-to-the-southwest scarp (Hansen and others, 1981). This scarp may have, at least in part, an erosional origin. A canal follows the southwest (lower) side of the scarp. The lineament associated with this scarp is enhanced on the aerial photographs by a road that follows the slope break.

Northwest of the PCS4 scarp, the fault follows a northeast-trending bedrock escarpment for about 1.9 km (1 mi). The fault is either in rock or along the base of the slope in colluvium, so that surficial expression is not obvious.

Northwest of the rock escarpment, a northwest-trending, 0.9-km-long (0.5-mi-long), down-to-the-northeast scarp crosses an alluvial fan remnant that is graded to a level about 3 m (10 ft) above Pot Creek. This scarp is labeled PCS5 on Figure 10. The alluvial fan has a smooth, gently sloping surface. It is cut off from any source drainage. Light-colored areas that seem to delineate ridges and channels appear to be preserved beneath a surface of darker sediment that fills the channels. This expression may indicate that this surface is older than the ones with scarps to the southeast.

Immediately northwest of this scarp is a northwest-trending, down-to-the-northeast, 0.7-km-long (0.4-mi-long) scarp (labeled PCS6 on Figure 10) that could be a continuation of the PCS5 scarp to the southeast. The expression of the PCS6 scarp appears to have been enhanced by a drainage along its base and could be at least in part erosional in origin.

Northwest of the PCS6 scarp, the Pot Creek fault, if present, follows a north-facing escarpment in Precambrian Uinta Mountain Group. The fault is either in the rock or along the base of the slope in colluvium. There is no surficial expression of the fault northwest of this area. At the northwest end of the rock escarpment, two north-flowing drainages, Cow Creek and Simons Creek (west of the area shown in Figure 10), have built a smooth surface that shows no evidence of fault rupture. The southeastern drainage, Cow Creek, turns eastward at the rock escarpment and flows east-northeast before joining Pot Creek.

4.2.2. Quaternary activity on the Pot Creek fault

The scarps associated with the Pot Creek fault are shown by Hansen and others (1981, 1983) as displacing the Bishop Conglomerate, which implies that the underlying Gilbert Peak erosion surface is also displaced. Hansen and others (1981) and Hansen (1984, p. 25) reported that the scarps are Quaternary and inferred 5 to 6 m (17 to 20 ft) of Quaternary displacement. However, they also noted that the eroded character of the scarps suggests that the youngest displacement on the Pot Creek fault likely occurred during early Pleistocene.

The scarps along the Pot Creek fault have a maximum height of 20 to 24 m. On the basis of the eroded character of the scarps, their limited extent, and poor expression, we conclude that the scarps associated with the Pot Creek faults are probably no younger than 100 ka. They could be much older. Similar to the scarps along the Diamond Gulch fault to the southwest, cementation in the Bishop Conglomerate and the small sizes of the drainages may result in slow erosion so that the scarps are preserved for a long time.

4.3. South Flank or Marsh Peak Fault

The eastern portion of the South Flank fault, called the Marsh Peak fault in U.S. Bureau of Reclamation (1986) and Peterson (1989), is a curving, east-northeast-striking, down-to-the-southeast normal fault that bounds the south flank of the Uinta Mountains between east of the Whiterocks River and west of Ashley Creek (Figures 1 and 11). It is about 30 km (18 mi) long as mapped by Rowley and others (1985). The South Flank fault has a total length of about 130 km (80 mi) between the North Fork of the Provo River in central Utah and about Ashley Creek (Martin and others, 1985, p. 15; Hansen, 1986, his Figure 25). It is composed of shorter faults with similar characteristics (Kinney, 1955, p. 124). The eastern part of the South Flank fault juxtaposes Precambrian Uinta Mountain Group (primarily sandstone) against younger shale that is part of the Uinta Mountain Group or against Mississippian or Pennsylvanian rocks (Kinney, 1955, p. 124). Maximum displacement on the South Flank fault is greater than 1,220 m (4,000 ft) in central Utah (Huddle and others, 1951, *in* Martin and others, 1985, p. 15). Displacement gradually decreases to the east and dies out east of Ashley Creek (Kinney, 1955, p. 124).

A 5-km-long (3-mi-long) section near the east end of the South Flank fault is shown by Rowley and others (1985) to displace the Bishop Conglomerate (25 Ma-30 Ma) on two mesas between Brownie Creek Canyon and Ashley Creek (Figure 11). However, a section of the fault about 10 km (6 mi) to the west of these mesas is shown by them to be concealed by either the Bishop Conglomerate on Mosby Mountain or by Pleistocene glacial till between Dry Fork and the North Fork (Figure 11). Kinney (1955, his Plate 1) does not portray the South Flank fault as displacing the Bishop Conglomerate at Mosby Mountain or on the mesas to the east between the Dry Fork of Ashley Creek and Ashley Creek. Anderson and Miller (1979) portrayed the eastern South Flank fault as suspected of Quaternary displacement. It was not considered to be a Quaternary fault by Hecker (1993).

The eastern portion of the South Flank fault was examined on black-and-white, 1:40,000-scale and 1:80,000-scale aerial photographs (NAPP, #5855-99 and 5855-100, taken 6/20/93; #5861-74, taken 8/1/93; #5863-25, 5863-40, and 5863-41, taken 8/28/98; GS-VEFM project, #1-26 and 1-27, #2-99, #3-45 and 3-46, taken 8/76) and briefly on the ground.

4.3.1. Surficial expression of the eastern South Flank fault

Surficial expression of the eastern South Flank fault is best along a marked, down-to-the-southeast, linear escarpment near Brownie Canyon (red line, Figure 11). The 5-km-long (3-mi-long) escarpment is composed of Precambrian Uinta Mountain Group (sandstone) that is juxtaposed against Mississippian or Pennsylvanian rocks (sandstone, limestone, and shale) (Rowley and others, 1985). The escarpment continues about 2 km (1.2 mi) to the west to the North Fork (blue line, Figure 11), but this section has weaker expression than it does near Brownie Canyon. High ridges extending across the escarpment seem to have little displacement in contrast to the intervening areas along drainages. The area is generally tree-covered making assessment of the surficial expression of the fault difficult. However, where the road along Brownie Canyon crosses the escarpment, we found no evidence for faulting. Other than the rock escarpment, no surficial expression for the fault was noted. The abrupt changes in the expression of the escarpment, its best expression adjacent to Brownie Canyon and in nearby drainages, and its poorest expression on intervening ridges suggest that the escarpment formed, at least in part, by erosion along tributaries to the creek in Brownie Canyon.

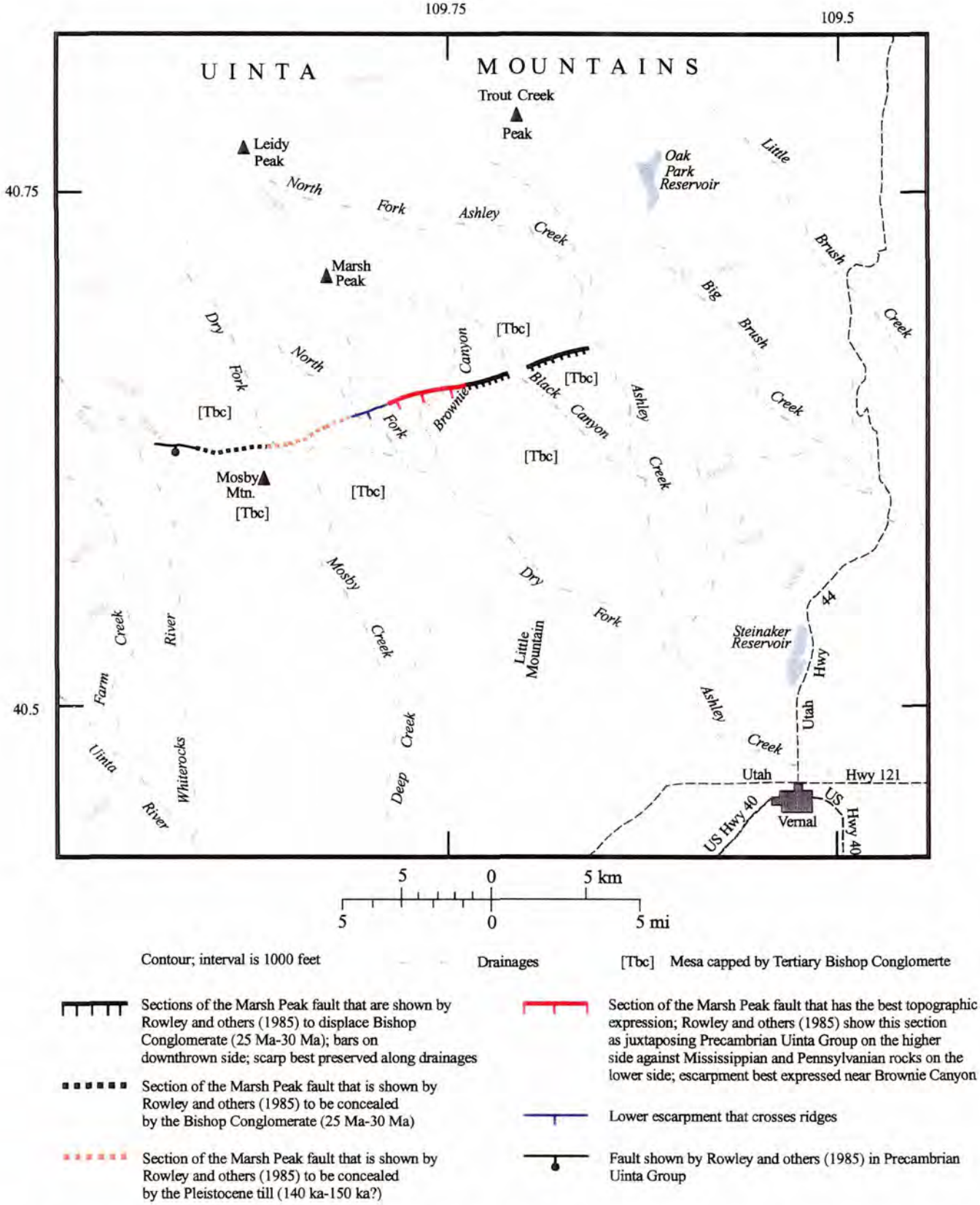

Figure 11. Map of the eastern South Flank or Marsh Peak fault between the Whiterocks River and Ashley Creek. The map is based on a portion of the 1:250,000-scale Vernal topographic map and portions of the 1:100,000-scale Dutch John and Vernal topographic maps.

East of Brownie Canyon, the South Flank fault is expressed as a 6.5-km-long (4-mi-long), down-to-the-southeast scarp on two mesas capped by Bishop Conglomerate (black line with hachures, Figure 11). The scarp is only weakly expressed on the eastern of these two mesas. Where a road crosses the west end of the scarp, an elevation difference between the surfaces of the Bishop Conglomerate northwest and southeast of the fault is not obvious and may be zero. As with the escarpment in rock to the west, the scarp on the surface of the Bishop Conglomerate is best expressed where it has a drainage adjacent to it. This relationship suggests that the scarp formed, at least in part, by erosion.

Between the North Fork and the Dry Fork of Ashley Creek (dashed orange line, Figure 11), no surficial expression of the South Flank fault was noted on the aerial photographs or during a brief field reconnaissance. This 5-km-long (3-mi-long) section is covered by Pleistocene glacial till of at least two different ages (Carrara, 1980; Rowley and others, 1985). The oldest of these tills is correlated by Carrara (1980) to the Bull Lake Glaciation in the Wind River Mountains in west-central Wyoming. The Bull Lake Glaciation in the Wind River Mountains is thought to have occurred between about 140 ka and 150 ka (Hall and Shroba, 1993).

West of the section concealed by Pleistocene glacial till is a 4-km-long (2.5-mi-long) section that is portrayed by Rowley and others (1985) as concealed by the Bishop Conglomerate. No evidence for fault displacement was observed on the aerial photographs.

Rowley and others (1985) show an east-striking, 2.5-km-long (1.5-mi-long), down-to-the-south fault in Precambrian Uinta Mountain Group just east of the Whiterocks River and west of the till-covered section. They connected this fault with the South Flank fault to the east. If this fault is included, then the total length of the eastern section of the South Flank fault is about 25 km (15 mi).

4.3.2. Quaternary activity on the eastern South Flank fault

Although the Bishop Conglomerate may be displaced at the east end of the South Flank fault, this displacement could have occurred before the Quaternary. The expression of the scarp on the surface of the Bishop Conglomerate suggests an erosional origin for at least part of the scarp. This is also true for a rock escarpment that coincides with the fault near Brownie Canyon. Precambrian quartzite is juxtaposed against weaker Mississippian and Pennsylvanian rocks across the escarpment, which suggests the escarpment is likely, at least in part, erosional in origin. In addition, the lack of evidence for fault rupture on surfaces of Pleistocene till near the North Fork and Dry Fork of Ashley Creek suggests that any displacement on the fault is older than at least 140 ka to 150 ka. The youngest displacement on the fault could be much older.

5. Seismicity

Flaming Gorge Dam lies within the Uinta Mountains, an east-trending salient of the Middle Rocky Mountain province. The Wyoming Basin lies to the north and the Colorado Plateau to the south (Figure 12). This is a region of modest seismicity and generally limited seismographic coverage. To evaluate the seismic hazard arising from earthquakes not associated with mapped surface faults, a study area covering parts of the Middle and Southern Rocky Mountains, the Colorado Plateau, and the Wyoming basin (Figure 12) was defined. The study area includes the transition zones between these tectonic provinces.

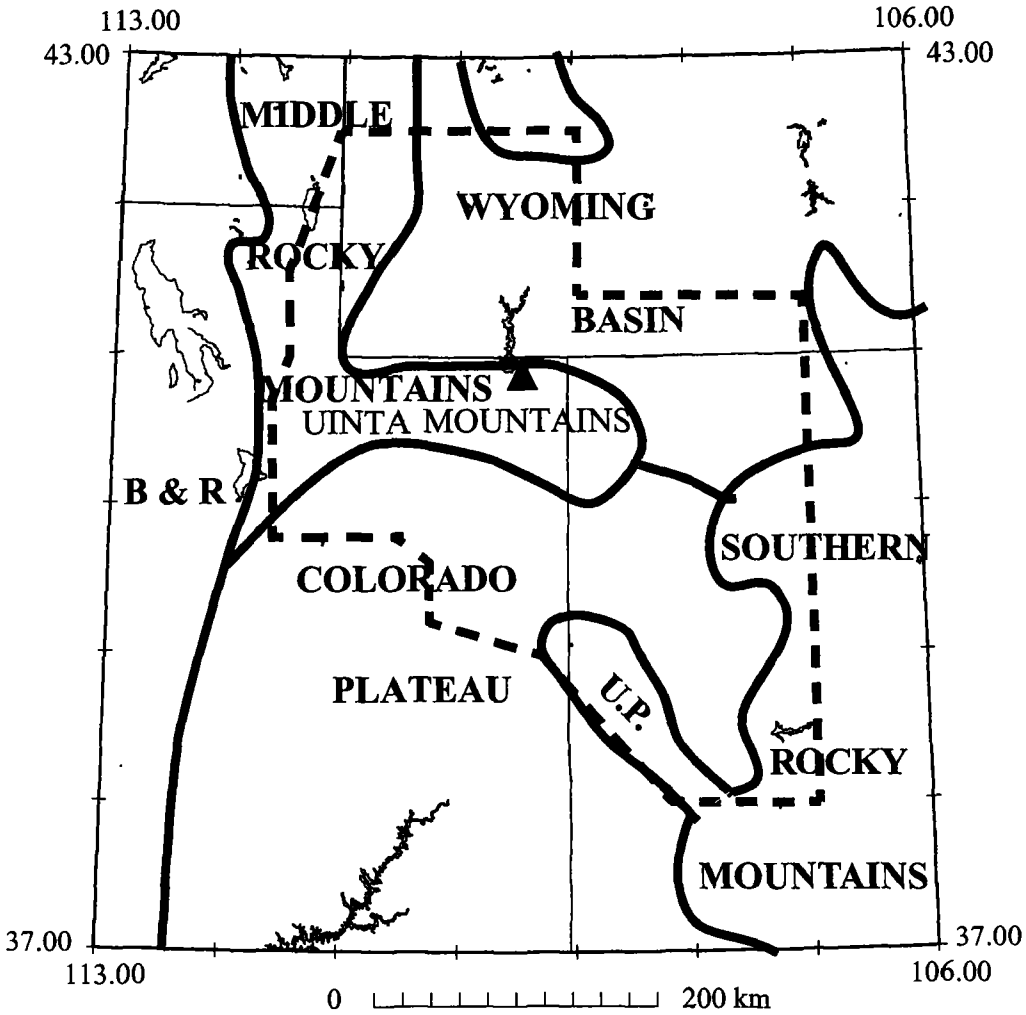

Figure 12. Location of Flaming Gorge Dam (black triangle) in relation to tectonic provinces (heavy solid lines). B & R = Basin and Range province, U.P. = Uncompahgre Plateau. Study area for earthquake recurrence indicated by dashed line.

The area surrounding Flaming Gorge Dam is characterized by moderate seismicity. Only one historical earthquake of magnitude >5 has occurred within the study area, an event on October 11, 1960, near Montrose, Colorado, which had a magnitude of M_w 5.5. All earthquakes of magnitude 2 and greater within the study area are plotted in Figure 13. Data sources for the seismicity assessment are: the Decade of North American Geology (DNAG) catalog of Engdahl and Rinehart (1991), which extends through 1985; the Preliminary Determination of Epicenters (PDE) catalog from 1986 through December 1995; and additional data from the catalog of the University of Utah and the Bureau of Reclamation's (USBR's) Ridgway and Paradox seismograph networks. Detection capabilities in the study region are highly variable. The best station coverage is in northeastern Utah and the part of southwest Colorado monitored by the USBR networks.

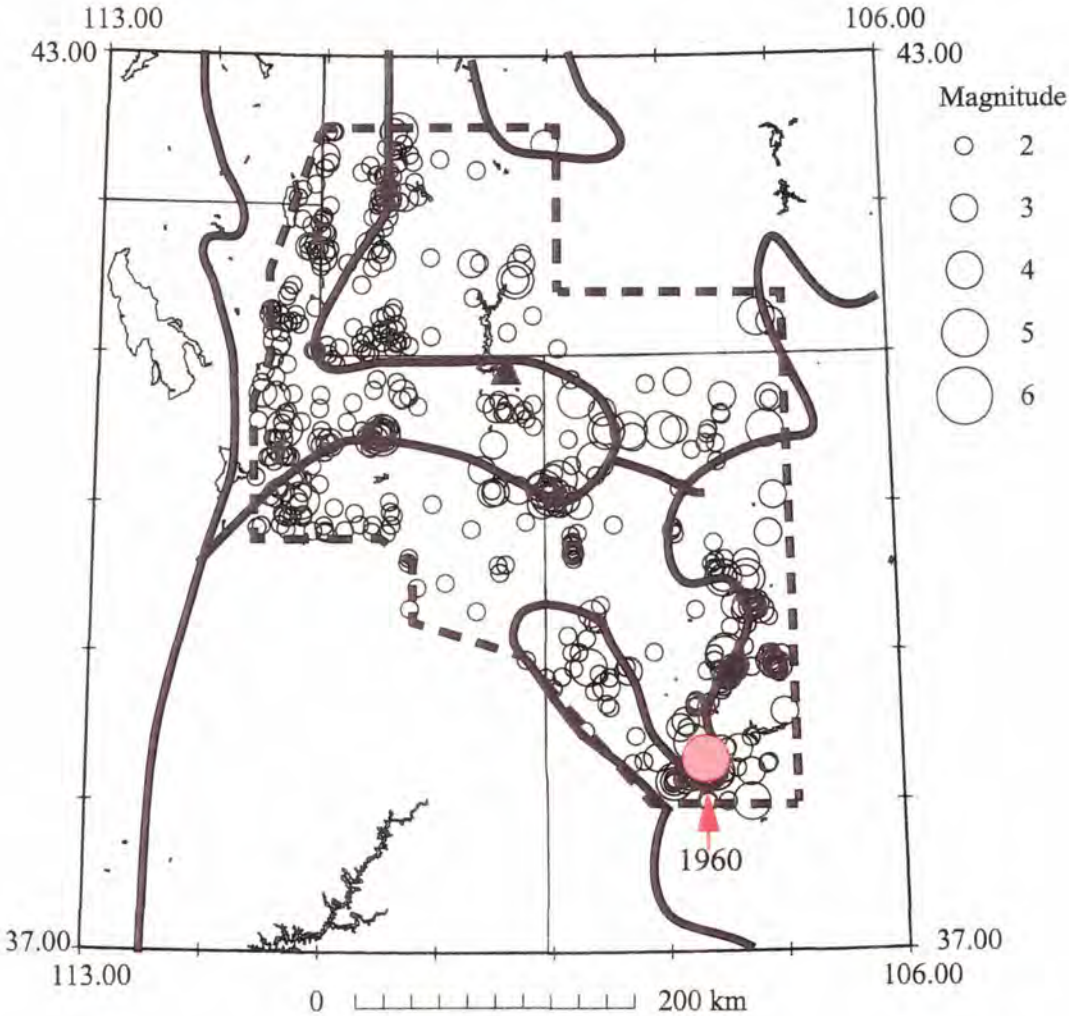

Figure 13. Seismicity of magnitude 2 and greater in study area (outlined by dashed line). Tectonic boundaries indicated by heavy solid lines (see Figure 12). Location of Flaming Gorge Dam indicated by solid triangle. The October 11, 1960, M_w 5.5 earthquake near Montrose, Colorado, is identified by the red circle.

No obvious correlation between seismicity and physiographic/tectonic boundaries, which would justify a division into smaller zones, exists within the study area. Knowledge of seismicity in Colorado and eastern Utah is handicapped by the lack of spatially and temporally comprehensive seismographic coverage. Using smaller seismic source zones based upon physiographic/tectonic features would result in areas with sparse earthquake data and therefore lead to significant uncertainties in calculated *a*- and *b*- values. Therefore, the study area was treated as a single, homogeneous seismic zone in the following calculations of the seismic hazard.

Studies of existing focal mechanisms in the area by Zoback and Zoback (1989) and Wong and Humphrey (1989) indicate predominantly normal faulting, with some strike-slip. Results within the Colorado Plateau suggest T-axes with NE-SW orientations and P-axes with NW-SE directions. In other portions of the study area, T-axes have E-W and P-axes N-S orientations (Zoback and Zoback, 1989).

5.1. Earthquake Recurrence

In order to compute earthquake recurrence it is necessary to delete aftershocks and other dependent events so that the catalog approximates a Poissonian or random data set, estimate completeness periods for various magnitude ranges, and estimate the maximum magnitude of randomly occurring earthquakes within the source zone.

The preferred magnitude scale for the calculations is $\mathbf{M_W}$ or moment magnitude, which is assumed to be similar to the Richter magnitude M_L in the magnitude range of interest here. Most pre-instrumental earthquake magnitudes in the catalog are based on the commonly used Modified Mercalli Intensity (MMI)-magnitude conversion, $M_I = 2/3\ I_o + 1$, where M_I is "Intensity magnitude" and I_o is the maximum recorded MMI. However, studies in Colorado (McGuire, 1993) and New Mexico (LaForge and Anderson, 1988) found that, when compared to instrumental magnitudes, magnitudes based on MMI were too high. Intensity magnitudes in the catalog used here were therefore recalculated using the McGuire (1993) formula, $M_I = 2/3\ I_o + .63$, which was based on a recent study of Colorado earthquakes.

The completeness periods listed in Table 6 were determined from plots of the number of earthquakes over time for the smaller magnitudes (Figures 14 a, b, c) and from Engdahl and Rinehart (1991) for the larger magnitudes ($M > 4.5$). Figures 15 a and b are space-time plots (latitude versus time and longitude versus time) for the catalog of magnitude ≥ 3 events with dependent events removed, starting in 1960. Figure 15 suggests generally random space-time properties for the corrected catalog. After filtering the catalog for the completeness periods summarized in Table 6, a total of 68 events remained. These are plotted in Figure 16.

Table 6. Completeness periods and event counts used in recurrence calculation

Magnitude range	Completeness period	Number of earthquakes
3.0 - 3.5	1/1960 - 12/1995	37
3.5 - 4.0	1/1960 - 12/1995	13
4.0 - 4.5	1/1960 - 12/1995	12
4.5- 5.0	1/1940 - 12/1995	5
5.0 - 5.5	1/1930 - 12/1995	0
5.5 - 6.0	1/1920 - 12/1995	1
6.0 - 6.5	1/1900 - 12/1995	0

Earthquake recurrence statistics were computed from the data set, using unequal observation periods for different magnitude ranges. The maximum likelihood method (Weichert, 1980) was used. Data variances were computed as suggested in Weichert (1980). Return period uncertainty bounds were calculated using the method of Bollinger and others (1989). These estimates incorporate significant uncertainty due to the spatial inhomogeneity of seismic monitoring in the region and lack of objective information regarding historic detection capabilities. Based on observation and judgement, it was assumed that the seismicity record is currently complete for magnitude 3 and greater. Although only one earthquake in the magnitude 5 to 6 range occurred in the study area, the October 1960 earthquake near Montrose in southwestern Colorado of magnitude 5.5, it is assumed that events unaccompanied by surface rupture in the magnitude 6 to 6.5 range can occur in this zone. This conclusion is consistent with the observations of dePolo (1994) for the western Basin and Range.

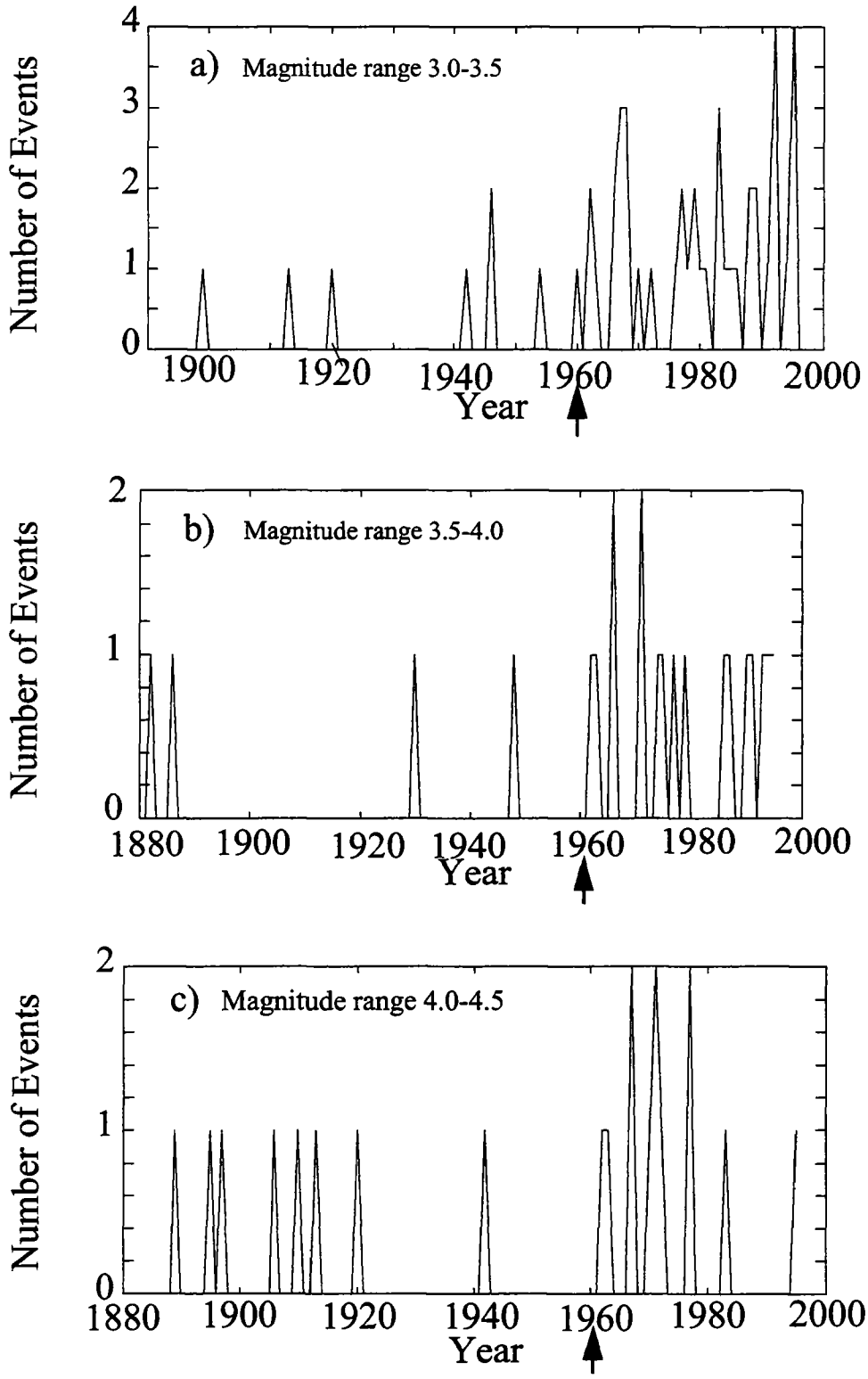

Figure 14. Number of earthquakes in three different magnitude ranges (a) 3.0-3.5, (b) 3.5-4.0, (c) 4.0-4.5 over time. Arrows indicate inferred beginning of complete recording for each magnitude interval.

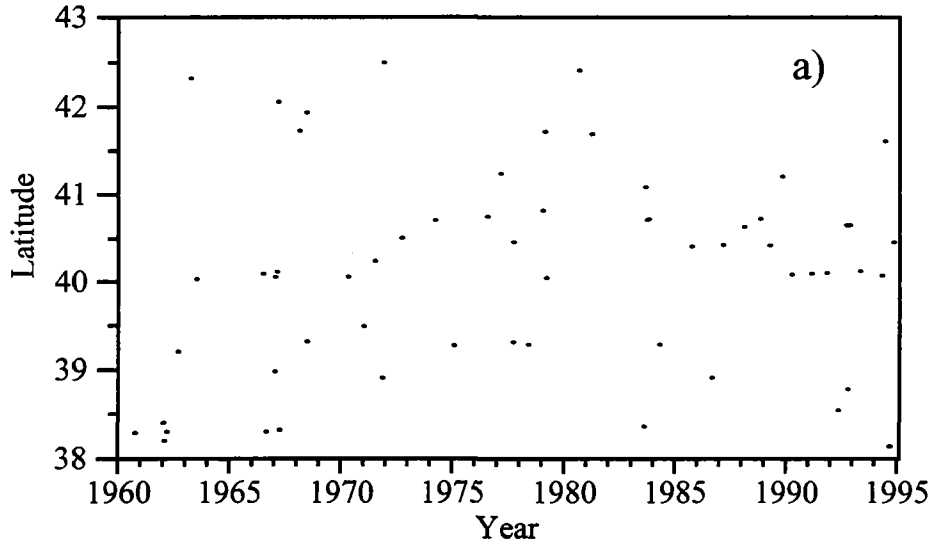

Figure 15a. Time versus latitude plot of independent events with magnitude ≥ 3 within Flaming Gorge study area.

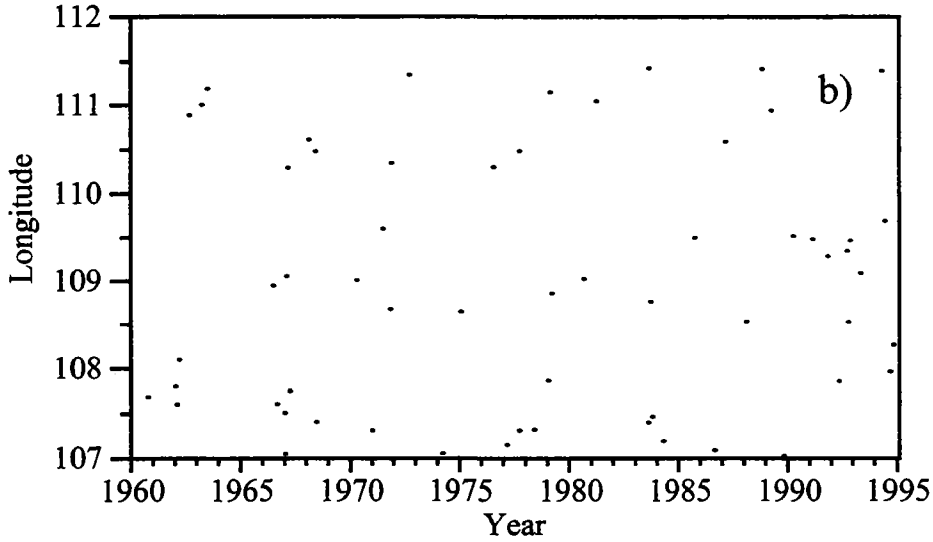

Figure 15b. Time versus longitude plot of independent events with magnitude ≥ 3 within Flaming Gorge study area.

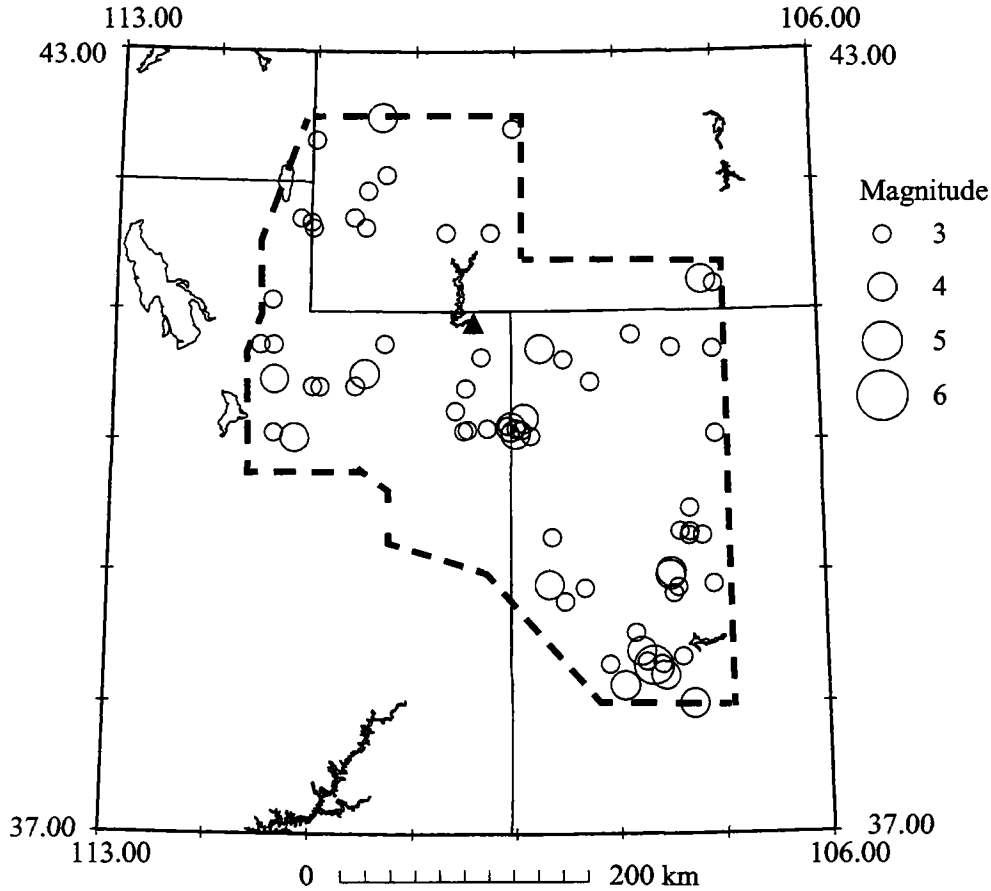

Figure 16. Earthquakes used in recurrence calculation, Flaming Gorge study area.

Figures 17 and 18 show the resulting maximum likelihood incremental and cumulative recurrence curves, and data and model bounds at the 95% confidence level for the magnitude range of 3.0 to 6.5. Each data point represents the annual rate for a given magnitude range. Table 7 lists the *a*- and *b*- values and their standard deviations, from the Gutenberg-Richter relation Log(N) = *a* - *b*(M), for both incremental and cumulative forms. The *a*- value is normalized to events per km^2 per year, based on the area of the study region of 133,230 km^2. The *b*- value for the cumulative relation is the same as for the incremental (Herrmann, 1975). Table 8 gives return periods for the different magnitude ranges, along with their 95% model confidence bounds as shown in Figures 17 and 18.

Table 7. Recurrence parameters

	a, incremental (σ)	*a*, cumulative (σ)	*b* (σ; inc,cum)
Flaming Gorge study area	-2.596 (.315)	-2.559 (.164)	.770 (.085,.047)

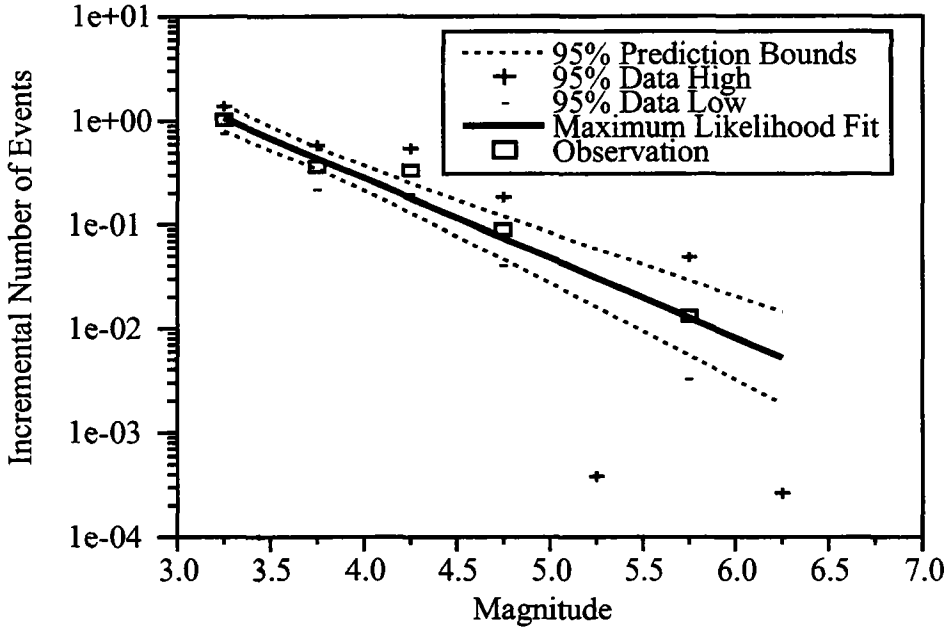

Figure 17. Incremental recurrence curve for the Flaming Gorge study area.

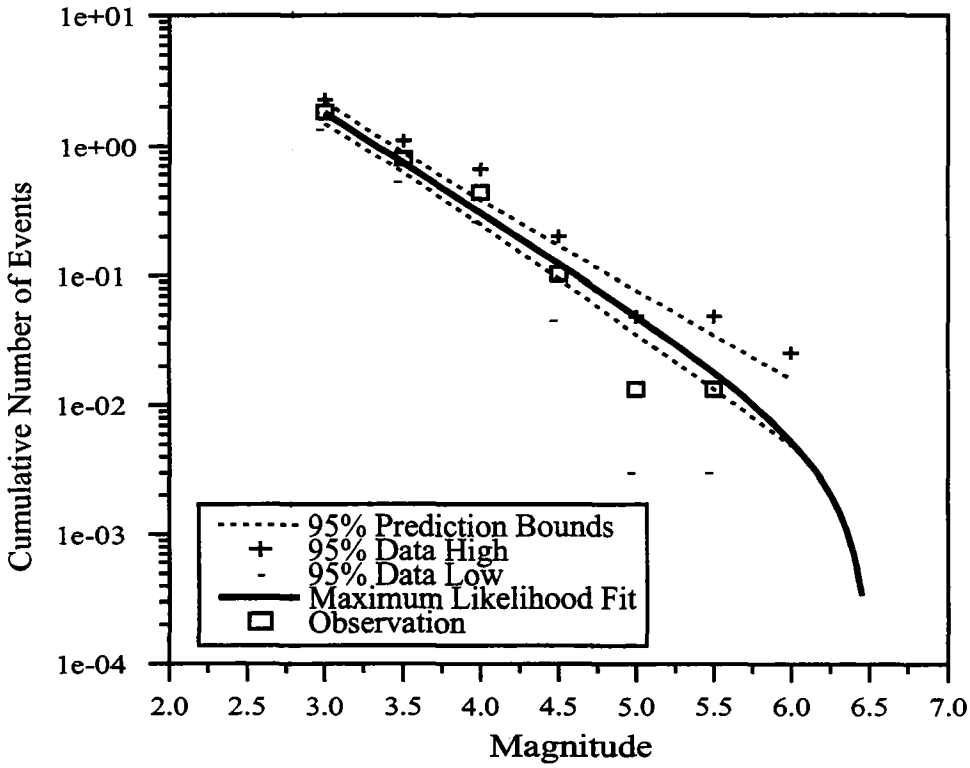

Figure 18. Cumulative recurrence curve for the Flaming Gorge study area.

Table 8. Observed and predicted return periods, with upper and lower bounds at 95% confidence for Flaming Gorge Dam

Magnitude range	Observed return period (yr)	Predicted return period (yr)	Lower bound	Upper bound
3.0 - 3.5	1.0	.9	.7	1.3
3.5 - 4.0	2.8	2.3	1.8	2.9
4.0 - 4.5	3.0	5.6	4.0	7.7
4.5 - 5.0	11	13	8.4	22
5.0 - 5.5	not observed	33	17	63
5.5 - 6.0	76	79	35	182
6.0 - 6.5	not observed	193	70	521

6. Evaluation of Faults As Potential Seismic Sources

Although a few faults in the area within about 50 km (30 mi) of the Flaming Gorge Dam have features suggestive of Quaternary surface rupture, we conclude that none has evidence for recurrent, large, latest Quaternary (since about 15 ka to 20 ka) ruptures. Characteristics of faults that were examined during this study for evidence of Quaternary surface rupture are summarized in Table 9.

A fault or faults that may be associated with the east-to-northeast-trending scarps along the north flank of Phil Pico Mountain do not appear to have experienced recurrent moderate to large earthquakes during the late Quaternary. Although the scarps are well expressed on an alluvial surface estimated to be between 130 ka-140 ka and 500 ka, the eroded character of the scarps and the presence of at least two and perhaps three younger alluvial-fan deposits that lack scarps suggest that surface rupture has not occurred here in a long time, since at least 13 ka to 14 ka, probably not since 30 ka to 40 ka, and perhaps not since 130 ka to 150 ka. The short length of surficial expression (about 4 km; 2.5 mi) and the small amount of net vertical displacement ($\leq$1.5 m; $\leq$5 ft) across the best-expressed graben also imply that any associated fault has not experienced a large amount of late Quaternary displacement. Thus, a fault that may be associated with the scarps along the north flank of Phil Pico Mountain is not considered to be a seismic source for Flaming Gorge Dam. This fault would come within about 40 km (24 mi) of the dam. Faults associated with similar scarps at Towanta Flat and near Elizabeth Ridge were not considered by Martin and others (1985, p. 71) or Sullivan and Ostenaa (1988, p. 1, 5) to be potential seismic sources for other dams in the region. Martin and others (1985, p. 71) concluded that faults associated with the scarps at Towanta Flat may have a nonseismogenic origin. This also could be true for the scarps along Phil Pico Mountain.

The presence of lineaments and a possible scarp along the southwest flanks of Diamond Peak and Middle Mountain suggests Quaternary tectonic displacement may have occurred on the northwest-striking Sparks fault that forms the northeastern boundary of the Uinta Mountains in northwest Colorado. However, a relationship between the scarps and the fault has not been established and is based solely on the close proximity of the surficial features to the mapped trace of the fault. The eroded character, short length, and discontinuity of the scarps and lineaments suggest that any associated fault rupture is older than latest Pleistocene (15 ka to 20 ka) and could be much older. Older Quaternary surfaces or deposits that could be used to evaluate such displacement are not preserved along the fault. On the basis of the characteristics of the lineaments and scarps, we conclude that the late Quaternary displacement rate has been very low, and thus, the fault should not be considered a seismic source for Flaming Gorge Dam. The Sparks fault is about 35 km (21 mi) east of the dam.

Because evidence for Quaternary surface displacement was not noted on the Uinta fault, which may be related to the Sparks fault, nor along any of the approximately east-striking faults between Flaming Gorge Dam and Browns Park, none of these faults is considered a seismic source. The closest of these faults is the Dutch John fault, which is about 2 km (1.2 mi) north of the dam.

Table 9. Characteristics of the faults examined for evidence of Quaternary activity in the area surrounding Flaming Gorge Dam[1]

Locality or fault (Possible related fault)	Surficial expression (evidence for Quaternary rupture)	Estimated amount of Quaternary surface displacement (m)	Youngest displaced unit; estimated age	Oldest undisplaced unit; estimated age	Estimated age of the youngest rupture	Quaternary surface expression (rupture length) (km)	Estimated average Quaternary displacement rate (mm/yr)	Estimated recurrence for Quaternary ruptures
North flank of Phil Pico Mountain (Henrys Fork fault)	Two 1-km-long graben; other scarps or slope breaks; lineaments	1.5 m across one graben that is bounded by scarps 10 and 5 m high; up to 1 m possible across lineaments	Scarps on alluvial surface ≤500 ka and older than 130 ka to 150 ka; lineaments on alluvial surface 130 ka -150 ka	Alluvial surface; 30 ka -40 ka to 13 ka-14 ka; surface 130 ka-150 ka may not be displaced	At least older than 13 ka to 14 ka; probably older than 30 ka to 40 ka; could be older than 130 ka to 150 ka	4.2	0.007 to 0.008 or less since 130 ka-150 ka; 0.003 or less since 500 ka	≥100 kyr?
Southwest flanks of Diamond Peak and Middle Mountain (Sparks fault)	Lineaments and a possible scarp on an alluvial fan at Diamond Peak	≤2	Older than 15 ka to 20 ka (could be much older)	--	Older than 15 ka to 20 ka (could be much older)	8.5 (includes a 2.5-km-long gap in expression)	≤0.001	--
Jessie Ewing Canyon (Uinta fault)	None observed	0?	--			0	0	--
Dutch John fault	None observed	0?	Bishop Conglomerate; 25 Ma-30 Ma	Alluvial surface on south flank of Goslin Mtn.; older than 130 ka to 150 ka	>1.6 Ma	0	0	--

Table 9. Characteristics of the faults examined for evidence of Quaternary activity in the area surrounding Flaming Gorge Dam[1] (Cont.)

Locality or fault (Possible related fault)	Surficial expression (evidence for Quaternary rupture)	Estimated amount of Quaternary surface displacement (m)	Youngest displaced unit; estimated age	Oldest undisplaced unit; estimated age	Estimated age of the youngest rupture	Quaternary surface expression (rupture length) (km)	Estimated average Quaternary displacement rate (mm/yr)	Estimated recurrence for Quaternary ruptures
Mountain Home fault	8-km-long linear slope break along the base of Mountain Home	0?	Browns Park Formation; 10 Ma-25 Ma	Dissecte alluvial fan 3.5 km east of Red Creek; older than 15 ka to 20 ka, perhaps >100 ka	>100 ka; perhaps >1.6 Ma	0?	0?	--
Beaver Creek fault	4-km-long lineament along the base of Cold Spring Mtn.	0?	Browns Park Formation; 10 Ma-25 Ma	Large alluvial fan at the mouth of Beaver Creek; older than 11 ka to 15 ka	>100 ka; perhaps >1.6 Ma	0?	0?	--
Diamond Gulch fault	Scarps and a linear drainage south of Diamond Gulch	Less than 25 to 30 (could be much less)	Alluvial surfaces; >100 ka (could be much older)	Alluvial fan near the south-east end; older than 10 ka to 15 ka	≥100 ka (could be much older)	19.5	<0.02 (could be much less)	--
Pot Creek fault	Poorly defined scarps south of Pot Creek	<20 (could be much less)	Alluvial surfaces; ages unknown	--	>100 ka (could be much older)	9.4	<0.01 (could be much less)	--
Whiterocks River to Ashley Creek (Eastern portion of the South Flank fault or Marsh Peak fault)	5.5-km-long escarpment in Precambrian through Pennsylvanian rocks or scarps onBishop Conglomerate	0?	Bishop Conglomerate; 25 Ma-30 Ma	Till correlated to the Bull Lake Glaciation; older than 140 ka to 150 ka (Bishop Conglomerate along part?)	Older than 140 ka to 150 ka; (could be much older)	0?	0?	--

[1]Based on expression on aerial photographs and field reconnaissance
Dashes indicate data that are not known or cannot be estimated on the basis of available studies.

For the faults along or adjacent to the south flank of the Uinta Mountains, the Diamond Gulch and Pot Creek faults have scarps associated with them. However, these scarps are short, very rounded, and markedly dissected. They appear to be best expressed where they are underlain by the Bishop Conglomerate near drainages. These characteristics suggest that the scarps, even if they have a tectonic origin, are quite old, perhaps pre-Quaternary. It is possible that the scarps are very old and have been preserved at the surface because of the induration of the Bishop Conglomerate or because they have been exhumed. Thus, we conclude that neither of these faults should be considered seismic sources. The Diamond Gulch fault is 27 km (16 mi) south of Flaming Gorge Dam. The Pot Creek fault is 22 km (13 mi) southeast of the dam.

The eastern section of the east-northeast-striking South Flank fault or Marsh Peak fault is shown by Rowley and others (1985) to displace the Tertiary Bishop Conglomerate (25 Ma-30 Ma). This fault is about 30 km south-southwest of Flaming Gorge Dam. Weakly expressed scarps appear to coincide with this section. However, the best expression of the fault is an escarpment where Precambrian Uinta Group on the higher side of the escarpment is juxtaposed against weaker Mississippian and Pennsylvanian rock on the lower side. The best expression of both the scarps on the Bishop Conglomerate and the escarpment is near drainages, which suggests that the feature are likely, at least in part, erosional rather than entirely tectonic in origin. In addition, the lack of evidence for fault rupture on surfaces of Pleistocene till near Dry Fork of Ashley Creek suggests that any displacement on the fault is older than at least 140 ka to 150 ka. The youngest displacement on the fault could be much older. Consequently, the Marsh Peak fault is not considered to be a seismic source for Flaming Gorge Dam.

7. Probabilistic Seismic Hazard Analysis

7.1. Methodology

A probabilistic seismic hazard analysis (PSHA) was performed for Flaming Gorge Dam. Based upon the lack of faults considered to be potential seismic sources (as summarized in Chapter 6), a single areal seismic source zone was considered. The basic methodology follows that of Cornell (1968) and McGuire (1974, 1978). A gridded point-source model was used to represent the hazard at the site. The geographic configuration of the zone is shown in Figures 12 and 13.

The ground motion attenuation relations of Sadigh and others (1997) and Spudich and others (1996) for rock site conditions were used. The Sadigh and others (1997) relation is based on recordings from shallow crustal earthquakes, with multiplicative factors to account for different faulting types. The relation of Spudich and others (1996) is derived from recordings from extensional tectonic environments, and is thus relevant to the study area. In both relations ground motion is for the randomly oriented horizontal component. Equal weights were assigned to the two relationships in the PSHA.

Because the Spudich and others (1996) function uses the closest distance to the surface projection of the fault as the distance measure, the depth distribution of earthquakes is not an issue for that relation. For the Sadigh and others (1997) relation, however, distance is defined as the closest distance to the fault rupture surface, and therefore the depth distribution of earthquakes in the region must be accounted for. Earthquake depths from studies by several authors in Utah, Montana, and Idaho were summarized by Smith and Arabasz (1991). That study suggested that the base of the seismogenic layer within the ISB is at a depth of about 10 to 15 km (6 to 9 mi). Within the Colorado Plateau and the Rocky Mountains, where the lithosphere is inferred to be cooler, focal depths can sometimes reach 30 to 40 km (18 to 24 mi; Wong and Chapman, 1990). For southwestern Colorado, some depth information is available since installation of the two USBR seismic networks in southwestern Colorado. Figure 19 shows depth statistics from earthquakes that occurred between 1989 and 1995 in southwestern Colorado and that were recorded by the Ridgway and Paradox seismic networks. From these sources of information a depth range for the seismicity in the Flaming Gorge study area was assumed to be zero to about 16 km (10 mi). The depth distribution was handled similarly to LaForge and Ake (1999). For the ground motion calculations, hypocentral depths of earthquakes in the M_w 5.5 to 6.5 range were assumed to be limited to less than 16 km (10 mi), with a modal value of 8 km (5 mi). The modal value is reasonable given the peak seen in Figure 19. Minimum hypocentral depths should be a function of magnitude, due to fault area and hydrostatic stress considerations. In order to estimate the minimum depth of a non-surface rupturing earthquake, depths were assumed to be equivalent to the radius of a circular crack with a 100 bar stress drop, occurring on a 60°-dipping fault. The 100 bar value is consistent with estimates for continental earthquakes by Kanamori and Anderson (1975). Minimum depths were computed for midpoint values of the four magnitude ranges (Figure 20) used in the probabilistic model. Triangular probability distributions for each magnitude range are shown in Figure 20. Each distribution was discretized into 5 equal-probability values.

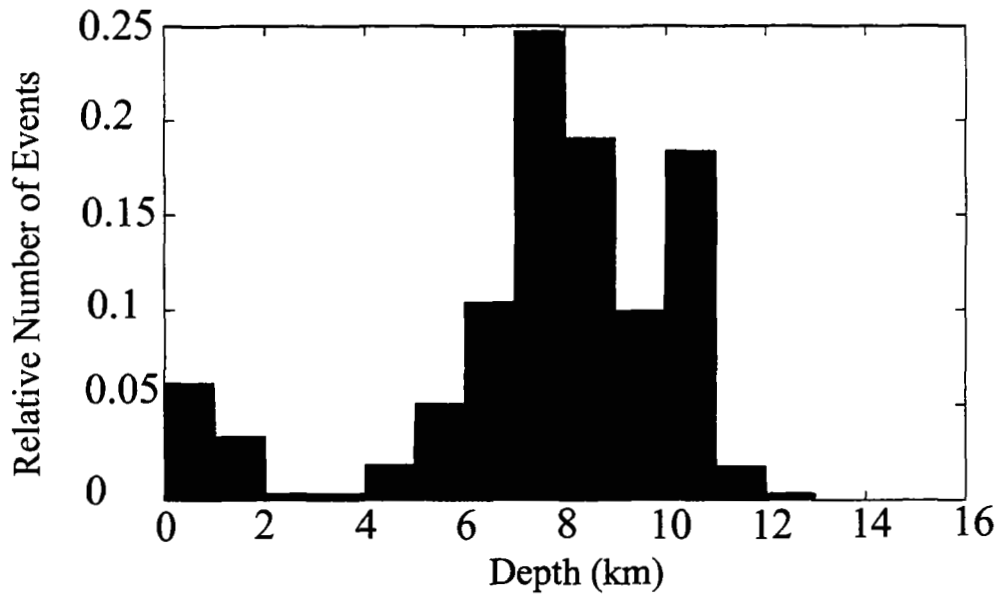

Figure 19. Depth histogram of earthquakes in the area of Ridgway seismic network. Uncertainties in depths are about ±2 km (as given by the location program Fasthypo; Herrmann, 1979).

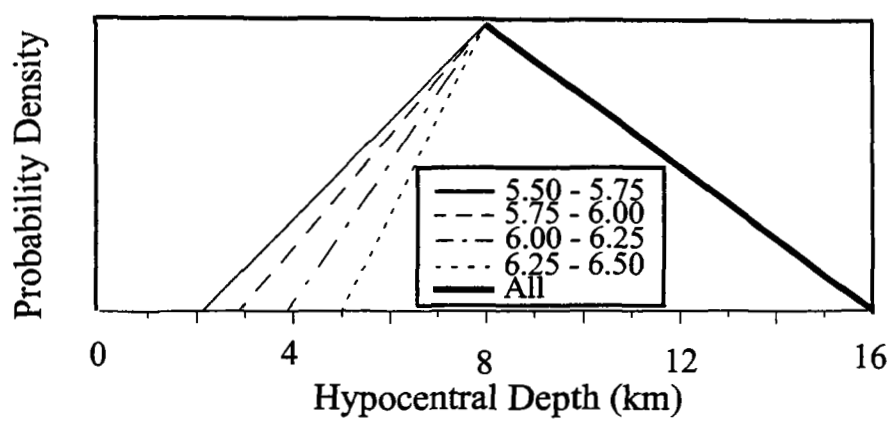

Figure 20. Schematic probability density functions of focal depths for the magnitude ranges used in the probabilistic analysis.

Uncertainties in ground motion attenuation and seismicity rates were treated by complete enumeration of the respective distributions (LaForge and Ake, 1999). This was accomplished by discretizing the log-normal distributions for each parameter into 50 equal-probability values, bounded at 2.5 standard deviations above and below the median value. The random source model was then executed for each parameter combination and each of the five depth values, resulting in

50^2 x 5 = 12,500 annual frequencies for each ground motion exceedance level. The arrays of annual frequency values for each exceedance level were then ordered and integrated into probability density functions.

7.2. Results

7.2.1. Peak Horizontal Acceleration (PHA) Hazard Curves

Figure 21 shows median hazard curves for the two attenuation relations. It can be seen that the attenuation relation of Spudich and others (1996) gives slightly lower PHA values for annual probabilities of exceedance $<10^{-3}$ than the relation of Sadigh and others (1997). Figure 22 shows the final weighted PHA hazard curves at 16th, 50th, and 84th percentile levels. Figure 23 shows return periods of PHA exceedances and their percentile levels in the form of a hazard probability surface. Median PHA for annual frequencies of exceedance values of 1×10^{-4} and 2×10^{-5} (return periods of 10,000 and 50,000 years) are listed in Table 10.

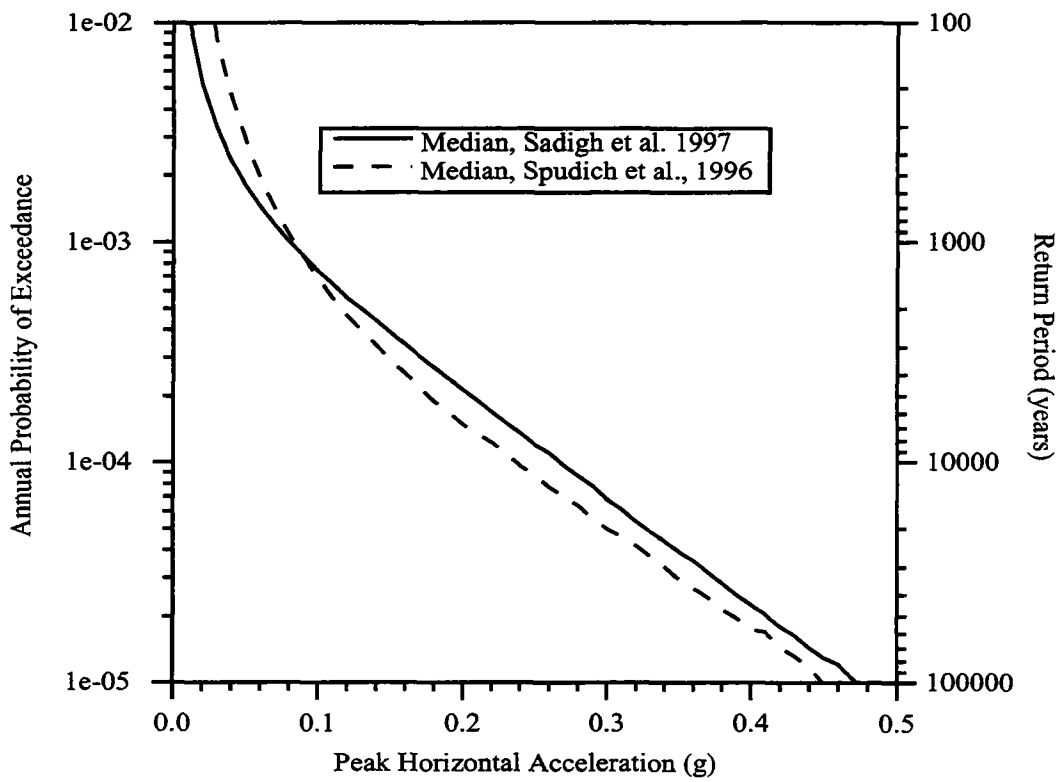

Figure 21. Median PHA hazard curves for Flaming Gorge Dam, calculated with the attenuation curves of Sadigh and others (1997) and Spudich and others (1996).

7.2.2. Spectrum Intensities

Acceleration and velocity spectrum intensities for the two annual probabilities of exceedance (return periods) were derived from the PSHA as defined in von Thun and others (1988). As before, median, 16th, and 84th percentile values were calculated. The results are given in Table 10.

Table 10. PHA and Spectrum Intensities

	PHA (g)			ASI (cm/sec)			VSI (cm)		
Return period	16th %	Median	84th %	16th %	Median	84th %	16th %	Median	84th %
10,000 yr	0.16	.25	0.32	144	217	276	36	63	82
50,000 yr	0.285	.40	0.46	236	346	404	67	103	123

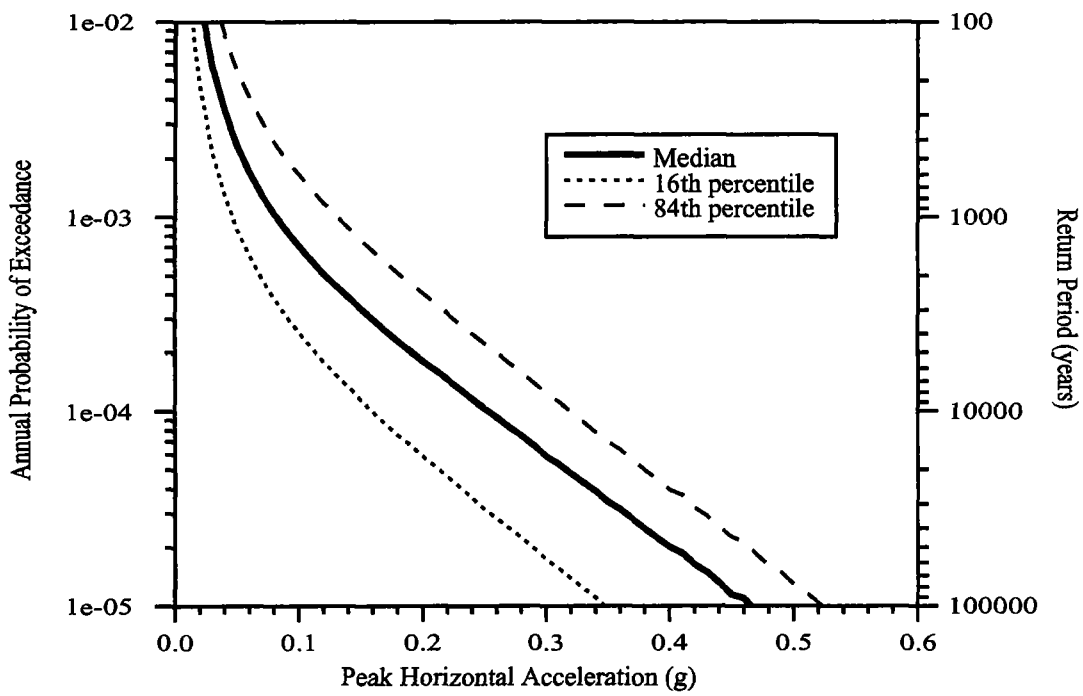

Figure 22. PHA hazard curves for Flaming Gorge Dam.

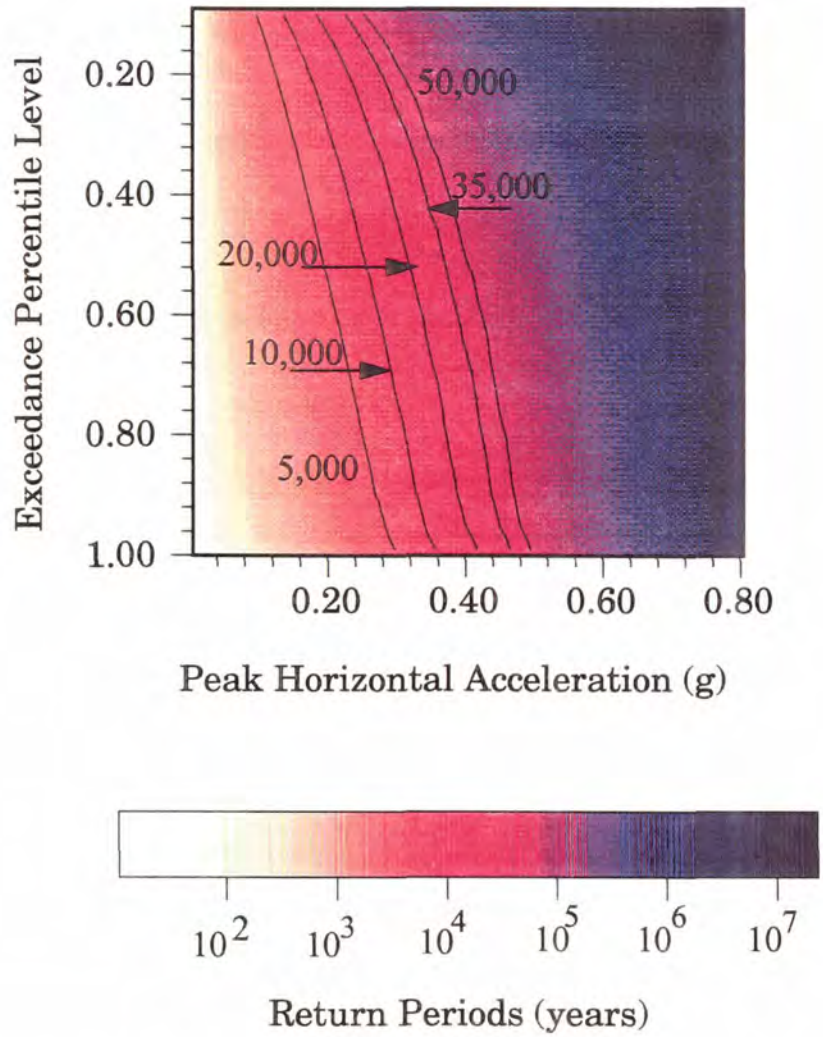

Figure 23. PHA hazard surface with contours indicating 5,000-, 10,000-, 20,000-, 35,000-, and 50,000-year return periods.

7.2.3. Uniform Hazard Spectra

A uniform hazard acceleration response spectrum (UHS) is defined as a spectrum where each ordinate has an equal probability of being exceeded. Acceleration response spectra (5% damping) were derived from the PSHA results. Figure 24 shows response spectra with uncertainties for annual probabilities of exceedance of 2×10^{-5} (50,000-year return period) and 1×10^{-4} (10,000-year return period), and Figure 25 shows the median UHS for the averaged attenuation relations for the two return periods.

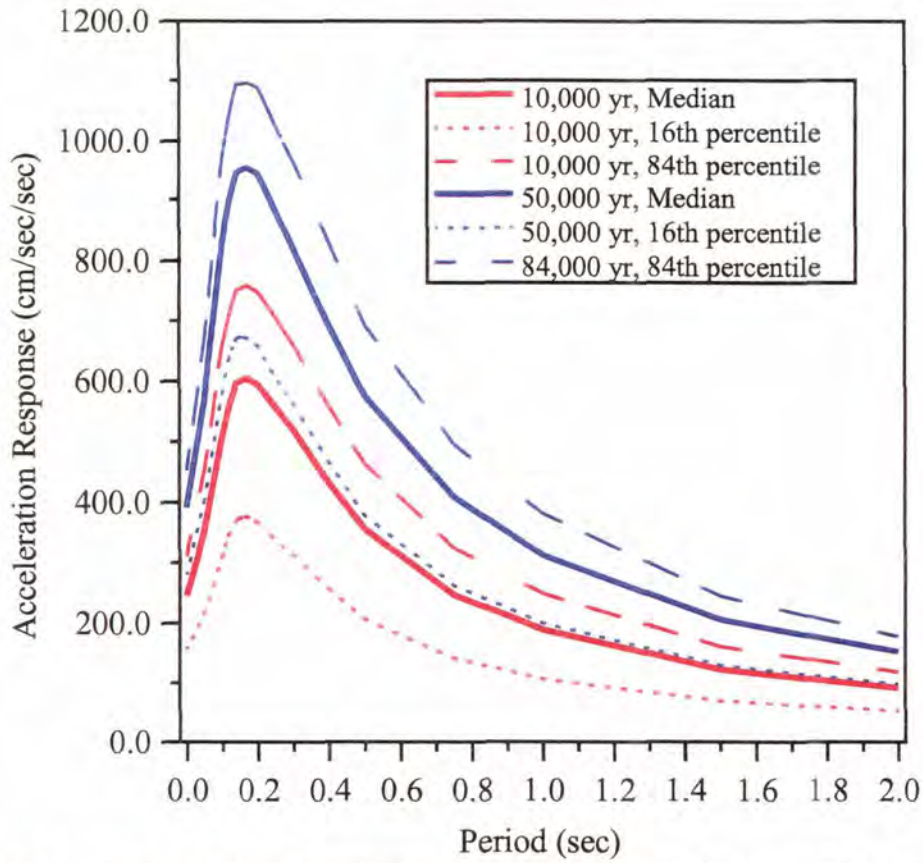

Figure 24. 5% damped acceleration response spectra for 10,000- and 50,000-year return periods, Flaming Gorge Dam.

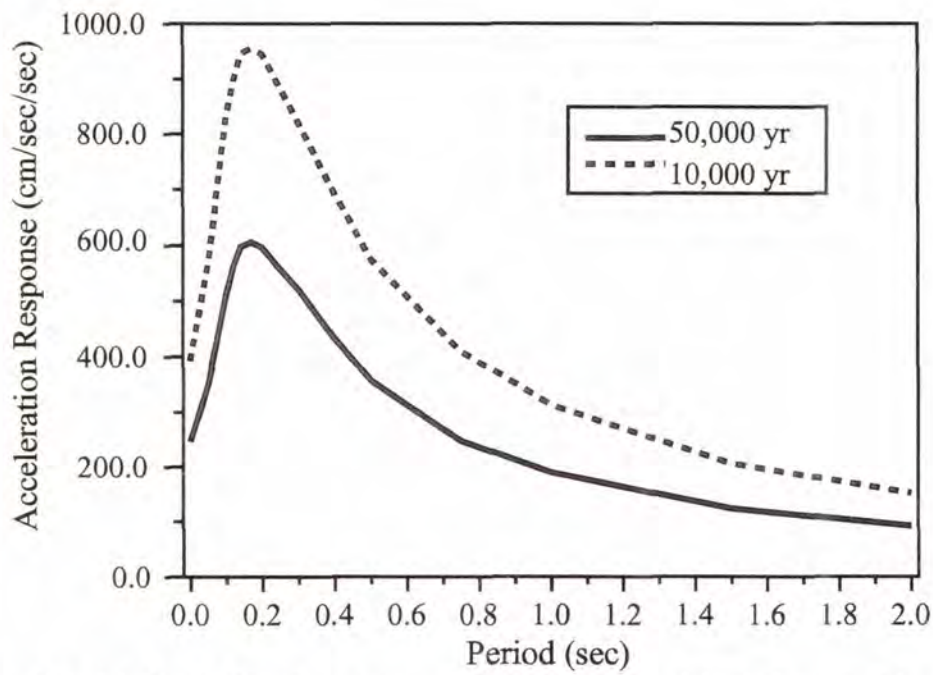

Figure 25. Median UHS for return periods of 50,000 and 10,000 years, Flaming Gorge Dam.

8. Acceleration Time Histories

The dynamic response of many structures depends not only on spectral amplitude but on the phase content of the waveforms as well (Abrahamson and Bolt, 1985). To ensure sufficient variability in phase content for dynamic analyses and to provide a three-dimensional characterization of ground motion, appropriate existing strong ground motion recordings have been selected. Flaming Gorge Dam has a critical response interval between about 0.15 and 0.5 seconds (Frank Jackmauh, oral communication, 1999). Three-component empirical time histories consistent with the UHS results for 50,000- and 10,000-year return periods were selected for use in the dynamic analysis of the dam.

For the 50,000-year return period, recommended time histories for the analysis of Flaming Gorge Dam are the recordings from the Long Valley Dam (upper left abutment) station, a rock site, that recorded the M_w 6.0 (M_L 6.2) Mammoth Lakes earthquake of May 27, 1980, 14:51 UTC. The earthquake was a shallow, oblique-slip event. The spectra of the horizontal components are compared to the target spectrum in Figure 26. Figure 27 shows the 50,000-year UHS together with the average of the two empirical horizontal spectra, and Figures 28 (a, b and c) show the three seismograms of the empirical records.

For the 10,000-year return period, recommended time histories for the analysis of Flaming Gorge Dam are the recordings from the Castlegate Street station in Compton, a deep soil site, that recorded the M_w 6.0 (M_L 5.9) Whittier Narrows earthquake of October 1, 1987, 14:42 UTC. The earthquake was an oblique-thrust event. The spectra of the two horizontal components are compared with the 10,000-year UHS in Figure 29. Figure 30 shows the 10,000-year UHS together with the average of the two empirical horizontal spectra, and Figures 31 (a, b and c) show the three seismograms of the empirical records.

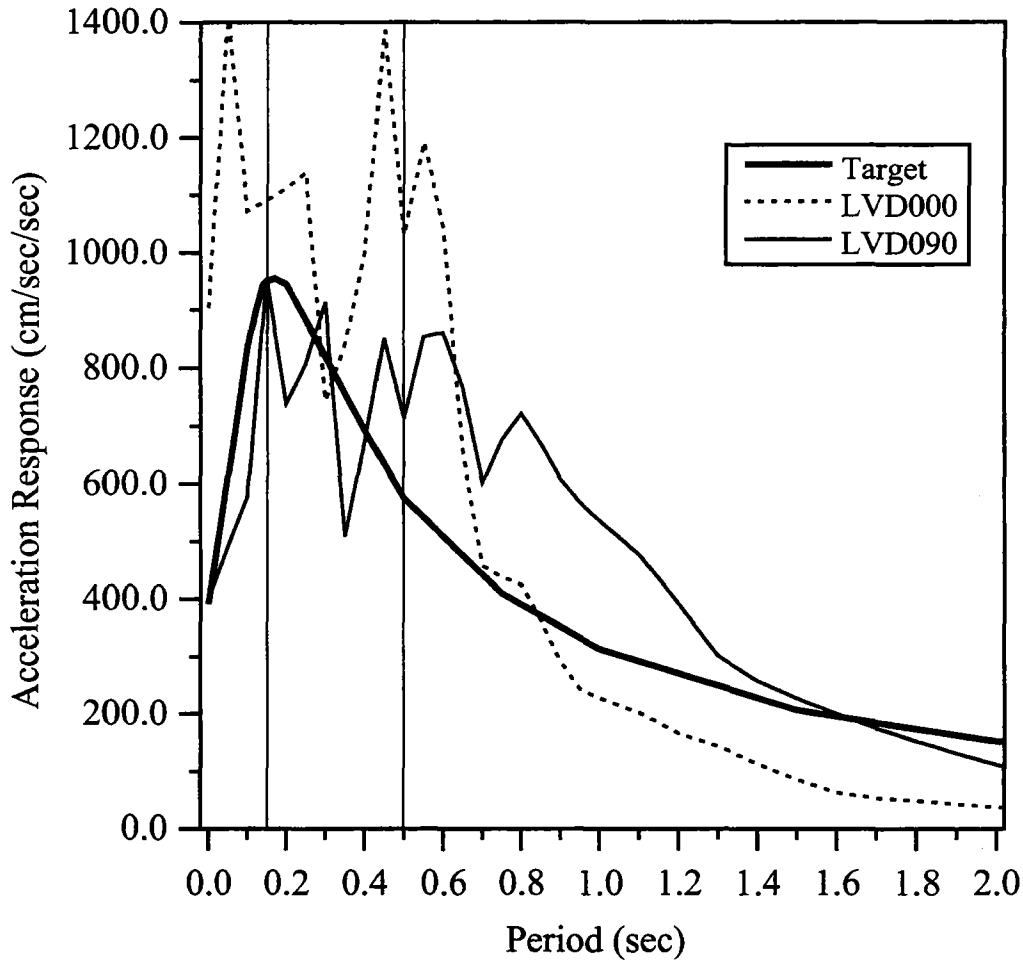

Figure 26. Comparison between median 50,000-year UHS (target) and two horizontal components (LVD000 and LVD090) of records from the May 27 1980, 14:51 UTC Mammoth Lakes earthquake, M_w 6.0, recorded at the Long Valley Dam (upper left abutment) station, which is a rock site. The two vertical lines mark the estimated response interval of Flaming Gorge Dam.

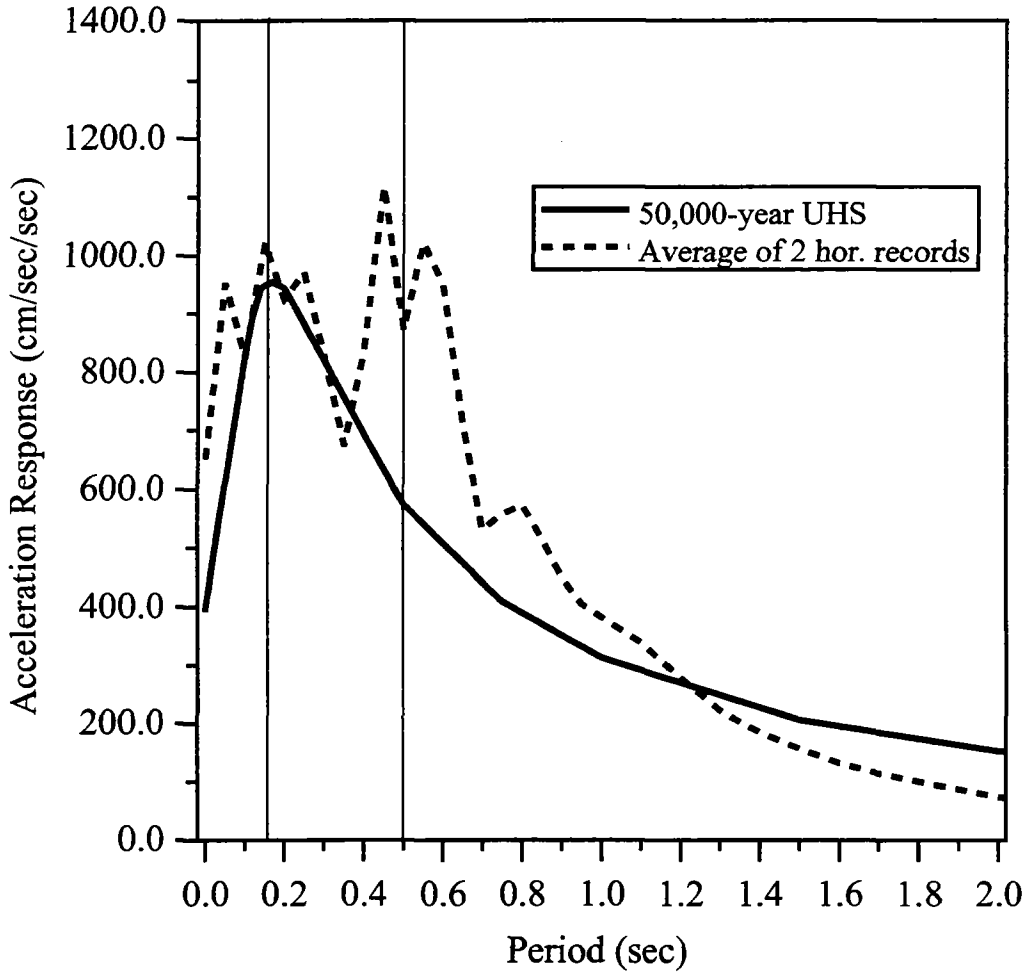

Figure 27. Comparison between median 50,000-year UHS (target) and the average of the two empirical horizontal spectra shown in Figure 26. The two vertical lines mark the estimated response interval of Flaming Gorge Dam.

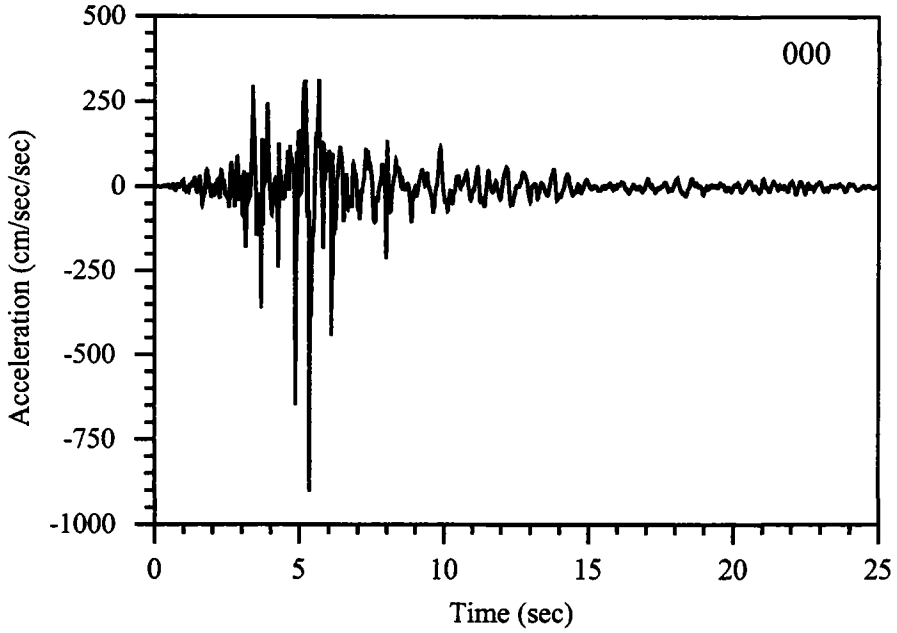

Figure 28a. 000-component of the Long Valley Dam (upper left abutment) record of the Mammoth Lakes earthquake of May 27, 1980, 14:51 UTC, M_w 6.0.

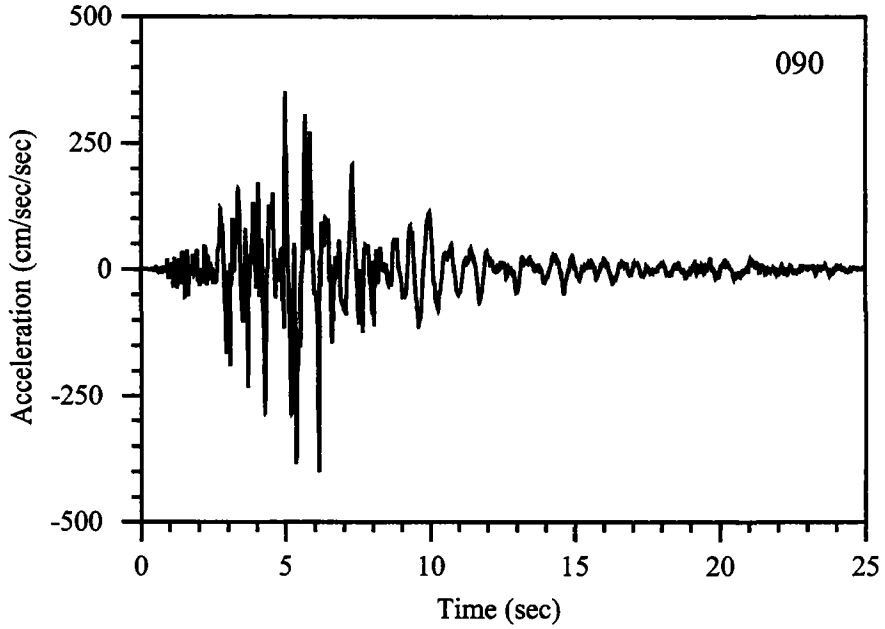

Figure 28b. 090-component of the same record as in Figure 28a.

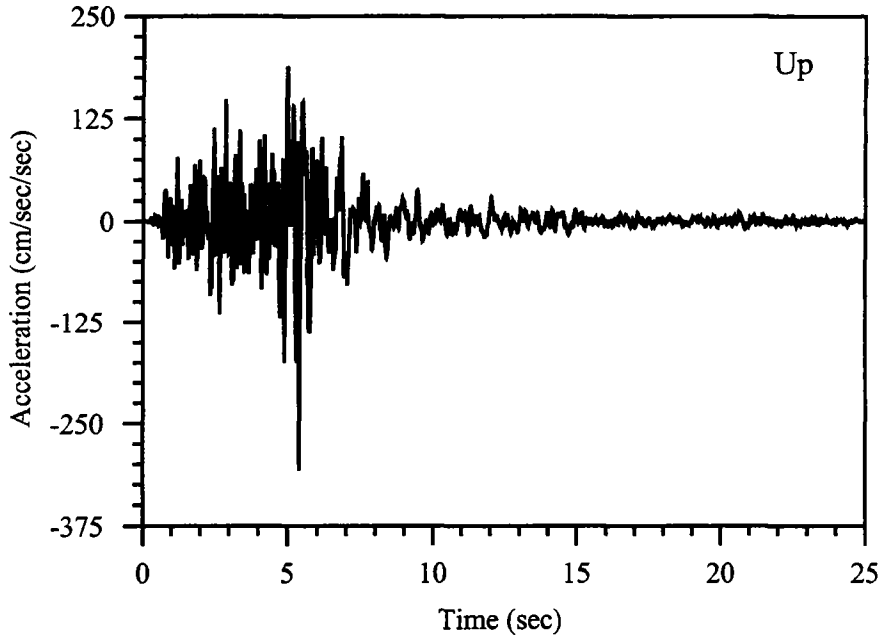

Figure 28c. Vertical component of the same record as in Figure 28a.

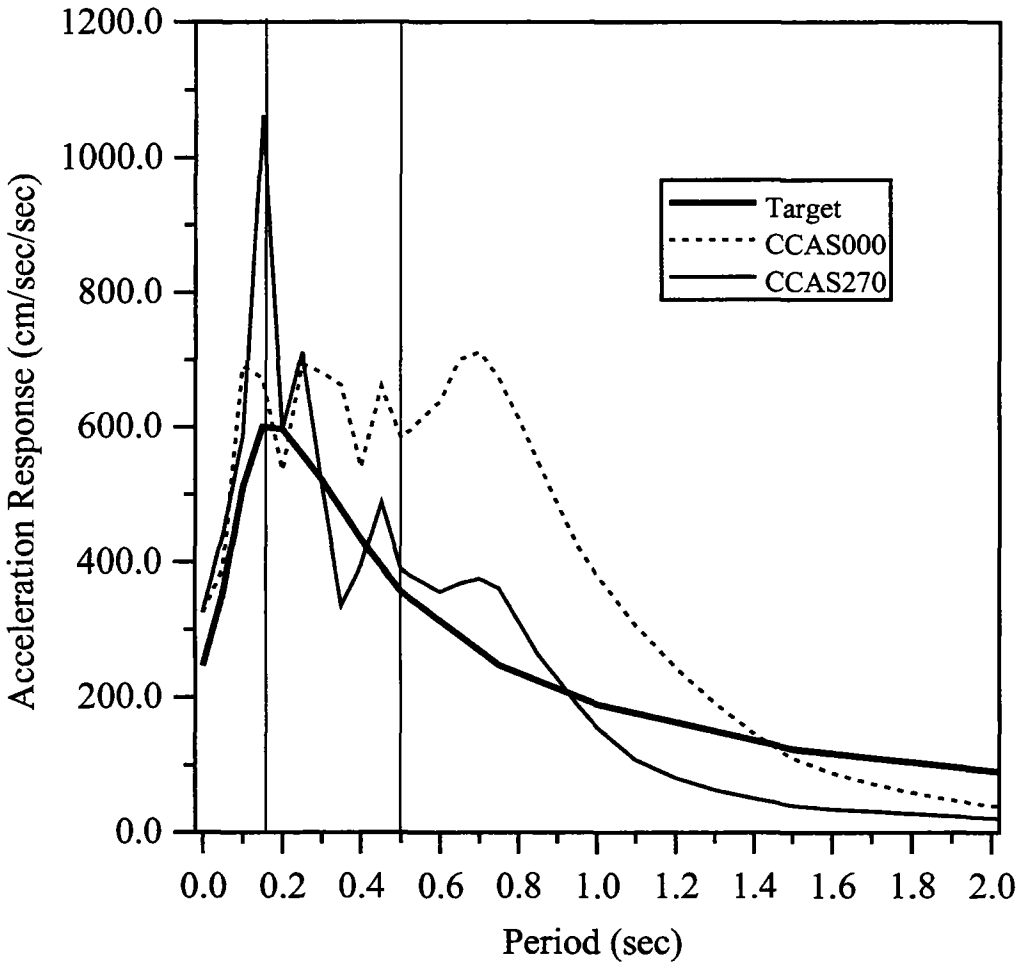

Figure 29. Comparison between median 10,000-year UHS (target) and the two horizontal components (CCAS000 and CCAS270) of records from the October 1, 1987, 14:42 UTC Whittier Narrows earthquake, M_W 6.0, recorded at the Compton - Castlegate Street station, which is a deep soil site. The two vertical lines mark the estimated response interval of Flaming Gorge Dam.

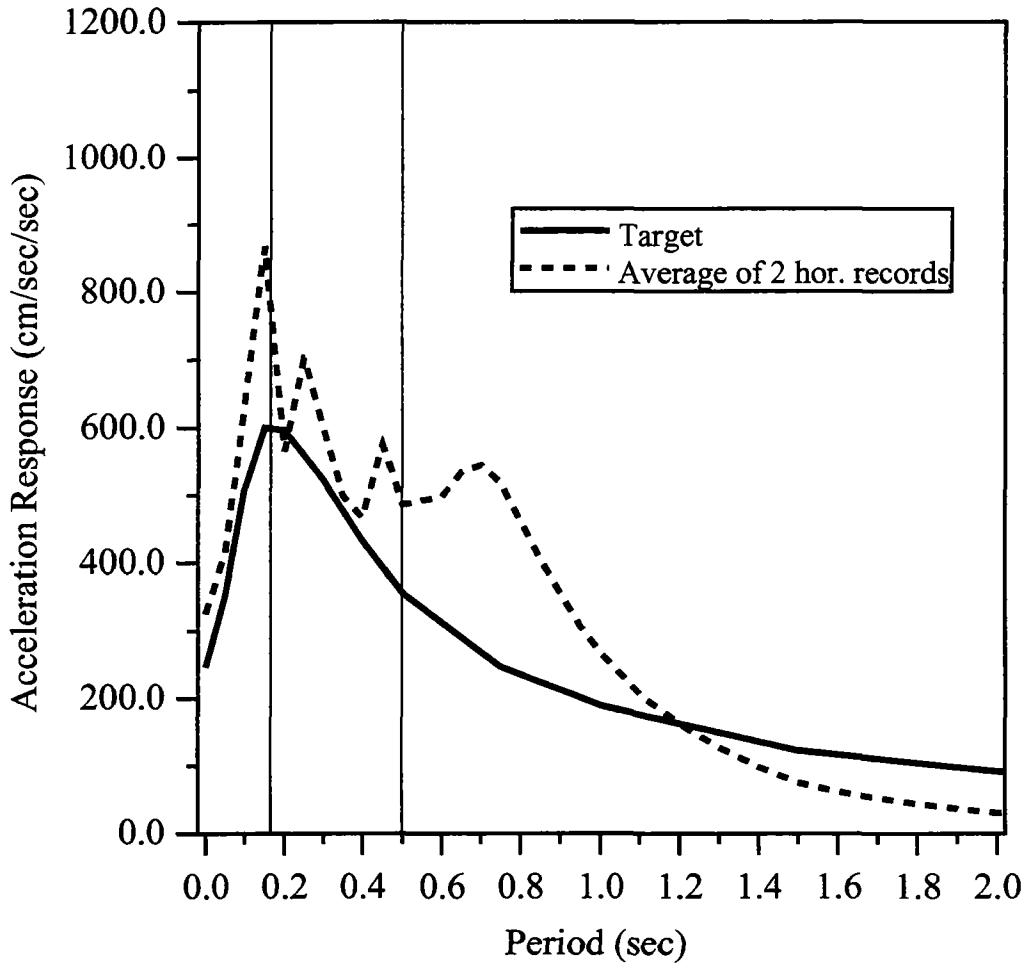

Figure 30. Comparison between median 10,000-year UHS (target) and the average of the two empirical horizontal spectra shown in Figure 29. The two vertical lines mark the estimated response interval of Flaming Gorge Dam.

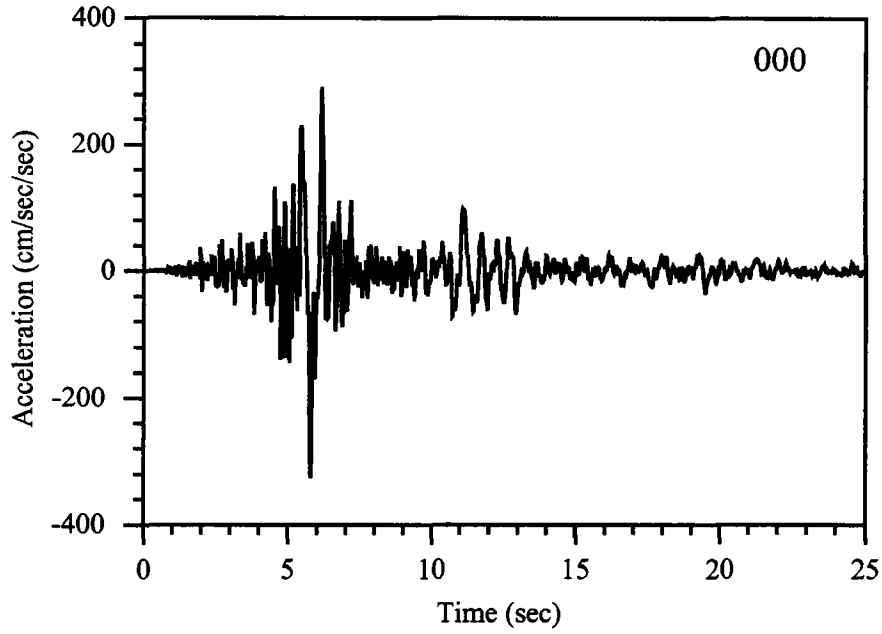

Figure 31a. 000-component of the Compton - Castlegate Street record of the Whittier Narrows earthquake of October 1, 1987, 14:42 UTC, M_w 6.0.

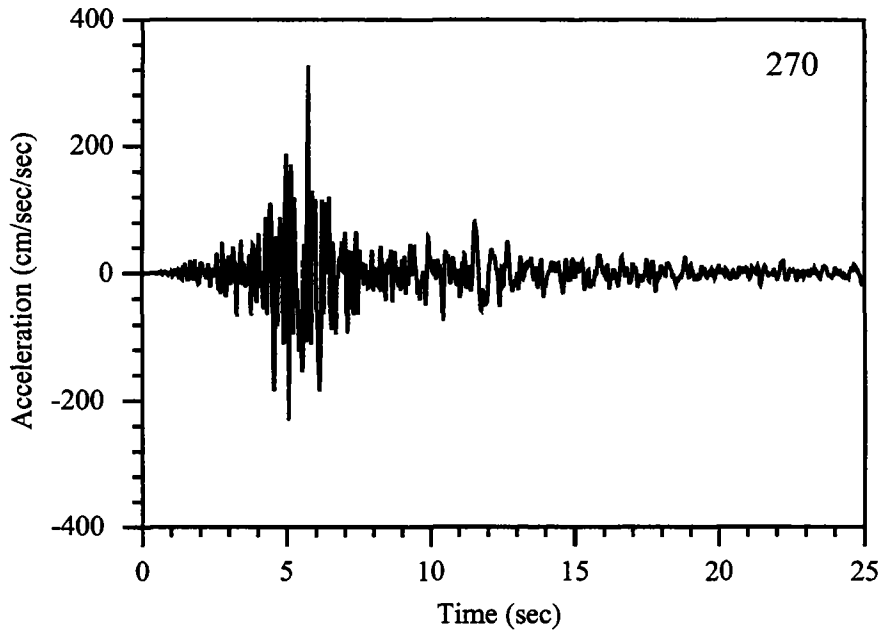

Figure 31b. 270-component of the same record as in Figure 31a.

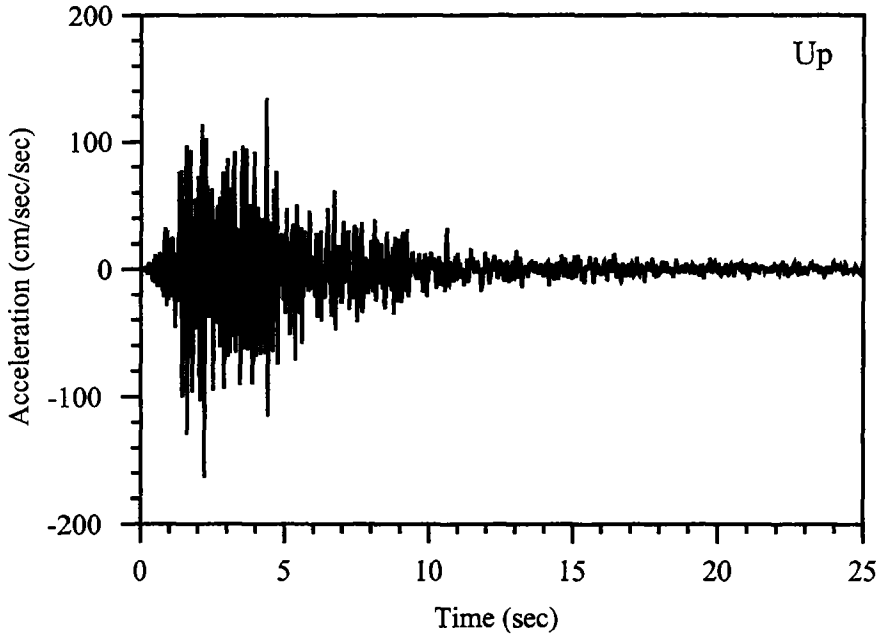

Figure 31c. Vertical component of the same record as in Figure 31a.

Peak horizontal acceleration, acceleration spectrum intensity (ASI), and velocity spectrum intensity (VSI) of the target UHS and the selected empirical records are compared in Table 11.

Table 11. Suggested ground motion characteristics

Parameter source	PHA (g)	ASI (cm/sec)	VSI (cm)
UHS 50,000 yr	0.40	346	104
LVD, 000 comp.	0.92	418	78
LVD, 090 comp.	0.41	305	125
average, LVD hor. records	0.66	361	102
LVD, up comp.	0.31	202	12
UHS, 10,000 yr	0.25	217	63
CCAS, 000 comp.	0.33	254	83
CCAS, 270 comp.	0.33	229	42
average, CCAS hor. records	0.33	242	63
CCAS, up comp.	0.17	74	3

LVD = Long Valley Dam (upper left abutment); CCAS = Compton, Castlegate Street.

Figures 32 and 33 compare the UHS for 50,000- and 10,000-year return with the average of the two selected horizontal empirical records.

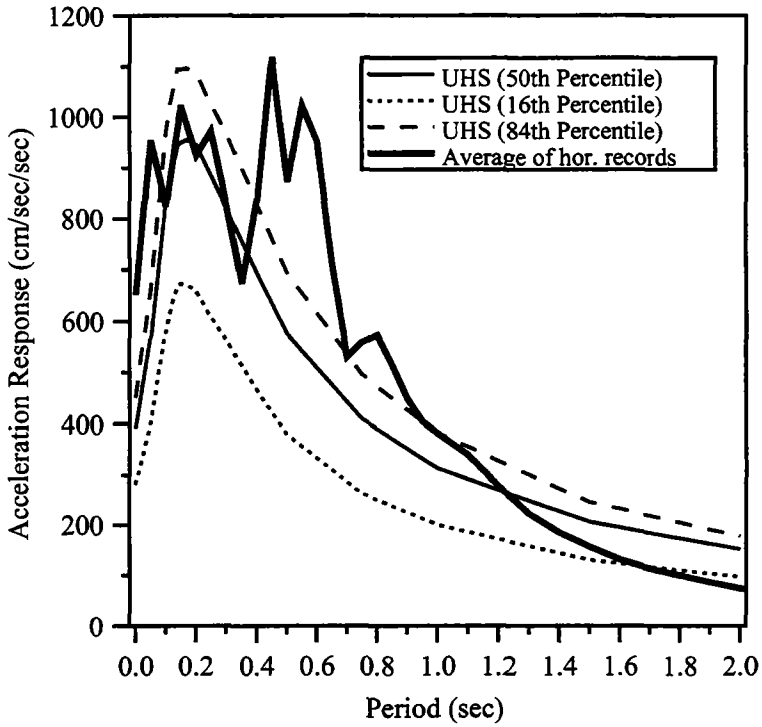

Figure 32. Comparison of UHS for 50,000 years (with confidence bounds) to average spectrum of suggested horizontal records of the Mammoth Lakes earthquake of May 27, 1980 (see Figure 26).

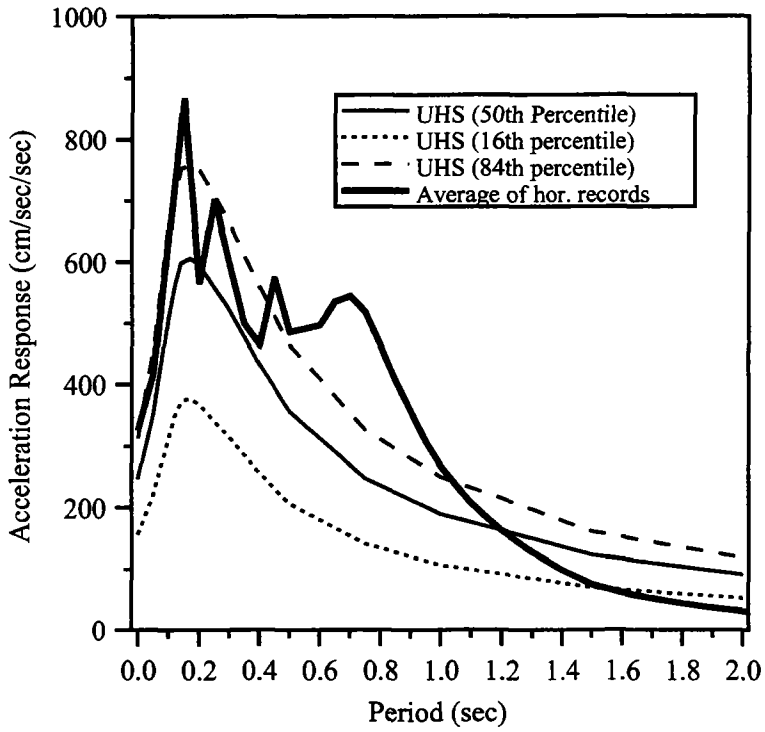

Figure 33. Comparison of UHS for 10,000 years (with confidence bounds) to average spectrum of suggested horizontal records of the Whittier Narrows earthquake of October 1, 1987 (see Figure 2).

9. References

Abrahamson, N.N., and Bolt, B.A., 1985, The spatial variation of the phasing of seismic strong ground motion: Bulletin of the Seismological Society of America, v. 75, p. 1247-1265.

Anderman, G.G., 1955, Tertiary deformations history of a portion of the north flank of the Uinta Mountains in the vicinity of Manila, Utah: Wyoming Geological Association, 10th Annual Field Conference Guidebook, Green River Basin, p. 130-134.

Anderson, L.W., and Miller, D.G., 1979, Quaternary fault map of Utah: Long Beach, California, Fugro, Inc., map scale 1:500,000, 35 p.

Birkeland, P.W., 1984, Soils and geomorphology: New York, Oxford University Press, 372 p.

Bollinger, G.A., Davison, F.C., Sibol, M.S., and Birch, J.B., 1989, Magnitude recurrence relations for the southeastern United States and its subdivisions: Journal of Geophysical Research, v. 94, p. 2857-2873.

Bucknam, R.C., and Anderson, R.E., 1979, Estimation of fault scarp ages from a scarp-height-slope-angle relationship: Geology, v. 7, no. 1, p. 11-14.

Bull, W.B., 1991, Geomorphic responses to climatic change: New York, Oxford University Press, 326 p.

Carrara, P.E., 1980, Surficial geologic map of the Vernal 1° x 2° quadrangle, Colorado and Utah: U.S. Geological Survey Miscellaneous Investigations Map I-1204, scale 1:250,000.

Carver, David, Richins, W.D., and Langer, C.J., 1983, Details of the aftershock process following the 30 September 1977 Uinta Basin, Utah, earthquake: Bulletin of the Seismological Society of America, v. 73, no. 2, p. 435-448.

Colman, S.M., 1985, Map showing tectonic features of late Cenozoic origin in Colorado: U.S. Geological Survey Miscellaneous Investigations Series Map I-1566, scale 1:1,000,000.

Cornell, C.A., 1968, Engineering seismic risk analysis: Bulletin of the Seismological Society of America, v. 58, p. 1583-1606.

dePolo, C.M., 1994, The maximum background earthquake for the Basin and Range province, western North America: Bulletin of the Seismological Society of America, v. 84,p. 466-472.

Engdahl, E.R., and Rinehart, W.A., 1991, Seismicity map of North America Project, *in* Slemmons, D.B., Engdahl, E.R., Zoback, M.D., and Blackwell, D.D., eds., Neotectonics of North America: Boulder, Colorado, Geological Society of America, Decade Map Volume 1.

Hall, R.D., and Shroba, R.R., 1993, Soils developed in the glacial deposits of the type areas of the Pinedale and Bull Lake Glaciations, Wind River Range, Wyoming, U.S.A.: Arctic and Alpine Research, v. 25, no. 4, p. 368-373.

Hansen, W.R., 1957, Geology of the Clay Basin quadrangle, Utah: U.S. Geological Survey Geologic Quadrangle Map GQ-101, scale 1:24,000.

Hansen, W.R., 1965, Geology of the Flaming Gorge area, Utah-Colorado-Wyoming: U.S. Geological Survey Professional Paper 490, map scale 1:48,000, 3 pls., 196 p.

Hansen, W.R., 1969, The geologic story of the Uinta Mountains: U.S. Geological Survey Bulletin 1291, 144 p.

Hansen, W.R., 1977, Geologic map of the Jones Hole quadrangle, Uinta County, Utah, and Moffat County, Colorado: U.S. Geological Survey Geologic Quadrangle Map GQ-1401, scale 1:24,000.

Hansen, W.R., 1984, Post-Laramide tectonic history of the eastern Uinta Mountains, Utah, Colorado, and Wyoming: The Mountain Geologist, v. 21, no. 1, p. 5-29.

Hansen, W.R., 1986, Neogene tectonics and geomorphology of the eastern Uinta Mountains in Utah, Colorado, and Wyoming: U.S. Geological Survey Professional Paper 1356, 78 p.

Hansen, W.R., and Bonilla, M.G., 1954, Laramide faulting and orogeny on the north flank of the Uinta Mountains in eastern Daggett County, Utah: Denver, Colorado, Colorado Scientific Society Proceedings, v. 17, no. 1, 3 pls., 29 p.

Hansen, W.R., and Rowley, P.D., 1991, Geologic map of the Hoy Mountain quadrangle, Daggett and Uintah counties, Utah, and Moffat County, Colorado: U.S. Geological Survey Quadrangle Map GQ-1695, scale 1:24,000.

Hansen, W.R., Carrara, P.E., and Rowley, P.D., 1981, Geologic map of the Crouse Reservoir quadrangle, Uintah and Daggett Counties, Utah: U.S. Geological Survey Geologic Quadrangle Map GQ-1554, scale 1:24,000.

Hansen, W.R., Carrara, P.E., and Rowley, P.D., 1982, Geologic map of the Canyon of Lodore North quadrangle, Moffat County, Colorado: U.S. Geological Survey Geologic Quadrangle Map GQ-1568, scale 1:24,000.

Hansen, W.R., Rowley, P.D., and Carrara, P.E., 1983, Geologic map of Dinosaur National Monument and vicinity, Utah and Colorado: U.S. Geological Survey Miscellaneous Investigations Map I-1407, scale 1:50,000.

Hecker, Suzanne, 1993, Quaternary tectonics of Utah with emphasis on earthquake-hazard characterization: Utah Geological Survey Bulletin 127, map scale 1:500,000, 2 pls., 157 p.

Herrmann, R.B., 1975, Recurrence relations: Earthquake Notes, v. 48, p. 47-49.

Herrmann, R.B., 1979, FASTHYPO -- A hypocenter location program: Earthquake Notes, v. 50, no. 2, p. 25-37.

Huddle, J.W., Mapel, W.J., and McCann, F.J., 1951, Geology of the Moon Lake area, Duchesne County, Utah: U.S. Geological Survey Oil and Gas Investigations Map OM-115.

Izett, G.A., 1975, Late Cenozoic sedimentation and deformation in northern Colorado and adjoining areas, *in* Curtis, B.F., ed., Cenozoic history of the southern Rocky Mountains: Boulder, Colorado, Geological Society of America Memoir 144, p. 179-209.

Kanamori, H., and Anderson, D.L., 1975, Theoretical basis for some empirical relations in seismology: Bulletin of the Seismological Society of America, v. 65, p. 1073-1079.

Kinney, D.M., 1955, Geology of the Uinta River-Brush Creek area, Duchesne and Uintah Counties, Utah: U.S. Geological Survey Bulletin 1007, map scale 1 in = 1 mi, 6 pls., 185 p.

Kirkham, R.M., and Rogers, W.P., 1981, Earthquake potential in Colorado -- A preliminary evaluation: Colorado Geological Survey Bulletin 43, 171 p.

LaForge, R.C., and Ake, J.P., 1999, Seismic hazard analysis, Central Valley Project, Folsom Unit, Mormon Island Auxiliary Dam [unpub. report]: Denver, Colorado, U.S. Bureau of Reclamation, Technical Service Center Seismotectonic Report 94-3, in prep.

LaForge, R.C., and Anderson, L.W., 1988, Seismotectonic study for Santa Cruz Dam, Santa Cruz Dam Modification Project, New Mexico [unpub. report]: Denver, Colorado, U.S. Bureau of Reclamation, Seismotectonic Report 88-2, 31 p.

Machette, M.N., 1982, Quaternary and Pliocene faults in the La Jencia and south part of the Albuquerque-Belen basins, New Mexico -- Evidence of fault history from fault-scarp morphology and Quaternary geology: New Mexico Geological Society Guidebook, 33rd Field Conference, Albuquerque County II, p. 161-169.

Martin, R.A., Jr., Nelson, A.R., Weisser, R.R., and Sullivan, J.T., 1985, Seismotectonic study for Taskeech Dam and Reservoir site, Upalco Unit, Upper Stillwater Dam and Reservoir site, Bonneville Unit, Central Utah Project [unpub. report]: Denver, Colorado, U.S. Bureau of Reclamation, Seismotectonic Report 85-2, 95 p.

McGuire, R.K., 1974, Seismic structural response risk analysis incorporating peak response regressions on earthquake magnitude and distance: Massachusetts Institute of Technology, Department of Civil Engineering, Research Report No. R74-51.

McGuire, R.K., 1978, FRISK -- Computer program for seismic analysis using faults as earthquake sources: U.S. Geological Survey Open-File Report 78-1007, 62 p.

McGuire, R.K., 1993, Seismic hazard analysis at Rocky Flats Plant: Fourth Department of Energy (DOE) Natural Phenomena Hazards Mitigation Conference-1993, p. 636-640.

Nelson, A.R., and Weisser R.R., 1985, Quaternary faulting on Towanta Flat, northwestern Uinta Basin, Utah, *in* Picard, M.D., ed., Geology and energy resources, Uinta Basin, Utah: Salt Lake City, Utah Geological Association Publication 12, p. 147-158.

Peterson, J.E., 1989, Seismotectonic analysis for SEED report for Flaming Gorge Dam, Colorado River Storage Project [unpub. report]: Denver, Colorado, U.S. Bureau of Reclamation, Technical Memorandum No. 3610-89-16, 7 p.

Ritzma, H.R., 1971, Faulting on the north flank of the Uinta Mountains, Utah and Colorado, *in* Renfro, A.R., ed., Symposium on Wyoming tectonics and their economic significance: Billings, Montana, Wyoming Geological Association, 23rd Field Conference Guidebook, p. 145-150.

Rowley, P.D., Hansen, W.R., Tweto, Ogden, and Carrara, P.E., 1985, Geologic map of the Vernal 1° x 2° quadrangle, Colorado, Utah, and Wyoming: U.S. Geological Survey Miscellaneous Investigations Series Map I-1526, scale 1:250,000.

Sadigh, K., Chang, C.-Y., Egan, J.A., Makdisi, F., and Youngs, R.R., 1997, Attenuation relationships for shallow crustal earthquakes based on California strong motion data: Seismological Research Letters, v. 68, no. 1, p. 180-189.

Smith, R. B., and Arabasz, W.J., 1991, Seismicity of the Intermountain Seismic Belt, *in* Slemmons, D.B., Engdahl, E.R., Zoback, M.D., and Blackwell, D.D., eds., Neotectonics of North America: Boulder, Colorado, Geological Society of America, Decade Map, Volume 1.

Spudich, P., Fletcher, J.B., Hellweg, M., Boatwright, J., Sullivan, C., Joyner, W.B., Hanks, T.C., Boore, D.M., McGarr, A., Baker, L.M., and Lindh, A.G., 1996, Earthquake ground motions in extensional tectonic regimes: U.S. Geological Survey Open File Report 96-292, 351 p.

Sullivan, J.T., and Ostenaa, D.A., 1988, Seismotectonic study for Meeks Cabin and Stateline Dams, Lyman Project, Wyoming [unpub. report]: Denver, Colorado, U.S. Bureau of Reclamation, Seismotectonic Report 88-11, 7 p.

Tweto, Ogden, 1976, Geologic map of the Craig 1° x 2° quadrangle, northwestern Colorado: U.S. Geological Survey Miscellaneous Investigations Series Map I-972, scale 1:250,000.

Tweto, Ogden, 1979, Geologic map of Colorado: U.S. Geological Survey, scale 1:500,000.

U.S. Bureau of Reclamation, 1986, Seismotectonic considerations for modification decision analysis -- Steinaker Dam, Central Utah Project, Utah [unpub.]: Denver, Colorado, Memorandum from Chief, Geologic Services Branch, to Chief, Embankment Dams Branch, 7 p.

von Thun, J.L., Roehm, L.H., Scott, G.S., and Wilson, J.A., 1988, Earthquake ground motions for design and analysis of dams, *in* Proceedings of Earthquake Engineering and Soil Dynamics II: Park City, Utah, GT Div/ASCE, p. 463-482.

Weber, J.R., 1971, Structural geology of the northeastern flank of the Uinta Mountains, Moffat County, Colorado: The Mountain Geologist, v. 8, p. 163-181.

Weichert, D., 1980, Estimation of the earthquake recurrence parameters for unequal observation periods for different magnitudes: Bulletin of the Seismological Society of America, v. 70, p. 1337-1347.

West, M.W., 1988, Geologic and tectonic studies in the vicinity of Meeks Cabin and Stateline Dams, Lyman Project, southwestern Wyoming and north-central Utah, 121 p., *in* Sullivan, J.T., and Ostenaa, D.A., Seismotectonic study for Meeks Cabin and Stateline Dams, Lyman Project, Wyoming [unpub. report]: Denver, Colorado, U.S. Bureau of Reclamation, Seismotectonic Report 88-11, 7 p.

Wong, I.G., and Chapman, D.S., 1990, Deep intraplate earthquakes in the western United States and their relationship to lithospheric temperatures: Bulletin of the Seismological Society of America, v. 80, p. 589-599.

Wong, I.G., and Humphrey, J.R., 1989, Contemporary seismicity, faulting, and the state of stress in the Colorado Plateau: Geological Society of America Bulletin, v. 101, p. 1127-1146.

Zoback, M.L., and Zoback, M.D., 1989, Tectonic stress field of the continental United States, *in* Pakiser, L.C., and Mooney, W.D., eds., Geophysical Framework of the Continental United States,: Boulder, Colorado, Geological Society of America Memoir 172, p. 523-540.